Universitat Autònoma de Barcelona

Departament de Geologia, Facultat de Ciències, Universitat Autònoma de Barcelona

Registre sedimentari i icnològic del fini-Carbonífer, Permià i Triàsic continentals dels Pirineus Catalans

Evolució i crisis paleoambientals a l'equador de Pangea

Memòria presentada per Eudald Mujal Grané per optar al títol de Doctor en Geologia

Juny de 2017

Tesi doctoral dirigida per:

Dr. Oriol Oms Llobet, Departament de Geologia, Universitat Autònoma de Barcelona

Dr. Josep Fortuny Terricabras, Institut Català de Paleontologia Miquel Crusafont

Dr. Oriol Oms Llobet **Dr. Josep Fortuny Terricabras**

Eudald Mujal Grané

Capítol 5. *Constraining the Permian/Triassic transition in continental environments: Stratigraphic and paleontological record from the Catalan Pyrenees (NE Iberian Peninsula)*

El capítol 5 correspon a l'article publicat a la revista *Palaeogeography, Palaeoclimatology, Palaeoecology* l'1 de març de 2016 (online el 21 de desembre de 2015):

Mujal, E., Gretter, N., Ronchi, A., López-Gómez, J., Falconnet, J., Diez, J.B., De la Horra, R., Bolet, A., Oms, O., Arche, A., Barrenechea, J.F., Steyer, J.-S., Fortuny, J., 2016. Constraining the Permian/Triassic transition in continental environaments: Stratigraphic and paleontological record from the Catalan Pyrenees (NE Iberian Peninsula). Palaeogeography, Palaeoclimatology, Palaeoecology, 445: 18–37.

https://doi.org/10.1016/j.palaeo.2015.12.008

En aquest article l'autor E. M. ha contribuït en: plantejament del treball; tasques de camp, incloent prospecció i documentació de les traces fòssils; elaboració dels models fotogramètrics 3D de les icnites; anàlisis de sedimentologia i icnologia; interpretació i discussió de tots els resultats; redacció del manuscrit; preparació de les figures 6–14; maquetació de les figures 2, 6–14; preparació del material suplementari.

Palaeogeography, Palaeoclimatology, Palaeoecology 445 (2016) 18–37

Contents lists available at ScienceDirect

Palaeogeography, Palaeoclimatology, Palaeoecology

journal homepage: www.elsevier.com/locate/palaeo

Constraining the Permian/Triassic transition in continental environments: Stratigraphic and paleontological record from the Catalan Pyrenees (NE Iberian Peninsula)

Eudald Mujal [a], Nicola Gretter [b], Ausonio Ronchi [b], José López-Gómez [c], Jocelyn Falconnet [d], José B. Diez [e], Raúl De la Horra [f], Arnau Bolet [g], Oriol Oms [a], Alfredo Arche [c], José F. Barrenechea [c,h], J. -Sébastien Steyer [d], Josep Fortuny [d,g,*]

[a] Departament de Geologia, Universitat Autònoma de Barcelona, E-08193 Bellaterra, Spain
[b] Department of Earth and Environmental Sciences, University of Pavia, Via Ferrata 1, I-27100 Pavia, Italy
[c] Instituto de Geociencias (UCM, CSIC), c/ José Antonio Nováis 12, E-28040, Madrid, Spain
[d] C2RP, CNRS-MNHN-UPMC, 8 rue Buffon, CP38, F-75005 Paris, France
[e] Departamento de Xeociencias Mariñas e Ordenación do Território, Facultade de Ciencias do Mar, Universidade de Vigo, E-36310 Vigo, Spain
[f] Departamento de Estratigrafía, Facultad de Geología, Universidad Complutense de Madrid c/ José Antonio Nováis 12, E-28040, Madrid, Spain
[g] Institut Català de Paleontologia Miquel Crusafont, ICTA-ICP building, c/ de les columnes, s/n, E-08193 Cerdanyola del Vallès, Spain
[h] Departamento de Cristalografía y Mineralogía, Facultad de Geología, Universidad Complutense de Madrid c/ José Antonio Nováis 12, E-28040, Madrid, Spain

ARTICLE INFO

Article history:
Received 28 July 2015
Received in revised form 18 November 2015
Accepted 11 December 2015
Available online 21 December 2015

Keywords:
Permian
Triassic
Vertebrates
Palynology
Western Tethys
Pyrenees

ABSTRACT

The continental Permian–Triassic transition in southern Europe presents little paleontological evidence of the Permian mass extinction and the subsequent faunal recovery during the early stages of the Triassic. New stratigraphic, sedimentological and paleontological analyses from Middle–Upper Permian to Lower–Middle Triassic deposits of the Catalan Pyrenees (NE Iberian Peninsula) allow to better constrain the Permian–Triassic succession in the Western Tethys basins, and provide new (bio-) chronologic data. For the first time, a large vertebra attributed to a caseid synapsid from the ?Middle Permian is reported from the Iberian Peninsula—one of the few reported from western Europe. Osteological and ichnological records from the Triassic Buntsandstein facies reveal a great tetrapod ichnodiversity, dominated by small to medium archosauromorphs and lepidosauromorphs (*Rhynchosauroides* cf. *schochardti*, *R.* isp. 1 and 2, *Prorotodactylus–Rotodactylus*), an undetermined Morphotype A and to a lesser degree large archosaurians (chirotheriids), overall suggesting a late Early Triassic–early Middle Triassic age. This is in agreement with recent palynological analyses in the Buntsandstein basal beds that identify different lycopod spores and other bisaccate and taeniate pollen types of late Olenekian age (Early Triassic). The Permian caseid vertebra was found in a playa-lake setting with a low influence of fluvial water channels and related to the distal parts of alluvial fans. In contrast, the Triassic Buntsandstein facies correspond to complex alluvial fan systems, dominated by high-energy channels and crevasse splay deposits, hence a faunal and environmental turnover is observed. The Pyrenean biostratigraphical data show similarities with those of the nearby Western Tethys basins, and can be tentatively correlated with North African and European basins. The Triassic Pyrenean fossil remains might rank among the oldest continental records of the Western Tethys, providing new keys to decipher the Triassic faunal biogeography and recovery.

1. Introduction

The Permian–Triassic mass extinction represents one of the most extensively studied climatic and biological crises in the history of Earth (e.g., Erwin, 1994; Benton and Twitchett, 2003; Sahney and Benton, 2008; Benton and Newell, 2014; Smith and Botha-Brink, 2014). The extinction led to a profound remodeling of the ecosystems and a vertebrate faunal turnover (Benton et al., 2004) that covered a geologically short to extremely short period of time (Bowring et al., 1998; Ward et al., 2005). The Middle–Late Permian continental successions have been accurately constrained by tetrapod remains from Russia (Benton

* Corresponding author at: C2RP, CNRS-MNHN-UPMC, 8 rue Buffon, CP38, F-75005 Paris, France.
E-mail addresses: eudald.mujal@uab.cat (E. Mujal), nicola.gretter@gmail.com (N. Gretter), ausonio.ronchi@unipv.it (A. Ronchi), jlopez@ucm.es (J. López-Gómez), falconnet@mnhn.fr (J. Falconnet), jbdiez@uvigo.es (J.B. Diez), rhorraba@geo.ucm.es (R. De la Horra), arnau.bolet@icp.cat (A. Bolet), joseporiol.oms@uab.cat (O. Oms), aarche@ucm.es (A. Arche), barrene@ucm.es (J.F. Barrenechea), steyer@mnhn.fr (J.-S. Steyer), josep.fortuny@icp.cat (J. Fortuny).

http://dx.doi.org/10.1016/j.palaeo.2015.12.008
0031-0182/

et al., 2004, 2012; Surkov et al., 2007), Morocco (Voigt et al., 2010), France (Gand et al., 2000; Reisz et al., 2011), Italy (Valentini et al., 2007, 2009; Avanzini et al., 2011; Bernardi et al., 2015), Brazil (e.g., Cisneros et al., 2012, 2015; Costa da Silva et al., 2012), China (e.g., Xu et al., 2015) and South Africa (e.g., Smith and Botha-Brink, 2014), whereas the earliest part of the Triassic provides a much more scarce paleontological record. In fact, most of the Early Triassic continental record is late Olenekian in age, with the exception of a few areas and basins with Induan sediments and vertebrate fossils (e.g., the South African Karoo Basin, Smith and Botha-Brink, 2014, or the Russian East European Platform, Benton et al., 2004).

Accordingly, the basal Triassic record of the Iberian Peninsula and Balearic Islands has not yet been documented, as the older Triassic successions have been attributed to a late Early Triassic (Olenekian) age (Dinarès-Turell et al., 2005; Linol et al., 2009; Bourquin et al., 2011; López-Gómez et al., 2012; Galán-Abellán et al., 2013; Borruel-Abadía et al., 2015). Until now, vertebrate fossils have been characterized only from the Middle and Late Triassic of both fluvial and coastal–alluvial facies (e.g., Calzada, 1987; Demathieu and Saiz de Omeñaca, 1990; Pérez-López, 1993; Gand et al., 2010; Fortuny et al., 2011a,b; Díaz-Martínez and Pérez-García, 2012; Mateus et al., 2014; Brusatte et al., 2015; Díaz-Martínez et al., 2015; Mujal et al., 2015 and references therein).

In the Catalan Pyrenean Basin (NE Iberian Peninsula), Robles and Llompart (1987) reported tetrapod footprints that correlated the equivalent fossil-bearing red sediments to the Late Permian. Moreover, in the nearby Palanca de Noves tracksite (Ribera d'Urgellet, Catalonia), Fortuny et al. (2010) preliminarily identified four morphotypes of tetrapod footprints, here re-described and analyzed in detail. However, the age of this unit, together with the geology of this area, is still a subject of uncertainties. Here we present new geological, paleontological (i.e., vertebrate assemblages), and palynological data from the Permian and Triassic sequences of selected areas of the Catalan Pyrenees. Our data, framed in an interregional stratigraphic picture (i.e., Spanish Cantabrian Mountains, northern Italy, northern Morocco and southern France), precise with more confidence the transition from the Permian to the Triassic periods, and sheds light on the first onset of recovery after the end-Permian mass extinction of the Western Tethys.

2. Geological setting

All the studied tetrapod remains come from the continental succession that includes the Upper Carboniferous (?)–Lower Triassic of the Gramós Basin in the SE Catalan Pyrenees (Fig. 1). Since the last century this stratigraphic succession has been described from a sedimentological, petrological, structural and stratigraphical point of view (e.g., Viennot, 1929; Dalloni, 1930; Schmidt, 1931; Ashauer, 1934; Mey et al., 1968; Nagtegaal, 1969; Hartevelt, 1970; Gisbert, 1981; Martí, 1983; Speksnijder, 1985; Saura, 2004; Saura and Teixell, 2006; Pereira et al., 2014; Gretter et al., 2015). In this work we have adopted the most recent unit subdivision (Gisbert, 1981), comparing it with others (e.g., Mey et al., 1968; Nagtegaal, 1969). The Stephanian–

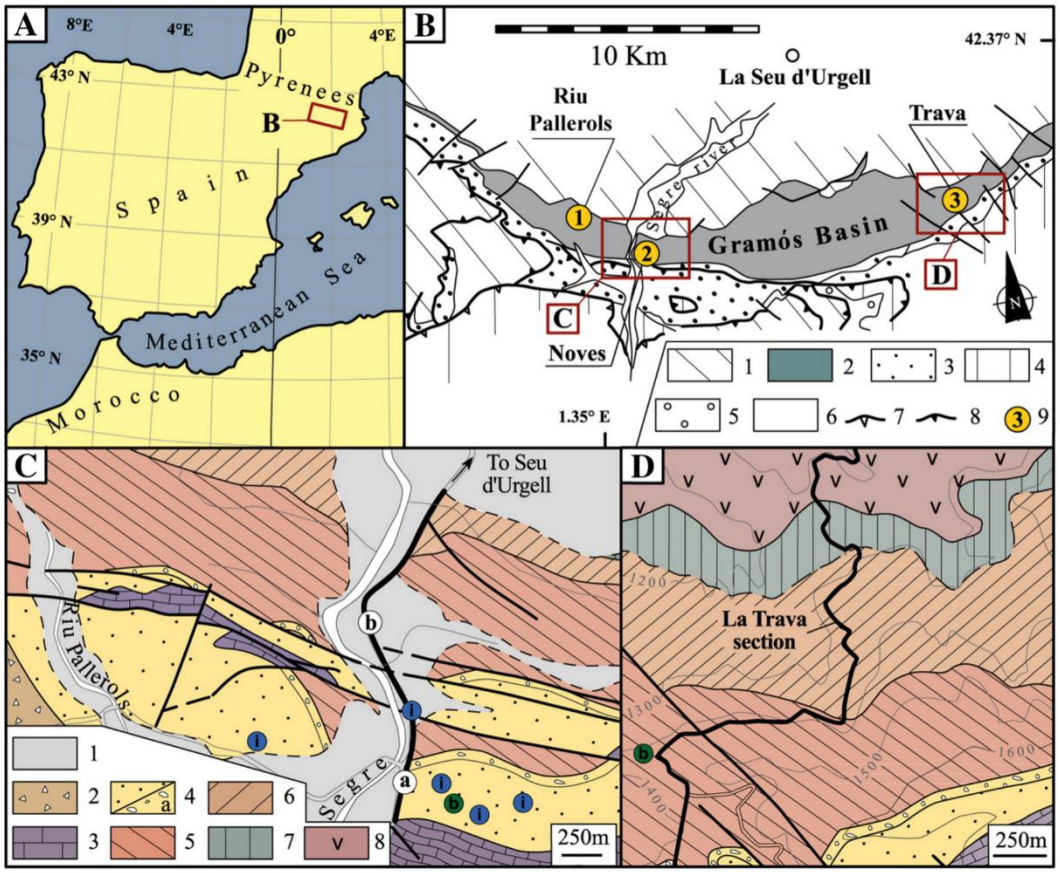

Fig. 1. A–B) Geographic location and simplified geological map of studied areas (modified from Hartevelt 1970; Saura and Teixell 2006). (1) Variscan Basement (2) Stephano-Permian deposits (3) Triassic (4) Jurassic–Cretaceous (5) Cenozoic cover (6) Quaternary (7) Alpine backthrusts (8) South-directed thrusts (9) Location of sampling sites and of measured sections. **C–D**) Geological sketch map of the Segre Valley and La Trava area: (1) Alluvial deposits, (2) Middle and Upper Triassic deposits, (3) Muschelkalk, (4) Buntsandstein, (5) Upper Red Unit, (6) Lower Red Unit, (7) Transition Unit, 8) Grey Unit (volcanic rocks).

Permian deposits are subdivided into four lithostratigraphic units (Fig. 2) which comprise, from base to top, the Grey Unit (GU), the Transition Unit (TU), the Lower Red Unit (LRU), and the Upper Red Unit (URU). It should be noted that the ages inferred by the floras of each unit must be updated and reviewed (e.g., Wagner and Álvarez-Vázquez, 2010), so we provide and summarize the available data for a general approach.

The GU ("Unidad Gris" of Gisbert, 1981 and "Stéphano-Permien gris" of Broutin et al., 1994; Fig. 2) is mostly made up of volcanic and volcaniclastic rocks and corresponds to the Aguiró Formation and to the Erillcastell Formation described by Dalloni (1930), Mey et al. (1968), and Nagtegaal (1969) in a more westerly area (see also Pereira et al., 2014). It rests uncoformably on the basement. The "Flora of Argestues" (Gisbert, 1981; Broutin and Gisbert, 1985) is equivalent to the "Flora of Aguiró" (Nagtegaal, 1969), and it is thought to be of Stephanian B age. Conversely, according to Talens and Wagner (1995), the flora of Aguiró could be dated as late Asturian (uppermost Westphalian) and earliest Cantabrian (lowermost Stephanian).

The TU ("Unidad de Tránsito" of Gisbert, 1981 and called "Permien alternant" by Broutin et al., 1994; Fig. 2) could correspond to the Malpàs Formation of Mey et al. (1968) and Nagtegaal (1969). It mainly consists of volcanic and volcaniclastic sequences at the base, grading upwards to grey sandstones and microconglomerates intercalated with grey and reddish siltstones. In the sector of Castellar de n'Hug (Berguedà; 43 km eastwards from La Trava section; see Gretter et al., 2015), a badly preserved tetrapod rib of 15 cm in length was found but not recovered. In any case, this finding demonstrates the presence of large tetrapods in those environments. The paleoflora of this unit suggest a Stephanian-Autunian or a Stephanian C-basal Autunian age (Gisbert, 1981; Broutin and Gisbert, 1985).

The LRU ("Unidad Roja Inferior" of Gisbert, 1981; Fig. 2) is composed of reddish alluvial fan and meandering river flood-plain deposits, including channels, overbank fines and paleosols. Volcaniclastic bodies are common at the base of the unit. Roger (1965), Mey et al. (1968), and especially Nagtegaal (1969) identified it with the name of Peranera Formation. The age of LRU was inferred as Permian, based on the floras and plant remains by Dalloni (1930), and Roger (1965). Mujal et al. (in press) inferred an Artinskian age (middle–late Early Permian) for the lower part of the LRU (Peranera Formation from the western Pyrenean area) based on tetrapod ichnoassociations including *Batrachichnus salamandroides*, *Limnopus* isp., cf. *Amphisauropus* (these three associated to *Characichnos* swimming traces), cf. *Ichniotherium*, *Dromopus* isp., cf. *Varanopus*, *Dimetropus leisnerianus*, as well as several invertebrate trace fossils. Above the LRU, the onset of the Upper Red Unit is defined by an angular unconformity.

The URU ("Unidad Roja Superior" of Gisbert, 1981 and "Permien rouge ou Saxonien" of Broutin et al., 1994; Figs. 2, 3A, D) is mainly composed of red conglomerates, sandstones and siltstones, paleosols with calcareous nodules and lacustrine deposits arranged in two fining upwards megasequences with volcanic intercalations in the lower part (Gisbert, 1983). To date, the absence of chronological data hampered the attribution of a precise age to the unit, even if it has been generically

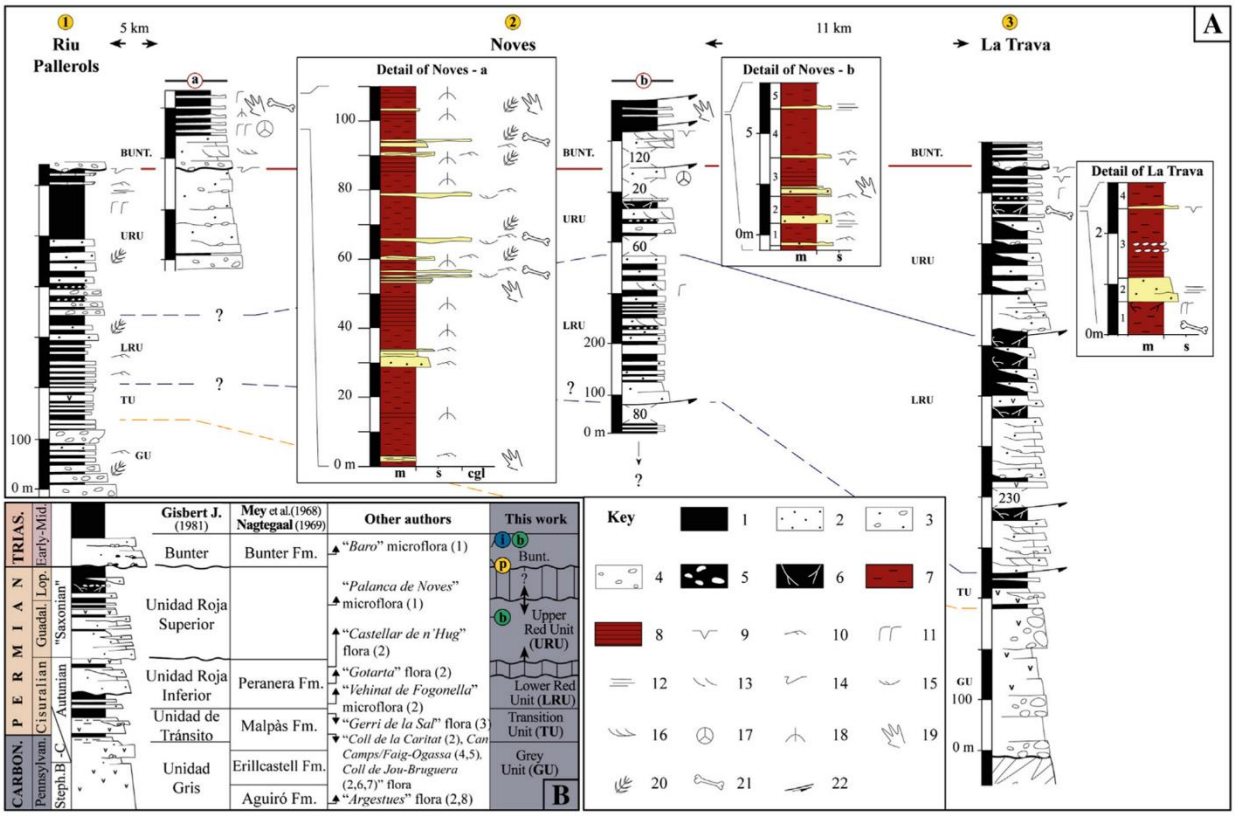

Fig. 2. A) Lithostratigraphic correlation chart of some simplified Permian stratigraphic sections from Central- Eastern Pyrenees (from 1 to 3). Lithology: (1) siltstones; (2) sandstones; (3) pebbly sandstones; (4) conglomerates; (5) carbonate nodules; (6) rhizolite concretions. (7) Thickly-bedded siltstones. (8) Thinly bedded siltstones/mudstones. Other symbols: (9) Mud cracks. (10) Ripple marks. (11) Bioturbation tracks. (12) Parallel laminations. (13) Planar laminations. (14) Flute casts. (15) Trough cross-stratification. (16) Eolian planar stratification. (17) Palynomorph samples (this work). (18) Incipient paleosol. (19) Tetrapod tracks (this work) (20) Paleoflora. (21) Bones. (22) Faults. For a more precise position of sections and sampling points see Fig.1B, C, D. **B**) Late Paleozoic–Mesozoic lithostratigraphy mostly based on Gisbert (1981), Mey et al. (1968) and Nagtegaal (1969). Other authors: (1) Broutin et al. (1988); (2) Broutin and Gisbert (1985); (3) Dalloni (1930); (4) Martin-Closas and Martinez-Roig (2007); (5) Álvarez-Ramis et al. (1971); (6) Doubinger et al. (1978); (7) Robert (1970); (8) Nagtegaal (1969). Carbon.: Carboniferous; Steph.: Stephanian; Guadal.: Guadalupian; Lop.: Lopingian; Trias.: Triassic; Mid.: Middle; Bunt.: Buntsandstein.

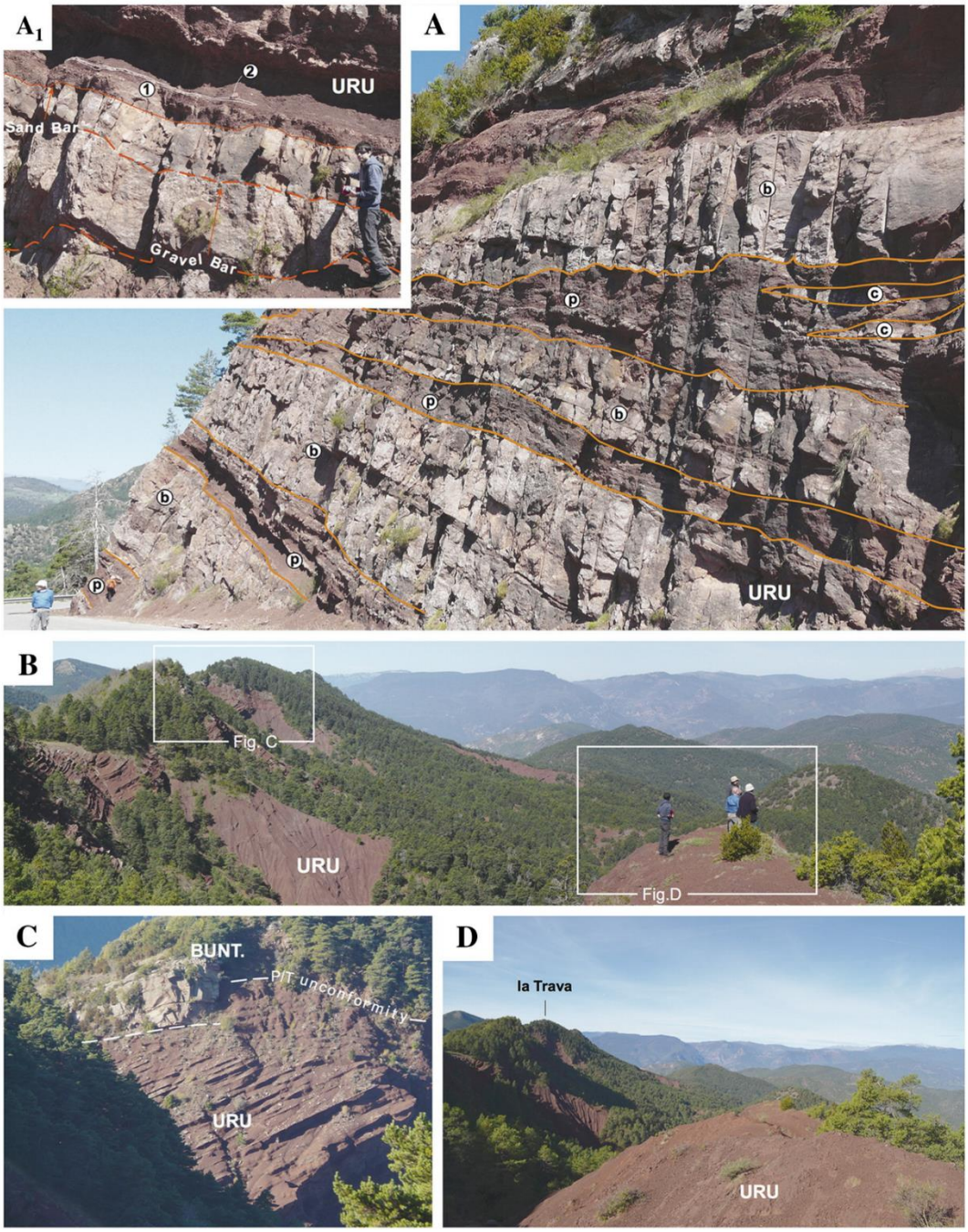

Fig. 3. A) Outcrop of URU beds characterized by gravel and sand bars (b) all overlain by fine grained paleosols (p). Some little sandy channels (c) can also be found. **A_1)** Detail of the aforementioned bars and paleosols showing a nodular horizon (1) and coalescing nodules (2). **B**) Overview of the eastern cliff of the Mirador de La Trava. **C**) Photographic panel showing the transition from the Upper Red Unit (URU) to the Buntsandstein facies (BUNT.) **D)** In the upper portion of the URU, the playa lake levels are clearly exposed just few meters beneath the P/T unconformity.

referred to as "Upper Thuringian" by López-Gómez et al. (2002) following Broutin et al. (1988). In the Palanca de Noves section, the URU fluvial conglomerates and sandstones above the alkaline basalt levels (Bixel and Lucas, 1983; Gisbert, 1983) were dated as "Thuringien" based on a palynomorph assemblage (Broutin et al., 1988).

The Buntsandstein facies (Bunter Formation, Mey et al., 1968; Fig. 2) consist of a sequence of 200 m thickness in average of fluvial red beds unconformably overlying the URU. In the studied areas the lower contact of the Buntsandstein facies (Fig. 3A) is deeply erosive and marks an angular unconformity of about 20–25°. The basal part of the coarse fluvial Buntsandstein deposits was ascribed to the Early Triassic (late Olenekian) by Bourquin et al. (2011) on the basis of previous works (Broutin et al., 1988; Diez, 2000; Diez et al., 2005). The fluvial Buntsandstein sedimentation started with a coarse oligomictic, quartz-

rich conglomerate followed by interbedded sandstones and siltstones forming a fining-upwards sequence. The upper part of the unit is constituted by dark-red micaceous sandstones, bioturbated mudstones and siltstones. The microflora reported in this upper portion ("microflora de Baro", Broutin et al., 1988), together with other palynomorph assemblages (Calvet et al., 1993; Diez, 2000; Diez et al., 2005) yielded a lower Anisian age (Aegean for Diez, 2000; Diez et al., 2005) for the mudstone-siltstone unit.

3. Materials and methods

The interpretation of sedimentary structures and lithologic associations of rocks has been carried out by the description of two complete stratigraphic sections (Fig. 2). Each column (Palanca de Noves and La Trava) is representative of the Stephano-Autunian succession of the Gramós sub-basin (in the sense of Saura and Teixell, 2006). Accordingly, we focused our sedimentological description on the Permian Upper Red Unit (URU) and the Triassic Buntsandstein facies as they are mostly related to the objectives of this work. In particular, we coupled the stratigraphic/sedimentological description of levels yielding tetrapod bones from the URU with the systematic study of the tetrapod bones and ichnites, and palynological analysis from the Buntsandstein facies. Our fieldwork included geological mapping (Fig. 1C–D), measurement of stratigraphic sections, sedimentological description and interpretation, and paleontological prospection. In general, sections were logged at a scale of 1:200, although the proposed stratigraphic panel has been drawn at a smaller scale (Fig. 2). The studied units were correlated between outcrops when possible, using marker beds.

Our ichnological study was based on the analysis of more than 70 *in situ* and *ex situ* specimens from different levels of the Palanca de Noves Buntsandstein succession. The samples collected are stored at the museum of the Institut Català de Paleontologia Miquel Crusafont (IPS, Sabadell, Spain). Silicone moulds and synthetic resin replicas (also at IPS) were made from some tetrapod footprints.

The qualitative and quantitative parameters analyzed in vertebrate tracks follow the methodology of Haubold (1971a, b) and Leonardi (1987). The descriptions and the biometric measurements (taken in both specimens and photos) were carried out on the best preserved material, avoiding extramorphological features (e.g., Haubold et al., 1995; Haubold, 1996; Bertling et al., 2006), using the software ImageJ (version 1.48r, available for download from http://rsbweb.nih.gov/ij/). 3D photogrammetric models, depth maps and contour-lines of 18 specimens have been generated following the procedures of Matthews (2008), Falkingham (2012) and Mujal et al. (2015; in press), in order to better define diagnostic features. The pictures, taken with a digital compact camera Sony DSC-T200 8.1 Megapixels, were processed with three different open access programs (i.e., VisualSFM v0.5.22 http://www.ccwu.me/vsfm/, MeshLab v.1.3.2 http://meshlab.sourceforge.net/, and ParaView v.4.1.0 http://www.paraview.org).

4. Results

4.1. Sedimentological description of vertebrate-bearing units

Vertebrate-bearing levels were found in the Permian URU (La Trava section) and the Triassic Buntsandstein sequence (Noves section). These units are composed of three main lithologies: conglomerates, sandstones and siltstones (Gretter et al., 2015).

The conglomerates consist of two grain-size classes of material, gravel clasts and sand/mud matrix. The proportion of each defines whether the deposits are clast or matrix supported. Conglomerates and breccias with sub-rounded/angular clasts, typically held together by a finer grained matrix, are more commonly referred to the lowermost portion of the URU (Fig. 3A, A_1). The conglomerates mainly consist of sub-angular to sub-rounded intra-clasts (polycrystalline quartz) and Cambro-Ordovician slate fragments. The matrix, locally abundant (>20%), is hematitic. The lowermost portion of the Buntsandstein facies is also characterized by coarse-grained lithologies; in this case (Fig. 4A, B), it consists of very coarse conglomerates, not exceeding a thickness of 15 m, with rounded clasts of quartz, quartzites and lidites. Clasts are white or pinkish.

The sandstones comprise moderately to poorly sorted fine- to medium-sized grains, although coarser intraclasts occur; their high content of iron oxides confers the typical red color. Well to poorly sorted, medium- to coarse-grained sandstones with variable litharenitic to arkose compositions mostly characterize the URU as well as the Buntsandstein facies. Sub-angular to sub-rounded grains are made up of quartz, feldspar, calcite and hematite. The main difference between the sandstones of both units is the much more abundant presence of detrital mica in the Buntsandstein beds.

Red siltstones and claystones are the most persistent lithologies in the upper portion of the URU and middle–upper Buntsandstein facies (dark red). Quartz, feldspar, calcite, dolomite and iron oxides (hematite) constitute the mineral composition as a whole. The clay minerals consist predominantly of illite and chlorite, with minor proportions of mixed-layered clays.

4.1.1. La Trava section

The vertebrate bone remains were found in a mudstone-siltstone layer, with rhizolits and root traces in its topmost part and deeply amalgamated by intense bioturbation. They were located in a promontory near the Mirador de la Trava (la Vansa i Fórnols, Alt Urgell, Catalonia; Fig. 3B). Specifically, the remains were located in the URU, 35 m below the unconformable contact with the Buntsandstein facies. In this part of the URU the deposits are mostly composed of thick alternations of fine-grained, often laminated dark-red silty-clay layers, and thin fine sandstone beds. Paleosols and rhizolits are usually preserved in silty claystones, under coarser levels. Bioturbation structures can be easily recognized by the absence of well-developed bedding in claystones and siltstones; these layers, in fact, display mottled structures of coarser grained size as well as plant fragments. Occasionally, greenish thin sandstone levels occur in this upper part of the URU. Although they are not tuff beds, these may be partly formed by alteration of volcanic rocks. As a whole, this part of the URU in the La Trava section has been related to a playa-lake environment (Robles and Llompart, 1987; Gretter et al., 2015).

4.1.2. Noves section

The studied tetrapod footprints are, in general, quite well preserved; they have been found in the reddish, fine-grained sediments of the Buntsandstein facies. The beginning of the Buntsandstein sedimentary record is composed of conglomerates and sandstones (Fig. 4A, B), which represent sandy and gravelly braided fluvial systems. In particular, the conglomerates are mostly made up of rounded to subrounded clasts of quartz, lidites and lithics. They are generally massive or crudely-bedded, usually matrix-supported, but locally clast-supported. Matrix is basically composed of red to pink medium to coarse sandstones. Trough and planar cross-stratified sandstones with ripples (Fig. 4C) and thin parallel laminations normally constitute thin levels with a fining-upwards tendency (see part 2, 3, 4 of Fig. 2A). Channel-fill deposits with concave-up erosive or planar base, gravel/sandstones bars (Fig. 4D) and bedforms are the most frequent elements of the basal portion of the Buntsandstein facies. The fine-grained levels, with footprints preserved, are represented by dark-red mudstones or siltstones with a massive aspect, containing vertically oriented root casts. They may show mud-cracks and occasionally well-developed paleosols (see part 1, 2, 3 of Figs. 2A and 4D, E). Fine red bioturbated sandstones with ripples may constitute centimetric beds found into dark-red massive siltstones (part 4, 5 of Figs. 2A, 4C). The fine-grained levels also show interbedded centimetric to decimetric microconglomerates, with the same aspect as those from the basal portion of the

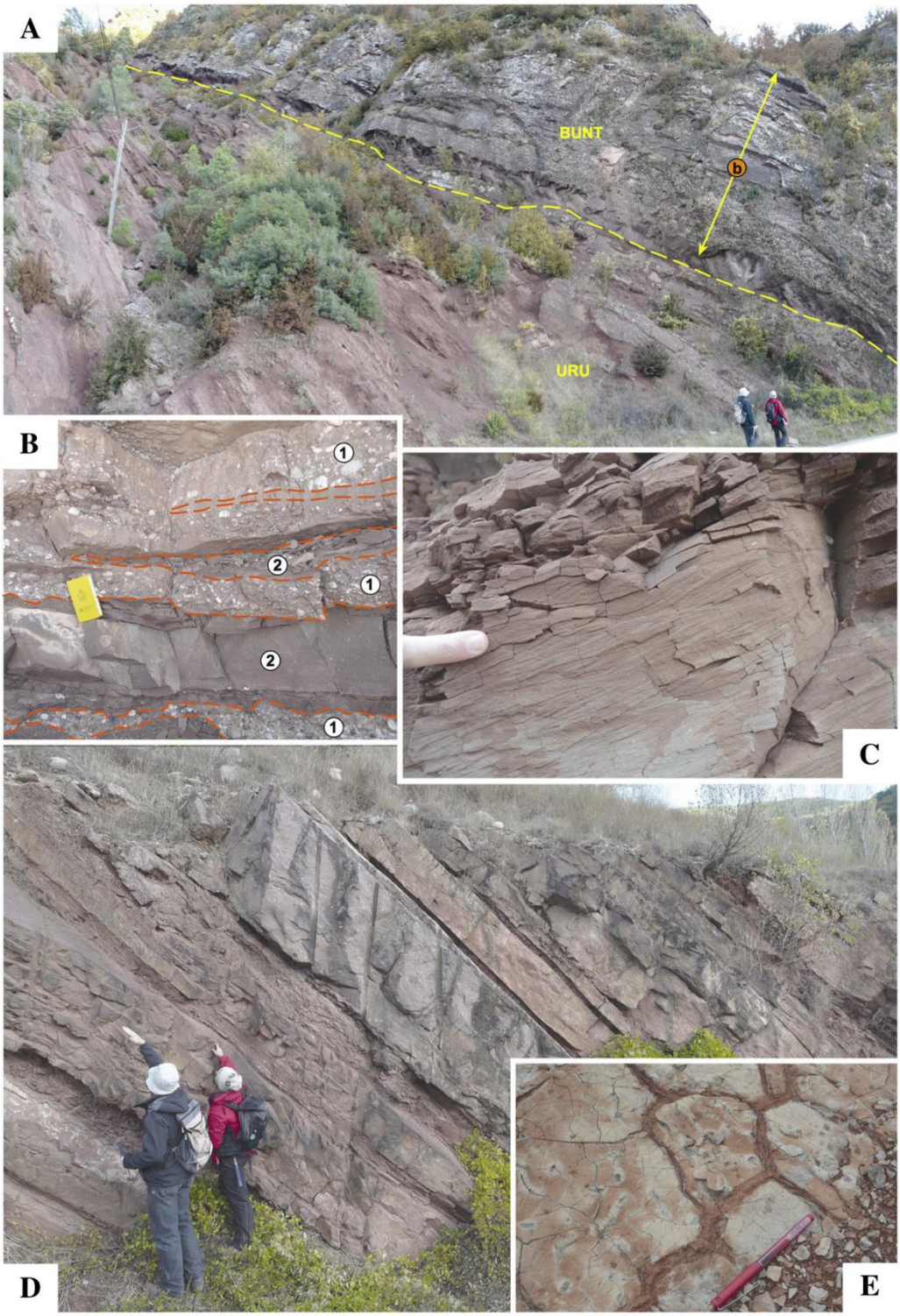

Fig. 4. A, B) Detail of the quartzitic conglomerates (1) with erosional base at the lower beds of Buntsandstein facies and fine sandstones (2) with tabular thin beds. **C**) Example of well-recognized stream ripples structures in the finer portion of Buntsandstein facies. **D)** Red mudstones alternating with fine-grained sandy metric-thick beds with mud-cracks structures in the thin siltitic levels (**E**) of the Buntsandstein facies.

Buntsandstein sequence. In these small channel deposits, scarce bone fragments are present and were recovered (Fig. 2A).

4.2. Systematic paleontology

4.2.1. Permian tetrapod vertebra

Synapsida Osborn, 1903
Caseidae Williston, 1911
Ennatosaurus Efremov, 1956
Ennatosaurus tecton Efremov, 1956
cf. *Ennatosaurus tecton*
Fig. 5A, B

Material: IPS-87365. Incomplete posterior dorsal vertebra including the dorsal half of a centrum and the base of the neural arch. The remainder of the vertebra is either missing or has been eroded.

Locality: A promontory near the lookout of the "Mirador de la Trava" (La Vansa i Fórnols, Alt Urgell, Lleida, Catalonia, Spain; Fig. 3B).

Horizon and age: Recovered in the URU, 35 m below the unconformable contact with the Buntsandstein facies. ?Middle Permian (?Wordian).

Description: IPS-87365 is a large vertebra. Its centrum is rounded, robust, and deeply amphicoelous to the point of being almost notochordal. The neural arch, in comparison, appears as a slender, tall triangular structure ending in a narrow neural spine. The base of a transverse process is preserved on the anterior half of the neurocentral suture. Located posteroventrally, on the centrum, there is also a distinct fossa including tiny laminae and foramina (arrow on Fig. 5A).

Discussion: In spite of its fragmentary state, the preservation and the anatomy of IPS-87365 provide enough information to allow its taxonomic identification. The neural arch lacks the typical swelling and zygapophyseal buttresses seen in diadectomorphs, parareptiles or captorhinids. It also shows nothing of the excavations seen at its base in sphenacomorphs and varanodontines. In fact, the whole conformation of the vertebra agrees well with that of posterior dorsals – the so-called "lumbar" vertebrae – of synapsid caseids (e.g., Romer and Price, 1940; Stovall et al., 1966; Olson, 1968; Reisz, 1986). The most significant anatomical feature of IPS-87365 is probably the presence of a small fossa on the lateral surface of the centrum. Shallow fossae have been observed by Olson (1968: p. 308) in this area in large caseid specimens, but he interpreted them as the mere result of crushing. The genus *Ennatosaurus* is the only caseid in which such true fossae have been described in dorsal vertebrae (Olson, 1968: p. 308, Fig. 22A–D). The presence of this unusual feature, diagnostic of *Ennatosaurus*, provides enough grounds for the tentative identification of IPS-87365 as cf. *Ennatosaurus tecton*.

4.2.2. Triassic remains

Tetrapoda indet.
Fig. 5C, D

Material: IPS-85043, IPS-85044, IPS-85046, IPS-85048.

Locality: Palanca de Noves (Ribera d'Urgellet, Alt Urgell, Catalonia).

Horizon and age: At 105 m, 115 m and 145 m from the base of the Buntsandstein facies sequence; Spathian (late Olenekian, Early Triassic).

Description: Some fragmentary and poorly-preserved bones were recovered during road construction in the Palanca de Noves site. Most of the remains cannot be identified with confidence but at least one of the remains presents a marked sculpture (IPS-85043, Fig. 5C) similar to the typical ornamentation found on the skull roof of the Stereospondyli tetrapods or on that of some archosauromorph reptiles.

Discussion: The fragmentary nature of the remains recovered in the Palanca de Noves site precludes a confident assessment of these remains to any group, but the ornamentation and thickness of the remains suggest a stereospondyl nature, although an archosauromorph reptile origin cannot be discarded. Stereospondyl remains have previously been recovered in the Middle Triassic of the Catalan Basin (Fortuny et al., 2011a,b). If the remains from Palanca de Noves happen to belong to Stereospondyli, they would represent the first occurrence of this group in the Pyrenean Basin and thus an enlargement of its record in the Triassic of southern Europe. On the contrary, if these remains finally

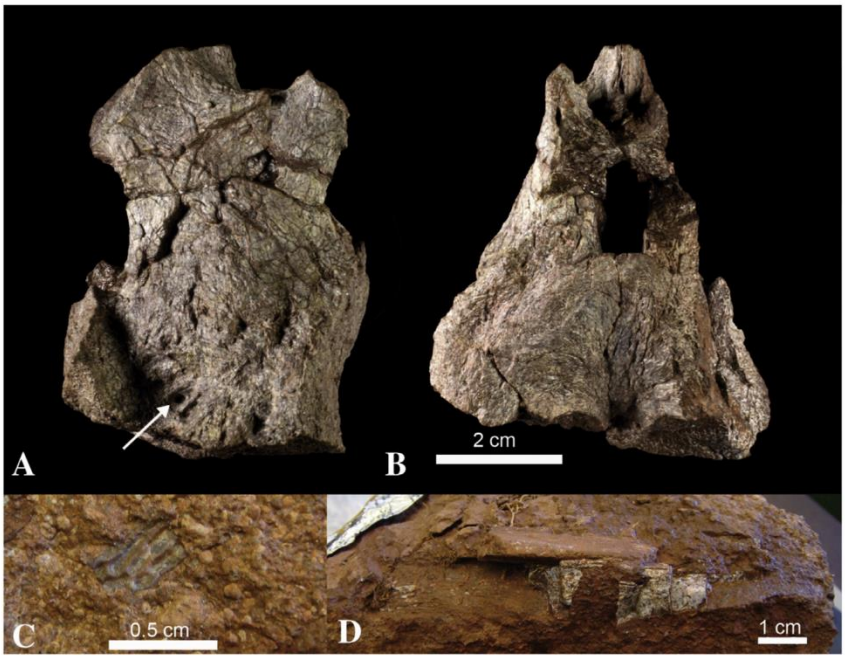

Fig. 5. A–B) IPS-87365, posterior dorsal vertebra of cf. *Ennatosaurus tecton*. **A**) right lateral view. The arrow indicates the fossa. **B)**, left lateral view. **C–D)** Tetrapod indet. remains. **C)** IPS-85043, small ornamented cranial fragment. **D)** IPS-85046, large bone fragment.

have an archosauromorph reptile affinity, their occurrence could represent the oldest finding of these reptiles in the Pyrenean Basin and in the Triassic of the Iberian Peninsula.

Ichnogenus *Rhynchosauroides* Maidwell, 1911

Remarks: Tracks corresponding to this ichnogenus are the most abundant and diverse in the Palanca de Noves site. There are several surfaces with mass occurrences of different morphotypes of *Rhynchosauroides*, which may correspond to different ichnospecies. All these footprints share the following diagnostic characters (the so called "lacertoid type") of the ichnogenus: (1) plantigrade to semiplantigrade pentadactyl manus, (2) digits I to IV increasing in length, (3) digit V rotated outwards and postero-laterally positioned, with a length between digits I and II, (4) digitigrade pes impressions, with digits II, III and IV mostly preserved, and overstepping manus footprints (e.g., Haubold, 1971a, b; Valdiserri and Avanzini, 2007; Gand et al., 2010; Klein and Lucas, 2010a). The pes impressions are often not preserved in the studied localities, as occurs in other tracksites (e.g., Valdiserri and Avanzini, 2007). The trackmakers referred to this ichnogenus are both lepidosauromorphs and archosauromorphs (Klein and Lucas, 2010a; Avanzini et al., 2011).

Ichnospecies *Rhynchosauroides* cf. *schochardti* (Rühle von Lilienstern, 1939)

Fig. 6

Material: IPS-82625, IPS-82626 (replicas with several ichnites), IPS-85058, IPS-85076, IPS-85078, IPS-86672, and several footprints not recovered.

Description: Plantigrade to semiplantigrade pentadactyl footprints, all corresponding to manus impressions, except one digitigrade pes imprint, with three digits preserved (Fig. 6A, B). The manus ichnites are longer than wide. The digits are relatively long and slender, increasing in length from I to IV. Digit V is slightly shorter than digit II. Digits I to IV are curved inwards. Digit V is postero-laterally positioned, straight or curved outwards, and rotated outwards. Digit tips are pointed, indicating the presence of claws. The outer side of digit IV is characteristically sinuous. The heel impression is convex with a sharp angle. The palm is the deepest impressed part. The digits present a triangular shape, wider

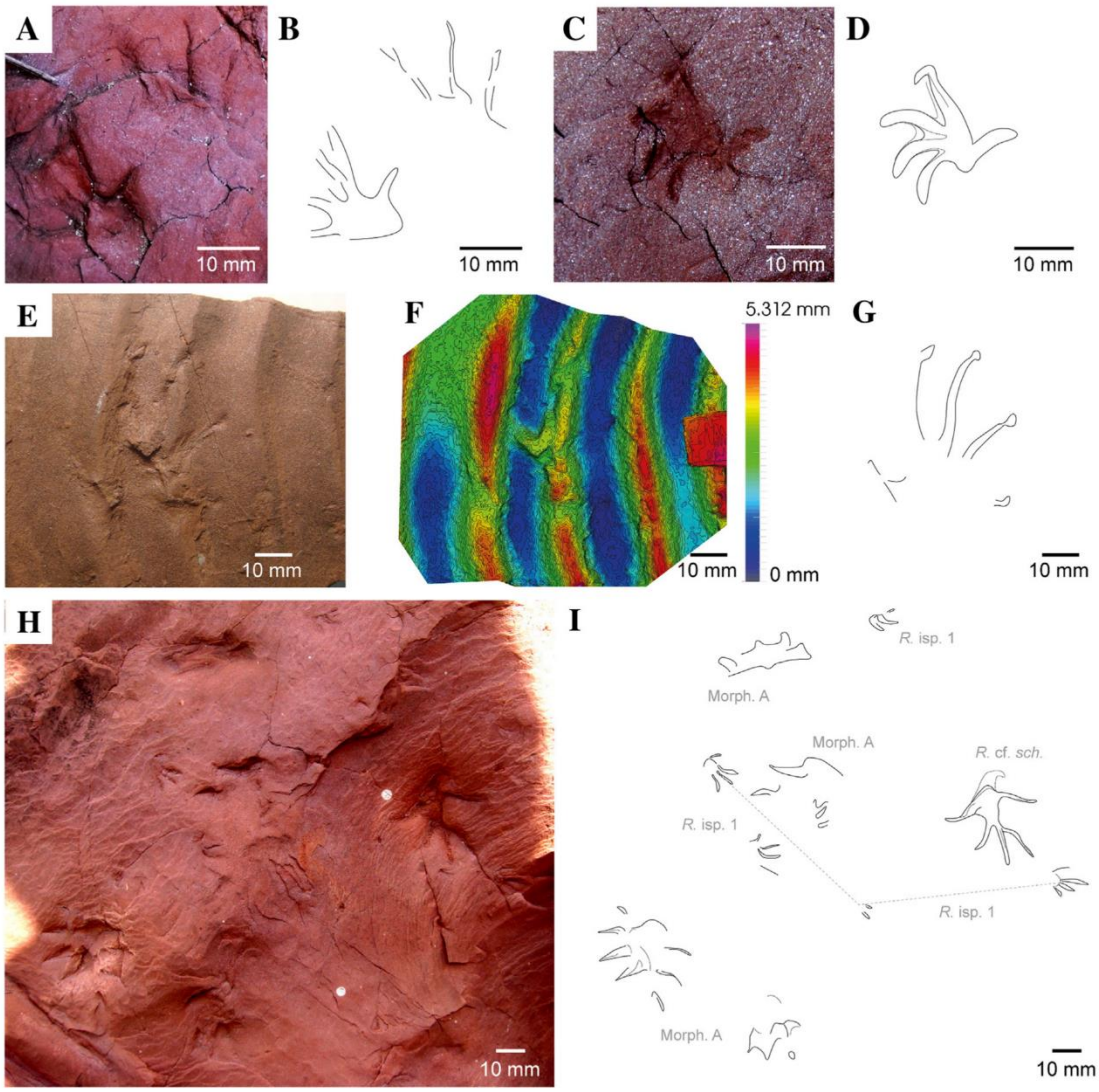

Fig. 6. A, B) *Rhynchosauroides* cf. *schochardti* manus–pes set. **C, D)** *R.* cf. *schochardti* manus and ichnite outline. **E–G)** *R.* cf. *schochardti* manus (IPS-86672), 3D model and ichnite outline. **H, I)** Mass occurrence of several ichnotaxa, including *R.* cf. *schochardti* (*R.* cf. *sch.*), *Rhynchosauroides* isp. 1 (*R.* isp. 1) and Morphotype A (Morph. A).

and deeper in the proximal part, with pointed tips. The angulation of digits I–II is higher than the other consecutive digit angulations. The tip of digit I is postero-medially directed.

Discussion: The angulation of digits I–IV, the shape of digits I and IV, the proportions and the shape of digit V, and the shape of the heel impression are characteristic of manus tracks of *Rhynchosauroides schochardti* (see Haubold, 1971a; Avanzini and Mietto, 2008; Klein and Lucas, 2010a). The specimens described here are smaller than those previously reported and, due to the lack of trackways (precluding the observation of some characters such as pace angulation, stride/body length rate, manus orientation in the trackway, and digits II–IV angle in pedes), we confer these ichnites to the ichnospecies *R. schochardti*. This ichnospecies is known from the late Early Triassic to the early Middle Triassic of Italy (Avanzini and Mietto, 2008; Avanzini et al., 2011), Germany (Haubold, 1971a), and the USA (Klein and Lucas, 2010a). Interestingly, Fortuny et al. (2010) described two footprints (Morphotype B) that are here assigned to this ichnospecies.

Ichnospecies *Rhynchosauroides* isp. indet. 1
Figs. 6H, I, 7

Material: IPS-82625, IPS-82626 (replicas with several ichnites), IPS-85050, IPS-85079.

Description: Plantigrade to semiplantigrade pentadactyl footprints. The ichnites are slightly longer than wide. The digits increase in length from I to IV, digit V is slightly shorter than the digit II. Digit V is straight, postero-laterally positioned and rotated outwards, separated from the other digits. Digits I to III are either rotated inwards or outwards, or straight. Digit IV is rotated outwards. The tips are the deepest impressed part of the digits, accentuated in digit I. The proximal part of the palm impression is diffuse. The trackway (Fig. 6H, I) is composed of three impressions, slightly rotated inwards. For one of them only two digits have been preserved. The trackway is relatively narrow with a pace of 28.5 mm, pace angulation of 131°, and a stride of 123.3 mm.

Discussion: The manus impressions are more common than the pes impressions within *Rhynchosauroides*, as they are usually more deeply impressed (e.g., Avanzini and Renesto, 2002; Valdiserri and Avanzini, 2007; Diedrich, 2008). Within trackways, the manus are parallel to the midline or rotated inwards, whereas the pedes are rotated outwards; thus all tracks herein described are attributed to manus impressions. The trackway presents the characteristic proportions (i.e., pace, pace angulation and stride) of all *Rhynchosauroides* ichnospecies (e.g., Haubold, 1971b; Avanzini and Renesto, 2002; Demathieu and Demathieu, 2004; Valdiserri and Avanzini, 2007; Diedrich, 2008; Gand et al., 2010). The scarcity of specimens presenting this morphology as well as the incompleteness of most of the tracks and the lack of manus–pes sets precludes the assignation of this material to any *Rhynchosauroides* ichnospecies.

Ichnospecies *Rhynchosauroides* isp. indet. 2
Fig. 8

Material: IPS-82624 (replica with several ichnites), IPS-85066, IPS-85075, IPS-85077.

Description: The manus tracks are plantigrade to digitigrade, elongated and pentadactyl. The digits increase in length from I to IV, digit V is slightly longer than digit I. Digits I to IV are curved inwards, and represent most of the length of the footprints. Digit V is straight and postero-laterally positioned, separated from the other digits. Digit I is represented by a shallow impression, often only observed in the 3D models, as well as digit V (Fig. 8A–F). Digit I is much shorter than digit II, which is similar in length to digit III. Digit I is in a more posterior position than digits II, III and IV. Digits II and III are nearly parallel. The digits of the specimens in Fig. 8A–C, G–H preserve phalangeal pads and claw impressions. The pes track is elongated, digitigrade, and pentadactyl. The digits increase in length from I to IV. Digit V, only preserved by the tip impression, is the shortest, and is rotated outwards. Digits I, II and III are nearly parallel. The pes impression (rotated outwards) is completely overstepping the manus impression (rotated inwards).

Discussion: The assignment of this morphotype is difficult due to the poor preservation of the tracks and the few specimens discovered (specimens in Fig. 8D–I correspond to undertracks). These tracks correspond to a different morphotype because they present particular characters (i.e., position of digit I in relation to digits II, III and IV, shape and orientation of digit V, digits angulations, and phalangeal pads) and all the footprints from this morphotype were found in the same facies as the other specimens attributed to *Rhynchosauroides*. The track shape of both manus and pes resemble those of *R. tirolicus* and *R. peabodyi*, but in these ichnospecies the pedes are often impressed much more anterior than the manus, and the manus and pedes cross axes within sets are nearly parallel (see Avanzini and Renesto, 2002; Diedrich, 2002, 2008).

Ichnospecies *Rhynchosauroides* isp. indet.
Fig. 9

Material: IPS-82627 (replica with several footprints), IPS-82628 (replica with several footprints), IPS-85052, several ichnites not recovered.

Description: Pentadactyl digitigrade footprints often with only three digits impressed. In the pentadactyl ichnites, the digits increase in length from I to IV, and digit V is similar in length to digit III. Digits I to IV are slender and slightly curved inwards. Digit V is rotated outwards and straight. The angulation of digits IV–V is about 90°. The footprints are relatively small, less than 10 mm in length (often of 4–5 mm length).

Discussion: These ichnites present the shape of the ichnogenus *Rhynchosauroides*, with the previously described diagnostic characters. However, the identification of the ichnospecies is not possible due to the lack of trackways and manus–pes sets. Similar specimens, also of unidentified ichnospecies, were reported by Haubold (1971b). Fortuny et al. (2010) also described footprints, named Morphotype A (not the same described below), with the same shape and in slightly lower stratigraphic levels. Nevertheless, the size of the ichnites and the angulation of digits IV–V are features not observed in the other *Rhynchosauroides* morphotypes herein reported. Moreover, these characters could also correspond to juvenile trackmakers. Therefore we assign these tracks to a different morphotype but not to a different ichnospecies, as they could be impressed by the same trackmakers of any other *Rhynchosauroides* morphotype herein described.

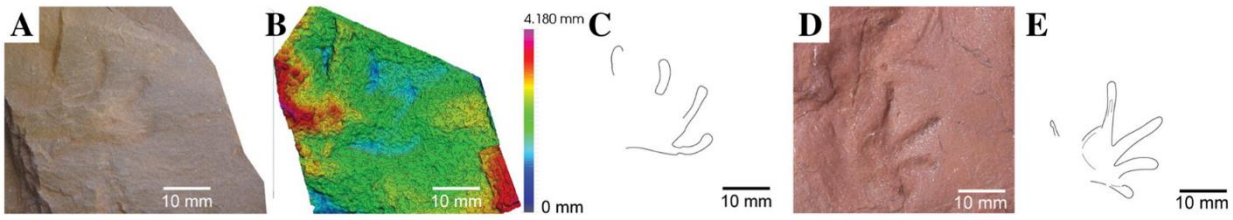

Fig. 7. *Rhynchosauroides* isp. 1. left manus tracks. **A-C)** Ichnite (IPS-85050) with the 3D model and outline drawing. **D, E)** Ichnite preserving the five digits, and outline drawing.

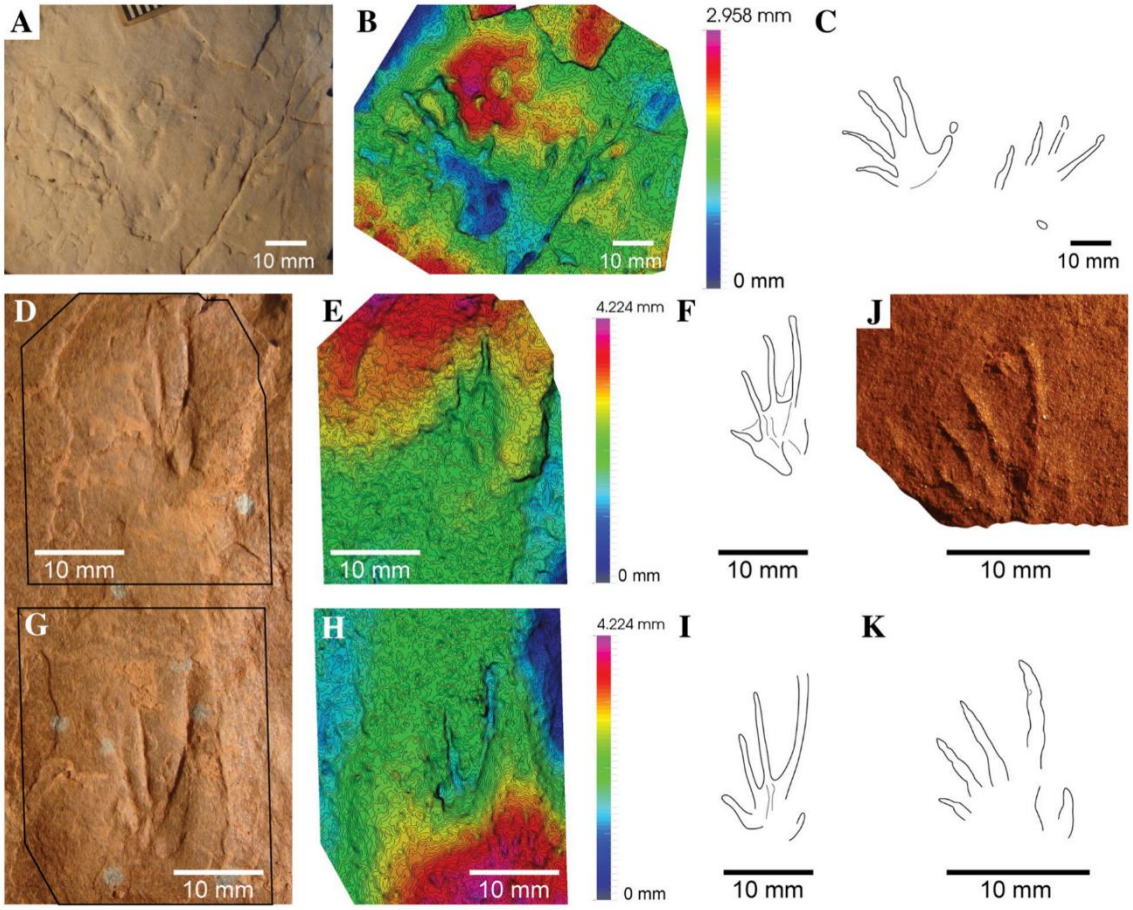

Fig. 8. *Rhynchosauroides* isp. 2. **A–C)** Large manus–pes set of the replica IPS-82624 with the corresponding 3D model and ichnites outline. **D–I)** IPS-85075, with the 3D models and ichnites outlines. **J, K)** Specimen IPS-85077 and ichnite outline.

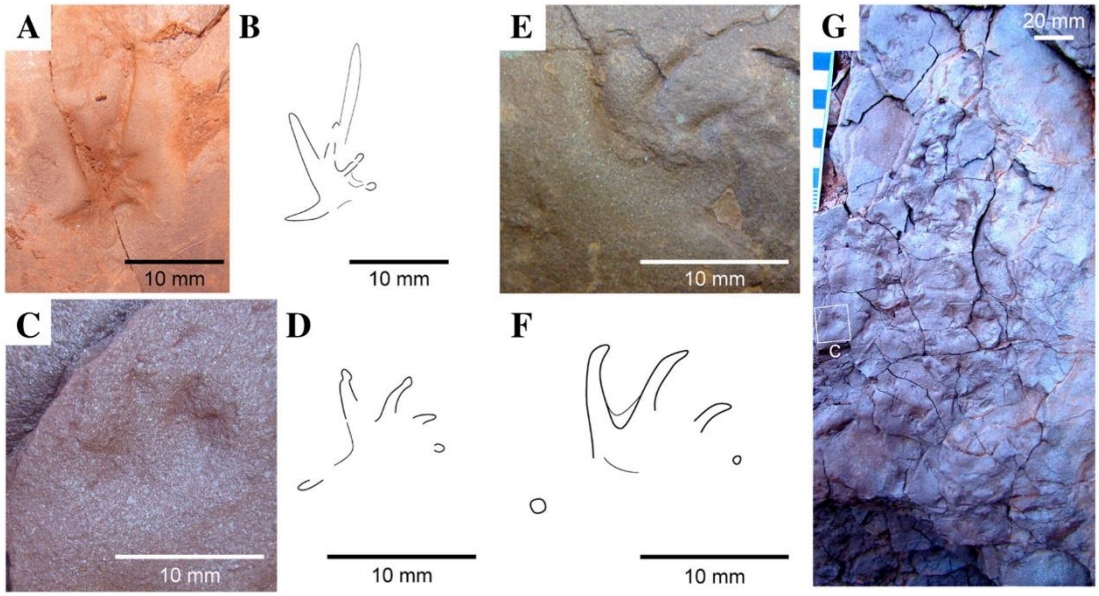

Fig. 9. *Rhynchosauroides* isp. indet. isolated tracks. **A–F)** Ichnites with the five digits impressed (E corresponds to IPS-85052). **G)** Mass occurrence of ichnites in a small very fine-grained surface.

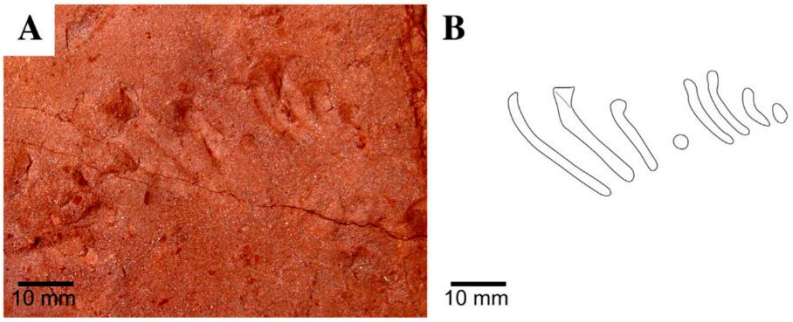

Fig. 10. A, B) *Prorotodactylus–Rotodactylus* manus–pes set with the ichnites outline.

Plexus *Prorotodactylus* Ptaszyński, 2000–*Rotodacytlus* Peabody, 1948
Fig. 10

Material: One manus–pes set not recovered.

Description: Both manus and pes tracks are digitigrade and preserve digits I, II, III and IV. The pes is larger than the manus and is antero-laterally overstepping it. The digits increase in length from I to IV in the pes track, whereas in the manus track, digit III is slightly longer than digit IV. Digit I in both manus and pes tracks is a rounded impression corresponding to the tip. Digits II, III and IV are relatively long, slender, with a slight inwards curvature accentuated on the tips. The angle of digits II–IV is low in the pes, whereas in the manus, digits II, III and IV are parallel.

Discussion: The digitigrady of the tracks, the overstepping pes to manus, the relative digits length, the shape of the digits and their angulation are diagnostic characters of both *Prorotodactylus* and *Rotodactylus* (e.g., Peabody, 1948; Ptaszyński, 2000; Brusatte et al., 2011; Klein and Niedźwiedzki, 2012; Fichter and Kunz, 2013; Niedźwiedzki et al., 2013). The main difference of these two ichnogenera is in digit V (Niedźwiedzki et al., 2013); in both, digit V is postero-laterally positioned but, in the manus tracks of *Rotodactylus*, it is usually completely rotated, whereas in *Prorotodactylus* it is just slightly rotated outwards (Ptaszyński, 2000; Brusatte et al., 2011; Klein and Niedźwiedzki, 2012; Fichter and Kunz, 2013; Niedźwiedzki et al., 2013). Otherwise, in the manus of *Prorotodactylus* and some ichnospecies of *Rotodactylus* digit III is the longest. The pes is overstepping the manus, but they are

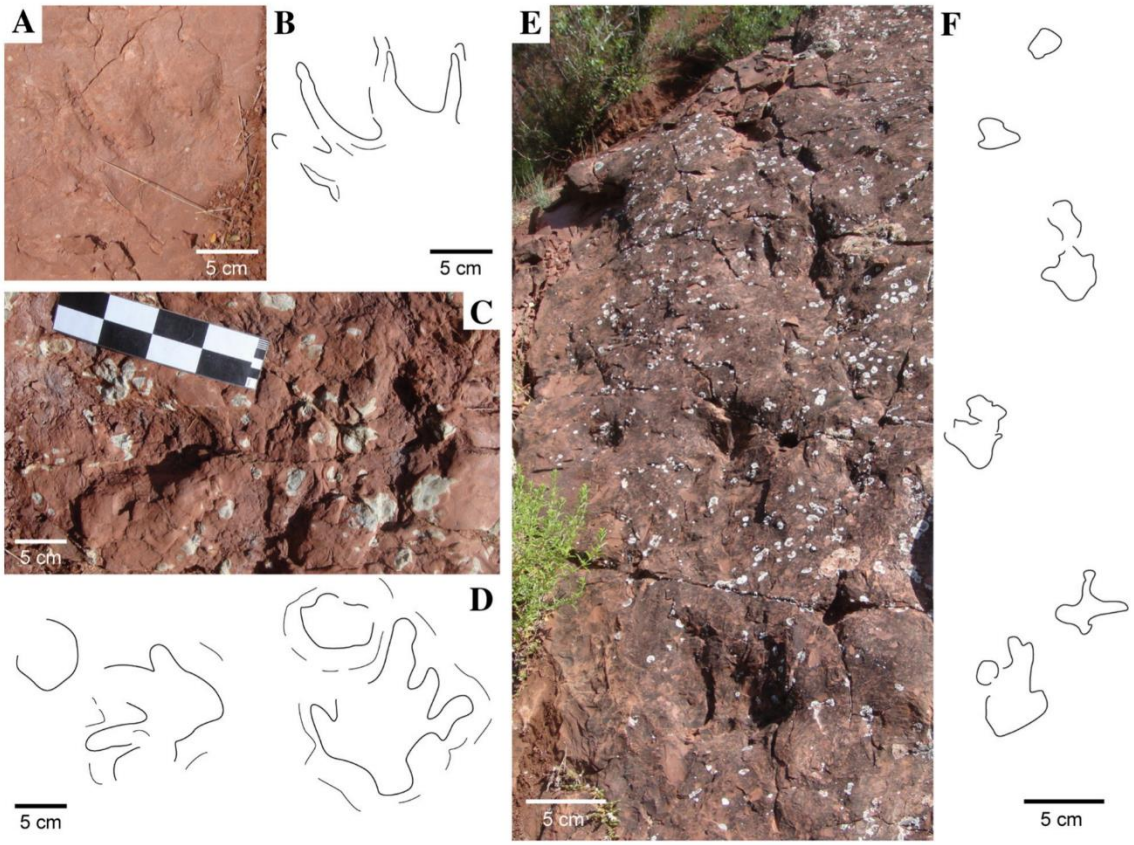

Fig. 11. Chirotheriid ichnites and the corresponding outline drawings. **A, B)** Isolated pes track. **C, D)** Isolated manus–pes sets. **E, F)** Possible trackway.

relatively close, being similar to *Prorotodactylus*, while in *Rotodactylus* the manus–pes distance is greater (see Niedźwiedzki et al., 2013 for a revision), so the relative track distances may suggest a closer resemblance to *Prorotodactylus*. In any case, the nomenclature for the Palanca de Noves ichnites remains open due to the scarcity of specimens and the lack of digit V impressions.

Chirotheriidae indet.
Fig. 11

Material: Two isolated footprints, two manus–pes sets and one trackway. Ichnites not recovered.

Description: Large (10–15 cm long) and deep impressions, with long, triangular, pointed digits. There are four impressions probably corresponding to two manus–pes sets. Manus tracks are just rounded impressions, partially overstepped by the larger pes tracks, which are longer than wide with robust digits. There are also five aligned impressions forming a trackway.

Discussion: The size of the footprints and the digit morphology observed resemble those of the ichnofamily Chirotheriidae (e.g., Haubold, 1971a, b). Fortuny et al. (2010) preliminarily reported a large footprint (Morphotype D). After the reexamination of the material, *Chirotherium* features have been observed. Thus the similarity in size with the herein reported ichnites is indicative of the presence of chirotheriid footprints in the Palanca de Noves site. Avanzini (2003) and Avanzini et al. (2011) reported tracks of *Chirotherium rex* from the early Anisian of northern Italy that present a similar shape and size to the Palanca de Noves tracks.

Morphotype A
Figs. 6H, I, 12, 13, 14

Material: IPS-82624, IPS-82625, IPS-82626 (replicas with several ichnites, including a trackway), IPS-85053, IPS-85064, IPS-85067 and several ichnites not recovered.

Description: The manus footprints are plantigrade to semiplantigrade, pentadactyl, and slightly longer than wide. The digits increase in length

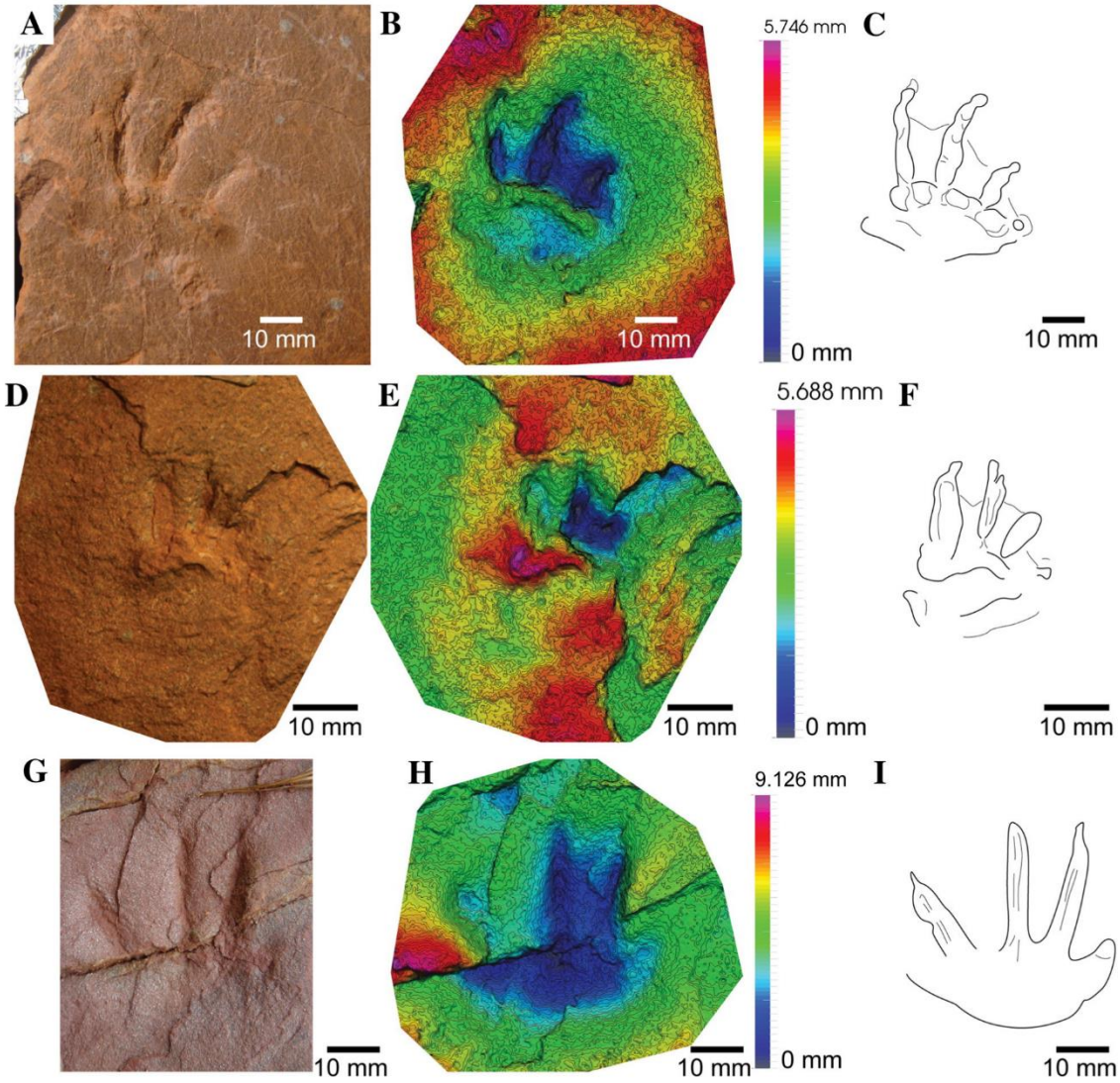

Fig. 12. Morphotype A, I. **A)** Left manus IPS-85064. **D)** Left manus IPS-85067. **G)** Right manus not recovered. **B, E, H)** 3D models. **C, F, I)** Ichnites outlines and corresponding outline drawings.

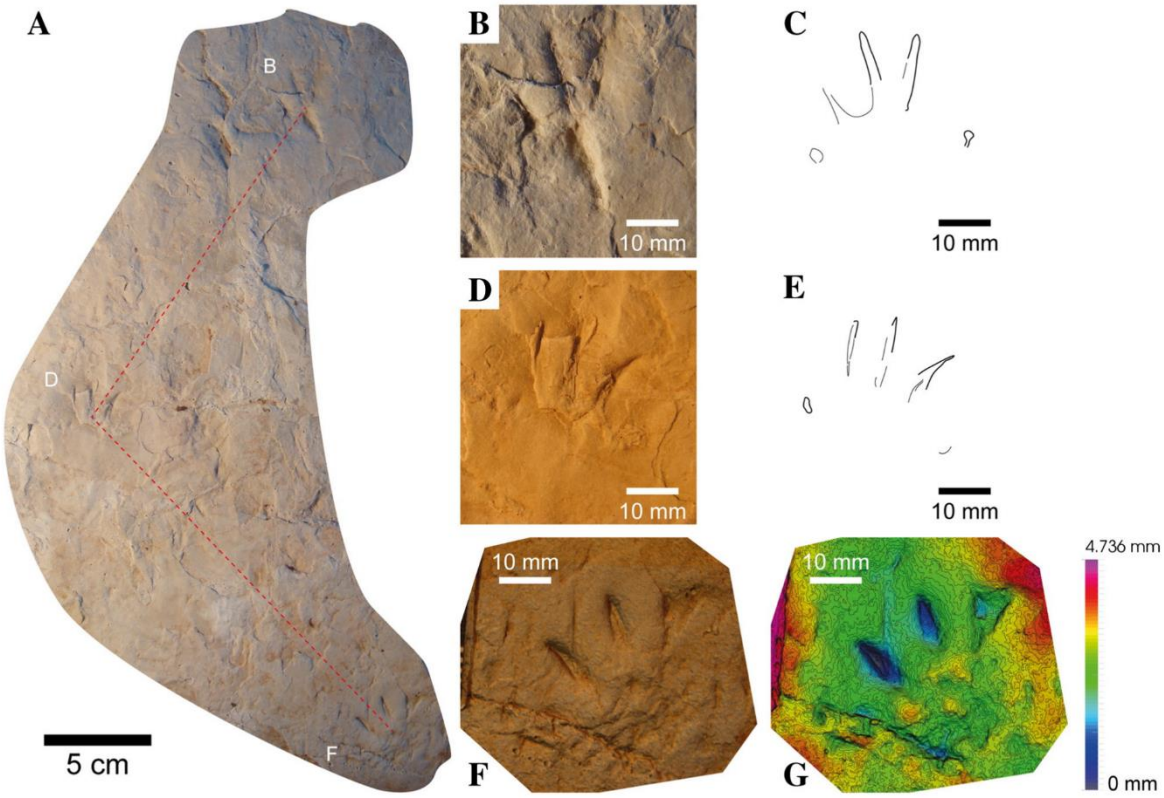

Fig. 13. Morphotype A, II. **A)** Trackway composed of three manus tracks. **B, D, F)** Detail of the footprints. **C, E, G)** Corresponding drawings and 3D model of B, D and F, respectively.

from I to III, digit IV is as long as digit III, or slightly shorter. The length of digit V is intermediate between the lengths of digits I and II. Digit I is preserved as a shallow rounded impression. Digits II, III and IV are slightly curved inwards, and present a triangular shape (wider on the proximal part) with clawed tips. Digits II and III are more separated than the digits III and IV. Digit V is separated from the other digits, and in a more postero-lateral position. Digit V is rotated outwards and curved towards the footprint cross axis (digit III axis). The palm impression is oval-shaped, wider below digits III and IV than below digits I and II. In some specimens, the palm is separated from digits II, III and IV by an edge, and in continuity with digits I and V. The base line of digits I to IV is perpendicular to the cross axis. Digits II and III are the deepest impressed followed by digit IV. The palm impression is deeper than digits I and V. Digits I and V are the shallowest impressed, in some cases not preserved. A low edge separating the pad impression of digit V from the palm is also observed (Figs. 12, 13). The posterior part of the palm impression is diffuse, steeper in the separating edge from digits II, III and IV. The digits represent about 2/3 of the length of the footprints (see Supplementary information). In the possible manus–pes set (Fig. 14A, B) the pes (rotated outwards) is overstepping the manus (rotated inwards), and is situated on the outer side of the midline, and laterally positioned. The pes footprint is digitigrade, preserving digits II, III and IV, which are subparallel and increasing in length. Digit IV is slightly curved inwards, more separated from digits II and III and much longer. The trackway (Fig. 13) is composed of three manus impressions, the coupled pedes are not preserved. The tracks are slightly rotated inwards. The low pace angulation (102.85°) indicates a sprawling gait for the trackmaker (see Supplementary information).

Discussion: The relative length of the digits, the fact that they are curved inwards, their clawed tips, the manus–pes proportions, the digitigrady of the pes related to the plantigrady of the manus, and the relative position of manus and pes are features of *Rhynchosauroides* described by Maidwell (1911), and also reported in Haubold (1966, 1971a, b). We should note that Klein and Niedźwiedzki (2012) reported several tracks assigned to *Rhynchosauroides* isp. that present general shape similarities to the tracks reported here (Klein and Niedźwiedzki, 2012: 48–49, Fig. 48). The Polish manus tracks also present a relatively short digit I and digit IV (the latter equal to digit III in length) and an elevated ridge separating the palm from digits II, III and IV, although in this case the ridge is not perpendicular to the axis of digit III as in the Pyrenean specimens. These authors noted the differences to other *Rhynchosauroides* species but due to preservational reasons a specific determination was not possible. Otherwise, the shape and the relative shortness of digit I, the relative length of digits III and IV, the shape of digit V, and the nearly parallel digits of the pes footprint are characters of the Early to Middle Triassic ichnogenera *Prorotodactylus* and *Rotodactylus*. However, they differ from them in the separation and angulation of digits II, III and IV, as well as in the manus width/length ratio and the low pace angulation of the trackway (see Brusatte et al., 2011; Klein and Niedźwiedzki, 2012; Niedźwiedzki et al., 2013 for a revision). Recently, Klein et al. (2015) revised the ichnogenus *Procolophonichnium*, with characters (relative length of digits III and IV, the tracks length/width ratio and divarication of digits I–IV) similar to those of the Pyrenean specimens. Despite that, the lack of more diagnostic features prevents the assignation to this ichnogenus.

The combination of the characters is indicative of a different morphotype from the previously mentioned ichnogenera. The differential features observed in these ichnites are all present in the manus impressions: (1) shape of the palm, (2) edge separating digits II, III and IV from the palm, (3) shape of digit V (curved inwards), and (4) length and depth of digits I and V (relatively short in comparison with digits II, III and IV, shallower than the palm impression). These characters are

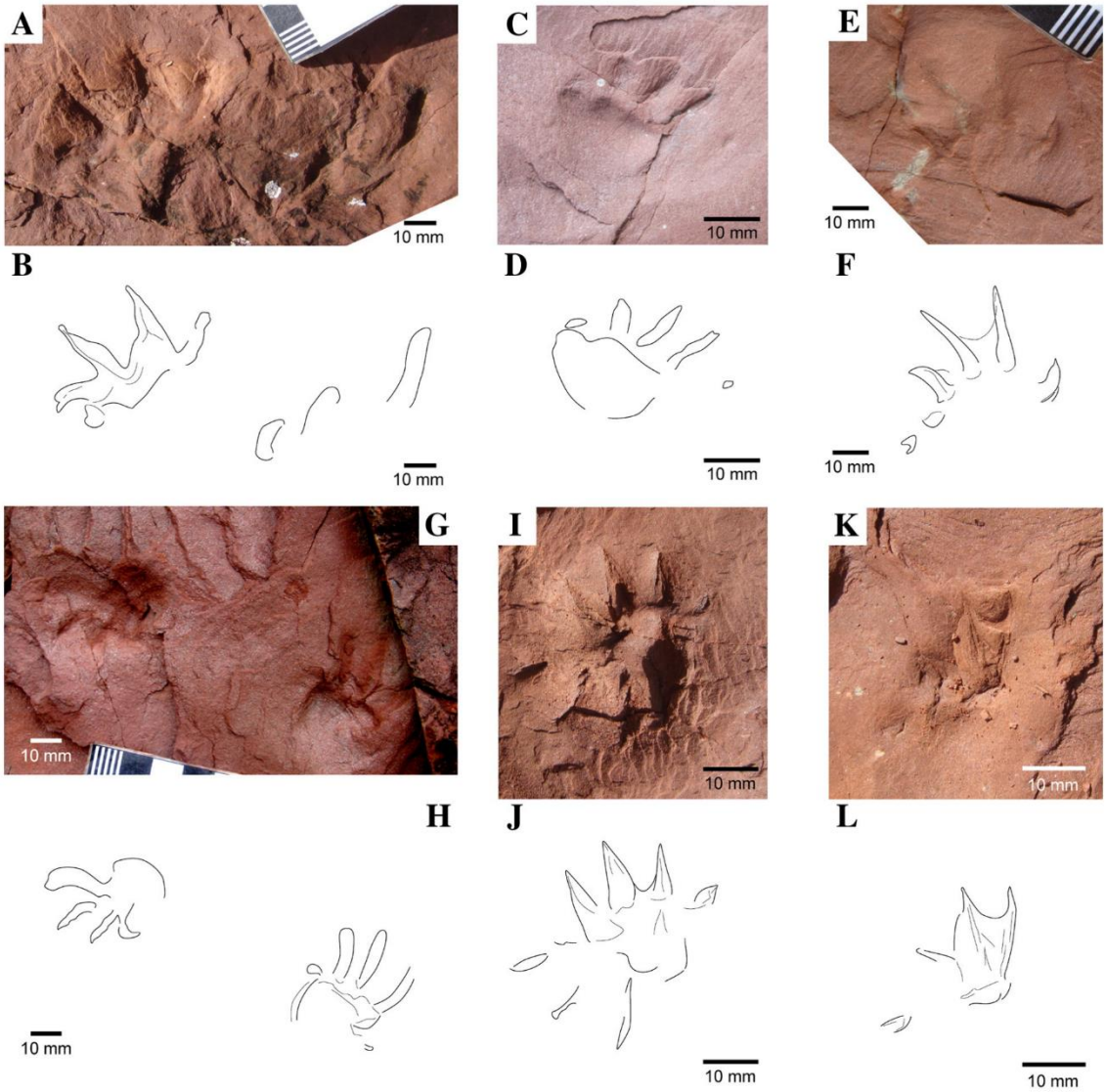

Fig. 14. Morphotype A, III. **A, B)** Possible manus–pes set. **C–L)** Isolated manus ichnites.

not observed among *Prorotodactylus*, *Rotodactylus* (see Peabody, 1948; Niedźwiedzki et al., 2013), and *Rhynchosauroides* (see Haubold, 1971a, b, 1984; Demathieu and Fichter, 1989; Fuglewicz et al., 1990; Ptaszyński, 2000; Diedrich, 2002, 2008, Gand et al., 2007, 2010; Valdiserri and Avanzini, 2007; Avanzini and Mietto, 2008; Klein and Lucas, 2010a; Avanzini et al., 2011; Klein et al., 2011; Krainer et al., 2012; Lovelace and Lovelace, 2012 for further comparisons). The separation of digit V from the palm, as well as the angulation of the base line with the cross axis are characters observed among chirotheriid ichnotaxa, and also in some specimens of *Prorotodactylus* (e.g., Klein

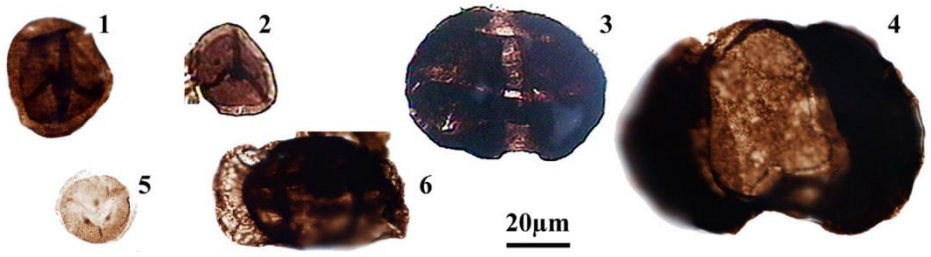

Fig. 15. Selected palynomorphs. All magnifications ×500. **1, 2**. *Densoisporites nejburgii* (Schulz) Balme 1970. **3.** *Lunatisporites albertae* (Jansonius) Fisher 1979. **4.** *Voltziaceaesporites heteromorpha* Klaus 1964. **5.** *Endosporites papillatus* Jansonius 1962. **6.** *Lunatisporites noviaulensis* (Leschik) Fisher 1979.

and Haubold, 2003; Niedźwiedzki et al., 2013). The relative length of digit III, slightly longer than digit IV, rejects the assignation to *Rhynchosauroides*, in which digit IV is always the longest. Therefore, we assign these ichnites to an undetermined morphotype (here Morphotype A), awaiting for further specimens and data to present a more confident diagnosis. The characters of these ichnites, together with the relatively low pace angulation, may be indicative of a potential non-archosaur archosauromorph trackmaker, although interpretations remain open.

4.3. Palynostratigraphy and age

The basal unit of the Buntsandstein facies of the Palanca de Noves section was assigned a Thuringian age (Middle–Late Permian) based on palynological data (Broutin et al., 1988; Diez, 2000; Diez et al., 2005). This temporal attribution was based on the abundance of common Permian miospores, although these authors already indicated the possibility of a more modern age based on the abundant presence of *Endosporites papillatus* and *Densoisporites nejburgii*. Our findings of different types of lycopod spores such as *Endosporites papillatus* and *Densoisporites nejburgii*, as well as other bisaccate pollen types such as *Voltziaceaesporites heteromorpha*, and various taeniate bisaccate pollens such as *Lunatisporites* or *Protohaploxipinus* (Fig. 15), allow to correlate this association with the Early Triassic levels described in Lucas (2010) and Kürschner and Herngreen (2010), and in particular with the *Densoisporites nejburgii* Zone of Orłowska-Zwolińska (1977, 1984) and the *nejburgii-heteromorphus* Phase (Brugman 1986), which correspond to an Early Triassic (late Olenekian) age.

5. Discussion

5.1. Vertebrate stratigraphy and age constraints

The presence of a caseid vertebra in La Trava indicates a minimum age of Middle Permian for the URU. This group of synapsids was relatively abundant during this time interval, although few specimens have been so far reported in Europe (e.g., Sigogneau-Russell and Russell,

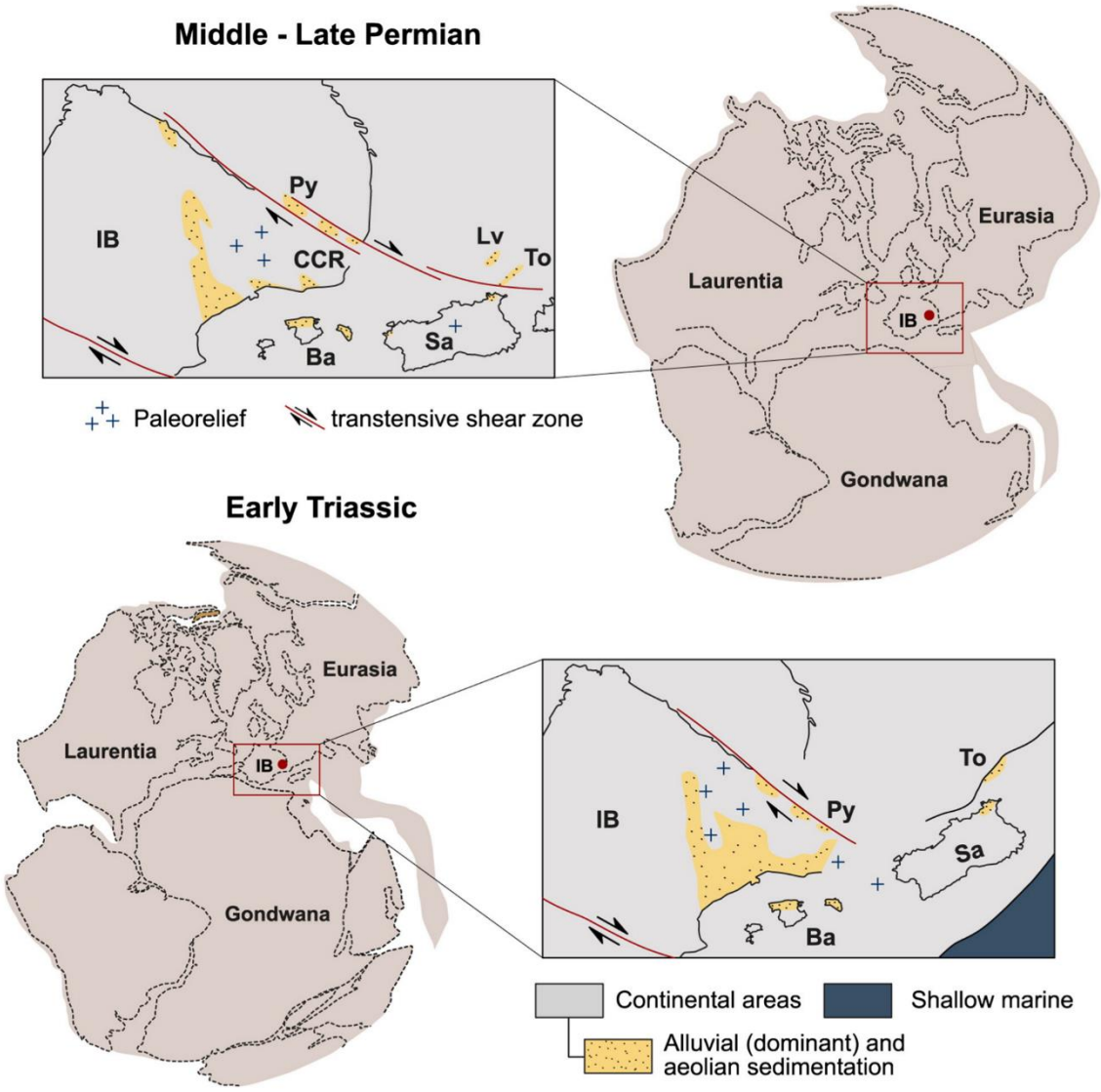

Fig. 16. Paleogeographic reconstructions for the Middle–Late Permian and the Early Triassic of the Iberian Plate. The paleogeographic sketches are slightly modified from Domeier et al. 2012. Ba: Balearic Islands. CCR: Catalan Coastal Ranges. IB: Iberian Plate. Lv: Lodève Basin. Py: Pyrenean Basin. Sa: Sardinia. To: Toulon-Cuers Basin.

1974; Wernerburg et al., 2007; Reisz et al., 2011; Ronchi et al., 2011; Romano and Nicosia, 2014). As a matter of fact, some of them have been poorly dated, especially *Euromycter* and *Ruthenosaurus*, from the Rodez Basin (France), whose ages range from the late Early to the early Late Permian (Reisz et al., 2011). The age of the *Cotylorhynchus* found in the Lodève Basin was until recently considered as Late Permian (Schneider et al., 2006), but the combination of new chronostratigraphic and magnetostratigraphic data on such Permian sequence (Evans, 2012; Evans et al., 2014; Michel et al., 2015) shows that the La Lieude Member was deposited from the Roadian to the Wordian, before the occurrence of the geomagnetic Illawarra Reversal event (i.e., middle Wordian according to Henderson et al., 2012). Regarding *Ennatosaurus tecton* itself, the Russian material has been recovered in the Mezen region from the Nijneoustinskaia and the Krasnoshelskaia formations (Ivakhnenko, 2008; Maddin et al., 2008), which are currently dated as Urzhumian and precede the Illawarra Reversal too (Gorsky et al., 2003). Since then, the regional stage Urzhumian has been correlated with the Wordian (Henderson et al., 2012), hence allowing the assignment of an early Wordian age to the Russian *Ennatosaurus tecton*. This age agrees with the supposed age of the other late European and North American caseids. At this point, the portion of the URU from which the vertebra IPS-87365 has been collected is tentatively assigned to the Middle Permian (possibly Wordian). Robles and Llompart (1987) reported large tetrapod footprints from the URU, which are similar to the well-known tracks of the Middle–Late Permian sites from La Lieude Member of the French Lodève Basin (Gand et al., 2000; Gand and Durand, 2006; see also Section 5.2 below), the Italian Southern Alps (Valentini et al., 2009), and the Cis-Urals region of European Russia (Surkov et al., 2007). Therefore, the inferred age for the footprints of Robles and Llompart (1987) is in agreement with that for the vertebra. Thus, awaiting further studies, we assign the latest part of the URU to, at least, the Middle Permian.

The other bones and ichnites from the Palanca de Noves site are 50 meters above the basal conglomerates of the Buntsandstein facies, which represent the beginning of the Triassic record. Previously, Fortuny et al. (2010) preliminary identified four ichnomorphotypes, erroneously considered as Late Permian following Robles and Llompart (1987), but corresponding to the Triassic record after the present study. The bones of Palanca de Noves are the first body fossil remains from the Buntsandstein of the Pyrenees. Until now, the nearest site with bone remains corresponded to the Middle Triassic of the Montseny area (Fortuny et al., 2011a, b) and Riera de Sant Jaume (Fortuny et al., 2011a), both in the Catalan Coastal Ranges (Catalan Basin).

Regarding the tetrapod ichnites, the stratigraphic range for *Rhynchosauroides* is assumed to span the Middle and Late Permian, the entire Triassic, and the Early Jurassic (Olsen et al., 2002; Gand and Durand; 2006; Klein and Lucas, 2010b), but the presence of potential *Rhynchosauroides* cf. *schochardti* suggests a late Early Triassic–early Middle Triassic age (e.g., Haubold, 1971a, b; Avanzini and Mietto, 2008; Klein and Lucas, 2010a). Chirotheriid tracks, as well as *Prorotodactylus* and *Rotodactylus*, have also been largely described in Early–Middle Triassic deposits (e.g., Peabody, 1948; Gand and Demathieu, 2005; Niedźwiedzki and Ptaszyński, 2007; Avanzini and Mietto, 2008; Klein and Lucas, 2010a, b; Tourani et al., 2010; Avanzini et al., 2011; Klein and Niedźwiedzki, 2012; Niedźwiedzki et al., 2013). Therefore, we propose that the age interval of the studied ichnoassemblage is late Early Triassic–early Middle Triassic, in concordance with the palynological results.

5.2. Environmental implications of the tetrapod remains

5.2.1. Permian tetrapods

In the URU from the Palanca de Noves site, 116 m below the Triassic unconformity, Robles and Llompart (1987) identified two tetrapod footprint morphotypes tentatively attributed to temnospondyl producers. Nevertheless, the forms described by these authors are more similar to the therapsid and caseid footprints of the La Lieude Member (French Lodève Basin) described by Gand et al. (2000) and by Gand and Durand (2006). Unfortunately, due to the loss of the Pyrenean footprints, the lack of data and the preservation, the ichnotaxa identification remains uncertain, although they could be equivalent to those of La Lieude Member. The Pyrenean footprints were preserved in a laminated mudstone sequence, with abundant mudcracks, interpreted as crevasse deposits from the distal parts of alluvial fans, corresponding to a general playa-lake setting (Robles and Llompart, 1987)—the same paleoenvironment interpreted for the deposits bearing the caseid vertebra. The inferred paleoenvironments for the URU (see also Gretter et al., 2015) are similar to those of the La Lieude Member, in the French Lodève Basin (Korner et al., 2003; Schneider et al., 2006; Lopez et al., 2008; Pochat and Van Den Driessche, 2011). Therefore, the paleoenvironmental conditions of the URU, as well as the faunal assemblage could be similar to that of the Salagou Formation, indicating a possible connection.

5.2.2. Triassic tetrapods

The relative diversity of fauna, based on the presence of several ichnotaxa, is indicative of (1) recovery signals after mass extinction, with a lepidosauromorph/ archosauromorph-dominated fauna, and (2) an initial gap on the fossil record, also indicated by the hiatus encompassing the earliest Triassic record of the Western Tethys (e.g., Cassinis et al., 2007; Linol et al., 2009; López-Gómez et al., 2010, 2012; Bourquin et al., 2007, 2011; Fortuny et al., 2011a; Galán-Abellán et al., 2013; Baucon et al., 2014; Gretter et al., 2015; Borruel-Abadía et al., 2015). In the same way, in the Palanca de Noves sequence there are about 30 m of stratigraphic record without fossils, corresponding to the basal conglomerates and associated coarse-grained deposits (Figs. 1C, 2, 4A, B).

The environmental setting was not restrictive for faunal distribution. The footprints attributed to *Rhynchosauroides* cf. *schochardti*, *R.* isp. 1, *R.* isp. 2, the *Prorotodactylus–Rotodactylus* plexus, the chirotheriid and the Morphotype A tracks are found in the same facies, composed of fine to very fine sandstone with abundant detrital micaceous minerals and a mudstone-texture matrix. Sedimentary structures, such as current ripples, wave ripples and climbing ripples are common. Our results reveal that strata are thin, and of little lateral continuity, surrounded by red mudstone floodplain deposits. These deposits are interpreted as crevasse splay deposits derived from meandering river channels (see also Gretter et al., 2015). The footprints assigned to the smallest *Rhynchosauroides* morphotype (Fig. 9) are preserved in finer facies (very fine sandstone-mudstone), where no other footprints are preserved. This is probably due to a taphonomic bias, as larger footprints could not be well-preserved in these deposits. Otherwise, the smallest *Rhynchosauroides* could not be preserved in the other facies because of the coarseness of the grain size.

The bone remains found in the Triassic sequence may correspond to stereospondyls or archosauromorphs, but no footprint evidence regarding the former has been found. It indicates that these animals may have lived, and died, in highly energetic flowing water channels, with rough substrates, composed of large pebbles, in which footprints have a low preservational potential.

5.3. Paleobiogeography of the Permian–Triassic Pyrenean succession

The Permian–Triassic Pyrenean basins were placed on the Western Tethys region (e.g., Dercourt et al., 2000; Cassinis et al., 2012; Domeier et al., 2012; Gretter et al., 2015; Fig. 16), a key zone for the understanding of tetrapod paleobiogeography, as well as the Permian–Triassic transition. In the nearby Permian basins of the Western Tethys, such as those from the Moroccan Argana Basin (e.g., Voigt et al., 2010), the French Lodève and Rodez basins (Gand et al., 2000; Gand and Durand, 2006; Reisz et al., 2011), the Spanish Cantabrian Basin (Demathieu et al., 2008), Sardinia (Ronchi et al., 2011) and the Italian Alps (Valentini et al., 2009; Avanzini et al., 2011), as well as in the Russian

Platform (Surkov et al., 2007), large faunas similar to those of the Pyrenees (i.e., the caseid vertebra and the footprints reported by Robles and Llompart, 1987) are known. Therefore, these findings suggest a widespread distribution of large synapsids and parareptiles during the Middle–?Late Permian. Considering the similar stratigraphic patterns and fossil distributions of the URU with the La Lieude Member of the Lodève Basin (see Schneider et al., 2006 and Lopez et al., 2008 in comparison with Robles and Llompart, 1987 and Gretter et al., 2015), a tentative connection or direct correlation of the Pyrenean and Lodève basins is inferred. Further findings and studies will shed light on the ichnoassemblage and the possible faunal exchanges with other Permian basins. Interestingly, an ichnofaunal turnover from the LRU (see Mujal et al., in press) to the URU is observed, as occurs in the Permian basins mentioned above, and probably related to the Early–Middle Permian extinction event (e.g., Sahney and Benton, 2008). Further works in progress on the Catalan Pyrenees will focus on this transition.

In the Triassic sequence studied, the footprints of small- to medium-size faunas dominate, whereas the chirotheriid ichnites are scarce and always poorly preserved. In contrast, the chirotheriid record of the Iberian Peninsula was until now only represented in the Middle Triassic, with well-preserved and abundant specimens (Calzada, 1987; Gand et al., 2010; Fortuny et al., 2011a; Díaz-Martínez and Pérez-García, 2012; Díaz-Martínez et al., 2015; Mujal et al., 2015). Thus the faunal composition of the Early Triassic of the Pyrenees differs from that of the Permian and Middle Triassic. The studied succession records a drastic faunal change, from large Permian synapsids and parareptiles to small-sized lepidosauromorphs and archosauromorphs. This is indicative of the faunal turnover after the end-Permian mass extinction, and the Triassic onset of ecosystems recovery (e.g., Benton et al., 2004; Sahney and Benton, 2008; Benton and Newell, 2014).

The Lower Triassic vertebrate record of the Western Tethys (all of late Early Triassic age) is scarce and limited to *Rhynchosauroides* footprints from the Italian Southern Alps (Avanzini et al., 2011), the chirotheriid-dominated ichnoassemblage of the Moroccan Argana Basin (Klein et al., 2010; Tourani et al., 2010), and the early Olenekian chirotheriid-dominated ichnoassemblage of southern Austria (Krainer et al., 2012). In the southern French basins there are no well-dated fossil remains of the Early Triassic, and the tetrapod record is mostly of Middle and Late Triassic age (Gand et al., 2007). Therefore, the Triassic Palanca de Noves ichnoassemblage is the most complete reported until now in the Western Tethys region, and the oldest reported from the Iberian Peninsula. The Pyrenean ichnoassemblage is dominated by *Rhynchosauroides* forms, which could represent the survivors of the end-Permian mass extinction, as also pointed out by Avanzini et al. (2011) in the Southern Alps. The *Rhynchosauroides* trackmakers are likely to belong to an opportunistic group associated to the main faunal recovery population. As stated by López-Gómez et al. (2012), the first signals of biotic recovery in the Iberian domain (mainly represented by root traces, bioturbations, and scarce tetrapod footprints) occurred 5 Ma after the mass extinction, but these authors considered that the diversification happened 1 Ma later, during the early Anisian (Middle Triassic; see also Béthoux et al., 2009; Gand et al., 2010; Galán-Abellán, 2011). Interestingly, the Palanca de Noves locality yields a relatively diverse biotic record, thus indicating that the recovery delay was not so prolonged, and that the initial recovery was prior to the present fossil record. This is in accordance with the suggested widespread terrestrial tetrapod distribution among Pangea (e.g., Sahney and Benton, 2008; Klein and Niedźwiedzki, 2012; Benton and Newell, 2014), so that the tetrapod (ichno-) faunal homogeneity may only be in a globally uniform recovery dominated by small- to middle-sized organisms. On the contrary, Sidor et al. (2013) pointed out a potential provincialization of the faunas throughout the end-Permian event.

The distribution of both the Triassic ichnofauna and the Buntsandstein facies, suggest a global scenario, where physical barriers within Pangea disappeared. The widespread extension at the end of the Variscan cycle, related to the breakup of Pangea (e.g., Torsvick and Cocks, 2013; Gretter et al., 2015) would have erased the topographic barriers of the Variscan chain, thus enhancing faunal connectivity (Fig. 16). Therefore, the breakup of Pangea would have triggered the global distribution of fauna. Nevertheless, following Sidor et al. (2013), other distribution constrictions such as climatic biomes and variations (e.g., Chumakov and Zharkov, 2003; Borruel-Abadía et al., 2015) should be investigated, as has been suggested for the Early and Late Permian (see Mujal et al., in press; Sidor et al., 2005, respectively). Thus, at the present state of knowledge, both global and endemics fauna should be considered. Further studies and interbasinal correlations will shed light on the evolution of paleobiogeographic patterns between the Permian and Triassic periods and its relation with the end-Permian extinction event.

6. Conclusions

The new findings in the Catalan Pyrenees provide new insights into the Permian–Triassic transition helping to constrain the boundary between these periods despite the existing long gap in the record. On the one hand, a large caseid vertebra represents the youngest tetrapod remains recovered in the Permian of the Iberian Peninsula. This vertebrate remain also permits to assign for the first time a ?Middle Permian age (possibly Wordian) to the Upper Red Unit of the Pyrenean succession. On the other hand, the ichnological and osteological recoveries provide the oldest Triassic vertebrate records from the Iberian Peninsula, confirmed by the palynological assemblage of late Olenekian age found in the lower part of the Buntsandstein facies. The Triassic ichnoassociation is dominated by small to medium archosauromorph and lepidosauromorph footprints (*Rhynchosauroides* cf. *schochardti*, *R.* isp. 1 and 2, *Prorotodactylus–Rotodactylus*, and Morphotype A). Archosaurian (chirotheriid) tracks, as well as either stereospondyl or archosauromorph bone fragments are also present, but scarce.

Our results show that the Permian URU paleoenvironment associated with the tetrapod remains corresponds to a playa-lake setting with low influence of fluvial water channels, indicative of the distal parts of alluvial fans. This paleoenvironment, as well as the corresponding faunas, drastically changed towards the Triassic period. The Buntsandstein facies correspond to complex alluvial fan systems. Therefore, the paleoenvironment is dominated by high energy channels containing bones and crevasse splay deposits, with the tetrapod footprints preserved in the quietest zones.

Globally, the Permian paleontological and sedimentological record presents similarities with those of the nearby Western Tethys basins. In the same way, the Lower Triassic of the Pyrenees can be tentatively correlated with that of Morocco, the Italian Southern Alps, and possibly extended to central Europe (e.g., Germany and Poland). This widespread distribution of the Triassic faunal ichnoassemblages may be related to the breakup of Pangea that would have led to a uniform recovery. Nevertheless, climatic controls on faunal distribution and the resulting increasing endemism should also be considered.

Since the contact between the Permian and Triassic rocks is represented by a deeply-erosive angular unconformity, a large time gap could be expected. The Middle Permian and Early Triassic ages obtained from the osteological and palynological records respectively, demonstrate that the time gap was prolonged for about 15–19 Ma. This hiatus implies that the Permian–Triassic boundary is not recorded in the studied localities of the Catalan Pyrenees. Moreover, even if a global faunal distribution in both Permian and Triassic periods is observed, the completely different paleoenvironments and faunas of the URU and the Buntsandstein facies are in agreement with a Permian–Triassic ecosystem turnover. The Pyrenean Triassic remains could represent some of the oldest record of the Western Tethys, and provide a clue to understand the recovery of continental fauna after the Permian–Triassic crisis.

Acknowledgments

Our special thanks go to Isabel Vila, Albert Garcia-Sellés and Ruben Garcia-Artigas for their help in the fieldwork tasks. We acknowledge Renaud Vacant (CNRS at the MNHN) for lab works. We thank Sharley Wilson and Judit Marigó for their kind revision of the English. E. Mujal and J. Fortuny received funding from the SYNTHESYS Project http://www.synthesys.info/ (DE-TAF-2560, FR-TAF-3621, FR-TAF-4808 to E. Mujal and FR-TAF-435 and FR-TAF-3353 to J. Fortuny) which is financed by European Community Research Infrastructure Action under the FP7 "Capacities" Program. E. Mujal acknowledges "Secretaria d'Universitats i de Recerca del Departament d'Economia i Coneixement de la Generalitat de Catalunya" (E.M., expedient number 2013 CTP 00013, at ISE-M, Université Montpellier-2) for funding used for visiting collections. E. Mujal obtained financial support from the PIF grant of the Geology Department at UAB. A. Arche, J. Barrenechea, R. De la Horra, J.B. Diez and J. López-Gómez received support from the CGL2011-24408 and CGL2014-52699 research projects of the Spanish Ministerio de Economía y Competitividad. This paper is also a contribution to the following research projects: "Sistemas Sedimentarios y Variabilidad Climática" (642853) of the CSIC, and Basin Analysis (910429), and Palaeoclimatology and Global Change (910198) of the Universidad Complutense de Madrid. J. Fortuny acknowledges the support of the Generalitat de Catalunya postdoc grant 2014 – BP-A 00048. Fieldwork campaigns have been developed under the projects "Vertebrats del Permià i el Triàsic de Catalunya i el seu context geològic" and "Evolució dels ecosistemes amb faunes de vertebrats del Permià i el Triàsic de Catalunya" (ref. 2014/100606), based by the Institut Català de Paleontologia and carried out thanks to the financial support of the Departament de Cultura (Generalitat de Catalunya). We acknowledge the company Knauf GmbH, and particularly Manuel Juan Fidalgo, who defrayed the fieldwork during the road construction at Palanca de Noves. Finally, we acknowledge four anonymous reviewers and the editor, Prof. Thomas Algeo for helpful and constructive comments on a previous version of the manuscript.

Appendix A. Supplementary data

Supplementary data to this article can be found online at http://dx.doi.org/10.1016/j.palaeo.2015.12.008.

References

Álvarez-Ramis, C., Doubinger, J., Diéguez Jiménez, M.C., 1971. Estudio paleobotánico de la flora de Ogassa (Gerona). Estud. Geol. XXVII, 267–277.
Ashauer, H., 1934. Die östliche endigung der Pyrenäen. Abh. Ges. Wiss. Goettingen, Math.-Phys. Kl. 3 (Heft 10), 2–115.
Avanzini, M., 2003. Tetrapod footprints from the Mesozoic carbonate platforms of the Italian Alps. Zubía 21, 175–186.
Avanzini, M., Bernardi, M., Nicosia, U., 2011. The Permo-Triassic tetrapod faunal diversity in the Italian Southern Alps. In: Dar, I.A. (Ed.), Earth and Environmental Sciences. InTech, pp. 591–608.
Avanzini, M., Mietto, P., 2008. Lower and Middle Triassic footprint-based biochronology in the Italian Southern Alps. Oryctos 8, 3–13.
Avanzini, M., Renesto, S., 2002. A review of *Rhynchosauroides tirolicus* Abel, 1926 ichnospecies (Middle Triassic: Anisian–Ladinian) and some inferences on *Rhynchosauroides* trackmaker. Riv. Ital. Paleontol. Stratigr. 108 (1), 51–66.
Balme, B.E., 1970. Palynology of Permian and Triassic strata in the Salt Range and Surghar Range, West Pakistan. In: Kummel, B, Teichert, C (Eds.), Stratigraphic Boundary Problems: Permian and Triassic of West Pakistan. University Press of Kansas, Department of Geology Special Publication 4, 305–453.
Baucon, A., Ronchi, A., Felletti, F., Neto de Carvalho, C., 2014. Evolution of Crustaceans at the edge of the end-Permian crisis: ichnonetwork analysis of the fluvial succession of Nurra (Permian–Triassic, Sardinia, Italy). Palaeogeogr. Palaeoclimatol. Palaeoecol. 410, 74–103.
Benton, M.J., Newell, A.J., 2014. Impacts of global warming on Permo-Triassic terrestrial ecosystems. Gondwana Res. 25, 1308–1337.
Benton, M.J., Newell, A.J., Khlyupin, A.Y., Shumov, I.S., Price, G.D., Kurkin, A.A., 2012. Preservation of exceptional vertebrate assemblages in Middle Permian fluviolacustrine mudstones of Kotel'nich, Russia: stratigraphy, sedimentology, and taphonomy. Palaeogeogr. Palaeoclimatol. Palaeoecol. 319-320, 58–83.
Benton, M.J., Tverdokhlebov, V.P., Surkov, M.V., 2004. Ecosystem remodelling among vertebrates at the Permian–Triassic boundary in Russia. Nature 432, 97–100.
Benton, M.J., Twitchett, R.J., 2003. How to kill (almost) all life: the end-Permian extinction event. Trends Ecol. Evol. 18, 358–365.
Bernardi, M., Klein, H., Petti, F.M., Ezcurra, M.D., 2015. The origin and early radiation of Archosauriforms: integrating the skeletal and footprint record. PLoS ONE 10 (6), e0128449 28 p.
Bertling, M., Braddy, S.J., Bromley, R.G., Demathieu, D.R., Genise, J., Mikuláš, R., Nielsen, J.K., Nielsen, K.S.S., Rindsberg, A.K., Schlirf, M., Uchman, A., 2006. Names for trace fossils: a uniform approach. Lethaia 39, 265–286.
Béthoux, O., De La Horra, R., Benito, M.B., Barrenechea, J.F., Galán-Abellán, B., López-Gómez, J., 2009. A new triadotypomorphan insect from the Anisian (Middle Triassic), Buntsandsteinfacies, Spain. J. Iber. Geol. 35 (2), 179–184.
Bixel, F., Lucas, C., 1983. Magmatisme, tectonique et sédimentation dans les fossés stéphano-permiens des Pyrénées occidentales. Rev. Géogr. Phys. Géol. Dyn. 24, 329–342.
Borruel-Abadía, V., López-Gómez, J., De la Horra, R., Galán-Abellán, B., Barrenechea, J.F., Arche, A., Ronchi, A., Gretter, N., Marzo, M., 2015. Climate changes during the Early–Middle Triassic transition in the E. Iberian plate and their palaeogeographic significance in the western Tethys continental domain. Palaeogeogr. Palaeoclimatol. Palaeoecol. 440, 671–689.
Bourquin, S., Durand, M., Diez, J.B., Broutin, J., Fluteau, F., 2007. The Permian–Triassic boundary and lower Triassic sedimentation in western European basins: an overview. J. Iber. Geol. 33 (2), 221–236.
Bourquin, S., Bercovici, A., López-Gómez, J., Diez, J.B., Broutin, J., Ronchi, A., Durand, M., Arche, A., Linol, B., Amour, F., 2011. The Permian–Triassic transition and the onset of Mesozoic sedimentation at the northwestern peri-Tethyan domain scale: palaeogeographic maps and geodynamic implications. Palaeogeogr. Palaeoclimatol. Palaeoecol. 299, 265–280.
Bowring, S.A., Erwin, D.H., Jin, Y.G., Matin, M.W., Davidek, K., Wang, W., 1998. U–Pb zircon geochronology and tempo of the end-Permian mass extinction. Science 280, 1039–1045.
Broutin, J., Cabanis, B., Chateauneuf, J.J., Deroin, J.P., 1994. Évolution biostratigraphique magmatique et tectonique du domaine paléotéthysien occidental (SW de l'Europe): implications paléogéographiques au Permien inférieur. Bull. Soc. Geol. Fr. 165, 163–179.
Broutin, J., Doubinger, J., Gisbert, J., Satta-Pasini, S., 1988. Premières datations palynologiques dans le faciès Buntsandstein des Pyrénées catalanes espagnoles. C. R. Acad. Sci. 2 (306), 159–163.
Broutin, J., Gisbert, J., 1985. Entorno paleoclimático y ambiental de la flora stephano-autuniense del Pirineo catalán. Compte Rendu du 10e Congrès International de Stratigraphie et de Géologie du Carbonifère, Madrid 3, pp. 53–66.
Brugman, W.A., 1986. A Palynological Characterization of the Upper Scythian and Anisian of the Transdanubian Central Range (Hungary) and the Vincentinian Alps (Italy) Ph.D Thesis University of Utrecht (95 pp.).
Brusatte, S.L., Butler, R.J., Mateus, O., Steyer, J.-S., 2015. A new species of *Metoposaurus* from the Late Triassic of Portugal and comments on the systematics and biogeography of metoposaurid temnospondyls. J. Vertebr. Paleontol. 35 (3), e912988 (23 pp.).
Brusatte, S.L., Niedźwiedzki, G., Butler, R.J., 2011. Footprints pull origin and diversification of dinosaur stem lineage deep into Early Triassic. Proc. R. Soc. B 278, 1107–1113.
Calvet, F., Solé de Porta, N., Salvany, J.M., 1993. Cronoestratigrafía (Palinología) del Triásico sudpirenaico y del Pirineo Vasco-Cantábrico. Acta Geol. Hisp. 28, 33–48.
Calzada, S., 1987. Niveles fosilíferos de la facies Buntsandstein (Trias) en el sector norte de los Catalánides. Cuad. Geol. Iber. 11, 256–271.
Cassinis, G., Durand, M., Ronchi, A., 2007. Remarks on the Permian and Permian–Triassic boundary in central and eastern Lombardy (Southern Alps, Italy). J. Iber. Geol. 33 (2), 133–142.
Cassinis, G., Perotti, C.R., Ronchi, A., 2012. Permian continental basins in the Southern Alps (Italy) and peri-Mediterranean correlations. Int. J. Earth Sci. (Geogr. Rundsch.) 101, 129–157.
Chumakov, N.M., Zharkov, M.A., 2003. Climate during the Permian–Triassic biosphere reorganizations. Article 2. Climate of the Late Permian and Early Triassic: general inferences. Stratigr. Geol. Correl. 11 (4), 361–375.
Cisneros, J.C., Abdala, F., Rubidge, B.S., Atayman-Güven, S., Celâl Şengör, A.M., Schultz, C.L., 2012. Carnivorous dinocephalian from the Middle Permian of Brazil and tetrapod dispersal in Pangaea. PNAS 109 (5), 1584–1588.
Cisneros, J.C., Marsicano, C., Angielczyk, K.D., Smith, R.M.H., Richter, M., Fröbisch, J., Kammerer, C.F., Sadleir, R.W., 2015. New Permian fauna from tropical Gondwana. Nat. Commun. 6, 8676. http://dx.doi.org/10.1038/ncomms9676 (8 pp.).
Dalloni, M., 1930. Étude géologique des Pyrénées catalanes. Ann. Fac. Sci. Marseille XXVI 1–373.
Demathieu, G., Demathieu, P., 2004. Chirotheria and other ichnotaxa of the European Triassic. Ichnos 11 (1), 79–88.
Demathieu, G., Fichter, J., 1989. Die Karlshafener Fährten im Naturkundemuseum der Stadt Kassel. Philippia 6 (2), 111–154.
Demathieu, G., Saiz de Omeñaca, J., 1990. Primeros resultados del estudio de un nuevo yacimiento de icnofauna triásica, en Peña Sagra (Cantabria, España). Estud. Geol. 46, 147–150.
Demathieu, G., Torcida Fernández-Baldor, F., Demathieu, P., Urién Montero, V., Pérez-Lorente, F., 2008. Icnitas de grandes vertebrados terrestres en el Pérmico de Peña Sagra (Cantabria, España). In: Ruiz-Omeñaca, J.I., Piñuela, L., García-Ramos, J.C. (Eds.), XXIV Jornadas de la Sociedad Española de Palaeontología, Museo del Jurásico de Asturias (MUJA), Colunga, pp. 27–28.
Dercourt, J., Gaetani, M., Vrielynck, B., Barrier, E., Biju-Duval, B., Brunet, M.F., Cadet, J.P., Crasquin, S., Sandulescu, M., 2000. Peri-Tethys Atlas, Palaeogeographical maps, CCGM/CGMW, Paris I-XX. pp. 1–269.

Díaz-Martínez, I., Castanera, D., Gasca, J.M., Canudo, J.I., 2015. A reappraisal of the Middle Triassic chirotheriid *Chirotherium ibericus* Navás, 1906 (Iberian Range NE Spain), with comments on the Triassic tetrapod track biochronology of the Iberian Peninsula. PeerJ 3, e1044 (36 pp.).

Díaz-Martínez, I., Pérez-García, A., 2012. Historical and comparative study of the first Spanish vertebrate paleoichnological record and bibliographic review of the Spanish chirotheriid footprints. Ichnos 19 (3), 141–149.

Diedrich, C., 2002. Vertebrate track bed stratigraphy at new megatrack sites in the Upper Wellenkalk Member and *orbicularis* Member (Muschelkalk, Middle Triassic) in carbonate tidal flat environments of the western Germanic Basin. Palaeogeogr. Palaeoclimatol. Palaeoecol. 183, 185–208.

Diedrich, C., 2008. Millions of reptile tracks—Early to Middle Triassic carbonate tidal flat migration bridges of Central Europe. Palaeogeogr. Palaeoclimatol. Palaeoecol. 259, 410–423.

Diez, J.B., 2000. Geología y Paleobotánica de la Facies Buntsandstein en la Rama Aragonesa de la Cordillera Ibérica. Implicaciones Paleogeográficasen el Peritethys Occidental. University of Zaragoza—U.P.M.C., Paris Ph.D Thesis. (424 pp.).

Diez, J.B., Broutin, J., Ferrer, J., 2005. Difficulties encountered in defining the Permian–Triassic boundary in Buntsandstein facies of the western Peritethyan domain based on palynological data. Palaeogeogr. Palaeoclimatol. Palaeoecol. 229, 40–53.

Dinarès-Turell, J., Diez, J.B., Rey, D., Arnal, I., 2005. "Buntsandstein" magnetostratigraphy and biostratigraphic reappraisal from eastern Iberia: Early and Middle Triassic stage boundary definitions through correlation to Tethyan sections. Palaeogeogr. Palaeoclimatol. Palaeoecol. 229, 158–177.

Doubinger, J., Robert, J.F., Broutin, J., 1978. Données complémentaires sur la flore Permo-Carbonifère de Surroca-Ogassa (province de Gérone, Espagne). 103e Congrès national des Sociétés savantes, Nancy 1978. Sciences II, 39–45.

Domeier, M., Van der Voo, R., Torsvik, T.H., 2012. Paleomagnetism and Pangea: the road to reconciliation. Tectonophysics 514-517, 114–143.

Efremov, J.A., 1956. American elements in the fauna of Permian reptiles of the USSR. Dokl. Akad. Nauk SSSR 111, 1091–1094.

Erwin, D.H., 1994. The Permo-Triassic extinction. Nature 367, 231–236.

Evans, M.E., 2012. Magnetostratigraphy of the Lodève Basin, France: implications for the Permo-Carboniferous reversed superchron and the geocentric axial dipole. Stud. Geophys. Geod. 56, 725–734.

Evans, M.E., Pavlov, V., Veselovsky, R., Fetisova, A., 2014. Late Permian paleomagnetic results from the Lodève, Le Luc, and Bas-Argens Basins (southern France): magnetostratigraphy and geomagnetic field morphology. Phys. Earth Planet. Inter. 237, 18–24.

Falkingham, P.L., 2012. Acquisition of high resolution three-dimensional models using free, open-source, photogrammetric software. Palaeontol. Electron. 15, 1–15.

Fichter, J., Kunz, R., 2013. "Dinosauromorph" tracks from the Middle Buntsandstein (Early Triassic: Olenekian) of Wolfhagen, northern Hesse, Germany. Comunicações Geol. 100 (1), 81–88.

Fisher, M.J., 1979. The Triassic palynofloral succession in the Canadian Arctic Archipelago. American Association of Stratigraphic Palynologists Contribution Series 5B, 83–100.

Fortuny, J., Bolet, A., Sellés, A.G., Cartanyà, J., Galobart, À., 2011a. New insights on the Permian and Triassic vertebrates from the Iberian Peninsula with emphasis on the Pyrenean and Catalonian basins. J. Iber. Geol. 37 (1), 65–86.

Fortuny, J., Galobart, À., De Santisteban, C., 2011b. A new capitosaur from the Middle Triassic of Spain and the relationships within the Capitosauria. Acta Palaeontol. Pol. 56 (3), 553–566.

Fortuny, J., Sellés, A.G., Valdiserri, D., Bolet, A., 2010. New tetrapod footprints from the Permian of the Pyrenees (Catalonia, Spain): preliminary results. Cidaris 30, 121–124.

Fuglewicz, R., Ptaszyński, T., Rdzanek, K., 1990. Lower Triassic footprints from the Świętokrzyskie (Holy Cross) Mountains, Poland. Acta Palaeontol. Pol. 35 (3-4), 109–164.

Galán-Abellán, B., 2011. Sedimentary, Mineralogical and Geochemical Variations inthe Buntsandstein facies, Lower–Middle Triassic, of the Iberian Ranges and Catalan Coastal Ranges: Implications in the Recovery of the Permian–Triassic crisis Ph.D Thesis Universidad Complutense, Madrid (383 pp.).

Galán-Abellán, B., López-Gómez, J., Barrenechea, J.F., Marzo, M., De la Horra, R., Arche, A., 2013. The beginning of the Buntsandstein cycle (Early–Middle Triassic) in the Catalan Ranges, NE Spain: sedimentary and palaeogeographic implications. Sediment. Geol. 296, 86–102.

Gand, G., De La Horra, R., Galán-Abellán, B., López-Gómez, J., Fernández-Barrenechea, J., Arche, A., Benito, M.I., 2010. New ichnites from the Middle Triassic of the Iberian Ranges (Spain): palaeoenvironmental and palaeogeographical implications. Hist. Biol. 22 (1), 1–17.

Gand, G., Demathieu, G., 2005. Les pistes dinosauroïdes du Trias moyen français: interprétation et réévaluation de la nomenclature. Géobios 38, 725–749.

Gand, G., Demathieu, G., Montenat, C., 2007. Les traces de pas d'amphibiens, de dinosaures et autres reptiles du Mésozoïque français: inventaire et interprétations. Palaeovertebrata 1-4, 1–149.

Gand, G., Durand, M., 2006. Tetrapod footprint ichno-associations from French Permian basins. Comparisons with other Euramerican ichnofaunas. In: Lucas, S.G., Cassinis, G., Schneider, J.W. (Eds.), Non-Marine Permian Biostratigraphy and Biochronology. Geological Society, Special Publications 265, pp. 157–177 (London).

Gand, G., Garric, J., Demathieu, G., Ellenberger, P., 2000. La palichnofaune de vertébrés tétrapodes du Permien supérieur du bassin de Lodève (Languedoc-France). Palaeovertebrata 29 (1), 1–82.

Gisbert, P., 1981. Estudio geológico–petrológico del Stephaniense-Pérmico de la sierra del Cadí. Diagénesis y Sedimentología. University of Zaragoza Ph.D Thesis. (314 pp.).

Gisbert, J., 1983. El Pérmico de los Pirineos españoles. In: Martínez García, E. (Ed.), Carbonífero y Pérmico de España. Ministerio de Industria y Energía, Madrid, pp. 405–420.

Gorsky, V.P., Gusseva, E.A., Crasquin-Soleau, S., Broutin, J., 2003. Stratigraphic data of the Middle–Late Permian on Russian Platform. Geobios 36, 533–558.

Gretter, N., Ronchi, A., López-Gómez, J., Arche, A., De la Horra, R., Barrenechea, J., Lago, M., 2015. The Late Palaeozoic–Early Mesozoic from the Catalan Pyrenees (Spain): 60 Myr of environmental evolution in the frame of the western peri-Tethyan palaeogeography. Earth Sci. Rev. 150, 679–708.

Hartevelt, J.J.A., 1970. Geology of the upper Segre and Valira valleys, central Pyrenees, Andorra/Spain. Leidse. Geol. Meded. 45, 349–354.

Haubold, H., 1971a. Die Tetrapodenfährten des Buntsandsteins in der Deutschen Demokratischen Republik und in Westdeutschland und ihre Äquivalente in der gesamten Trias. Paläntologische Abhandlungen, Abteilung A Paläozoologie, pp. 395–548.

Haubold, H., 1971b. Ichnia Amphibiorum et Reptiliorum fossilium. In: Wellnhofer, P. (Ed.). Encyclopedia of Paleoherpetology 18. Fischer Verlag, Stuttgart and Portland (124 pp.).

Haubold, H., 1984. Saurierfährten. Ziemsen Verlag, Wittenberg (231 pp.).

Haubold, H., 1996. Ichnotaxonomie und Klassifikation von Tetrapodenfährten aus dem Perm. Hallesches Jahrb. für Geowissenschaften B 18, 23–88.

Haubold, H., Hunt, A.P., Lucas, S.G., Lockley, M.G., 1995. Wolfcampian (Early Permian) vertebrate tracks from Arizona and New Mexico. N. M. Mus. Nat. Hist. Sci. Bull. 6, 135–165.

Henderson, C.M., Davydov, V.I., Wardlaw, B.R., 2012. The Permian Period. In: Gradstein, F.M., Hammer, O. (Eds.), The Geologic Time Scale 2012. Elsevier, Amsterdam, pp. 653–679.

Ivakhnenko, M.F., 2008. Subclass Ophiacomorpha. In: Ivakhnenko, M.F., Kurochkin, E.N. (Eds.), Fossil Vertebrates from Russia and Adjacent Countries. Fossil reptiles and birds. Part 1, pp. 95–100.

Jansonius, J., 1962. Palynology of Permian and Triassic sediments, Peace River area, Western Canada. Palaeontographica 110 B, 35–98.

Klaus, W., 1964. Zur sporenstratigraphischen Einstufung von gipsführenden Schichten in Bohrungen. (Playnostratigraphical correlation of gypsum-bearing layers in boreholes). Erdoel Zeitschrift 4, 119–132.

Klein, H., Haubold, H., 2003. Differenzierung von ausgewählten Chirotherien der Trias mittels Landmarkanalyse. Hallesches Jahrb. für Geowissenschaften 25, 21–36.

Klein, H., Lucas, S.G., 2010a. Review of the tetrapod ichnofauna of the Moenkopi formation/group (Early–Middle Triassic) of the American Southwest. N. M. Mus. Nat. Hist. Sci. Bull. 50, 1–167.

Klein, H., Lucas, S.G., 2010b. Tetrapod footprints—their use in biostratigraphy and biochronology of the Triassic. In: Lucas, S.G. (Ed.), The Triassic Timescale. Geological Society Special Publications 334, London, pp. 419–446.

Klein, H., Lucas, S.G., Voigt, S., 2015. Revision of the ?Permian–Triassic tetrapod ichnogenus *Procolophonichnium* Nopcsa 1923 with description of the new ichnospecies *P. lockleyi*. Ichnos 22, 155–176.

Klein, H., Niedźwiedzki, G., 2012. Revision of the Lower Triassic tetrapod ichnofauna from Wióry, Holy Cross Mountains, Poland. N. M. Mus. Nat. Hist. Sci. Bull. 59, 1–62.

Klein, H., Voigt, S., Hminna, A., Saber, H., Schneider, J., Hmich, D., 2010. Early Triassic Archosaur-dominated footprint assemblage from the Argana Basin (Western High Atlas, Morocco). Ichnos 17 (3), 215–227.

Klein, H., Voigt, S., Saber, H., Schneider, J.W., Fischer, J., Hminna, A., Brosig, A., 2011. First occurrence of a Middle Triassic tetrapod ichnofauna from the Argana Basin (Western High Atlas, Morocco). Palaeogeogr. Palaeoclimatol. Palaeoecol. 307, 218–231.

Körner, F., Schneider, J.W., Hoernes, S., Gand, G., Kleeberg, R., 2003. Climate and continental sedimentation in the Permian of the Lodève Basin (Southern France). Bollettino della Società Geologica Italiana e del Servizio Geologico d'Italia Volume speciale n. 2, pp. 185–191.

Krainer, K., Lucas, S.G., Ronchi, A., 2012. Tetrapod footprints from the Alpine Buntsandstein (Lower Triassic) of the Drau Range (Eastern Alps, Austria). Jahrb. Geol. Bundesanst. 152 (1-4), 205–212.

Kuerschner, W.M., Herngreen, W., 2010. Triassic palynology of central and northwestern Europe: a review of palynofloral diversity patterns and biostratigraphic subdivisions. In: Lucas, S.G. (Ed.), The Triassic Timescale. Geological Society Special Publications 334, pp. 263–283 (London).

Leonardi, G., 1987. Glossary and Manual of Tetrapod Footprint Palaeoichnology. Departamento Nacional de Produção Mineral, Brasilia (117 pp.).

Linol, B., Bercovici, A., Bourquin, S., Diez, J.B., López-Gómez, J., Broutin, J., Durand, M., Villanueva-Amadoz, U., 2009. Late Permian to Middle Triassic correlations and palaeogeographical reconstructions in south-western European basins: new sedimentological data from Minorca (Balearic Islands, Spain). Sediment. Geol. 220 (1-2), 77–94.

Lopez, M., Gand, G., Garric, J., Körner, F., Schneider, J., 2008. The playa environments of the Lodève Permian Basin (Languedoc-France). J. Iber. Geol. 34 (1), 29–56.

López-Gómez, J., Arche, A., Pérez-López, A., 2002. Permian and Triassic. In: Gibbons, W., Moreno, M.T. (Eds.), The Geology of Spain. Geological Society of London, London, pp. 185–212.

López-Gómez, J., Arche, A., Vargas, H., Marzo, M., 2010. Fluvial architecture as a response to two-layer lithospheric subsidence during the Permian and Triassic in the Iberian Basin, eastern Spain. Sediment. Geol. 223, 320–333.

López-Gómez, J., Galán-Abellán, B., De la Horra, R., Barrenechea, J.F., Arche, A., Bourquin, S., Marzo, M., Durand, M., 2012. Sedimentary evolution of the continental Early–Middle Triassic Cañizar Formation (Central Spain): Implications for life recovery after the Permian–Triassic crisis. Sediment. Geol. 249-250, 26–44.

Lovelace, D.M., Lovelace, S.D., 2012. Paleoenvironments and paleoecology of a Lower Triassic invertebrate and vertebrate ichnoassemblage from the Red Peak Formation (Chugwater Group), Central Wyoming. Palaios 27, 636–657.

Lucas, S.G., 2010. The Triassic timescale: an introduction. In: Lucas, S.G. (Ed.), The Triassic Timescale. Geological Society Special Publication 334, pp. 1–16 (London).

Maddin, H., Reisz, R.R., Sidor, C., 2008. Cranial anatomy of *Ennatosaurus tecton* (Synapsida: Caseidae) from the Middle Permian of Russia and the evolutionary relationships of Caseidae. J. Vertebr. Paleontol. 28 (1), 160–180.
Maidwell, F.T., 1911. Notes on footprints from the Keuper of Runcorn Hill. Proceedings of the Liverpool Geological Society 11, pp. 140–152.
Martí, J., 1983. La formación volcánica estefaniense Erill Castell (Pirineo de Lérida). Acta Geol. Hisp. 18 (1), 27–33.
Martín-Closas, C., Martínez-Roig, D., 2007. Plant taphonomy and palaeoecology of Stephanian limnic wetlands in the eastern Pyrenees (Catalonia, Spain). C.R. Palevol 6, 437–449.
Mateus, O., Butler, R.J., Brusatte, S.L., Whiteside, J.H., Steyer, J.S., 2014. The first phytosaur (Diapsida, Archosauriformes) from the Late Triassic of the Iberian Peninsula. J. Vertebr. Paleontol. 34 (4), 970–975.
Matthews, N.A., 2008. Aerial and close-range photogrammetric technology: providing resource documentation, interpretation, and preservation. Technical Note 428. Interior, Bureau of Land Management, National Operations Center, Denver, Colorado, U.S. Department of the 42 pp.
Mey, P.H.W., Nagtegaal, P.J.C., Roberti, K.J., Hartevelt, J.J.A., 1968. Lithostratigraphic subdivision of post-Variscan deposits in the South-Central Pyrenees, Spain. Leidse. Geol. Meded. 41, 153–220.
Michel, L.A., Tabor, N.J., Montañez, I.P., Schmitz, M., Davydov, V.I., 2015. Chronostratigraphy and paleoclimatology of the Lodève Basin, France: evidence for a pan-tropical aridification event across the Carboniferous-Permian boundary. Palaeogeogr. Palaeoclimatol. Palaeoecol. 430, 118–131.
Mujal, E., Fortuny, J., Oms, O., Bolet, A., Galobart, A., Anadón, P. Palaeoenvironmental reconstruction and early Permian ichnoassemblage from the NE Iberian Peninsula (Pyrenean Basin). Geol. Mag. http://dx.doi.org/10.1017/S0016756815000576 (in press, 23 pp.).
Mujal, E., Fortuny, J., Rodríguez-Salgado, P., Diviu, M., Oms, O., Galobart, A., 2015. First footprints occurrence from the Muschelkalk detritical unit of the Catalan Basin: 3D analyses and palaeoichnological implications. Span. J. Paleontol. 30 (1), 97–108.
Nagtegaal, P.J.C., 1969. Sedimentology, paleoclimatology, and diagenesis of post-Hercynian continental deposits in the south-central Pyrenees, Spain. Leidse. Geol. Meded. 42, 143–238.
Niedźwiedzki, G., Brusatte, S.L., Butler, R.J., 2013. *Prorotodactylus* and *Rotodactylus* tracks: an ichnological record of dinosauromorphs from the Early–Middle Triassic of Poland. In: Nesbit, S.J., Desojo, J.B., Irmis, R.B. (Eds.), Anatomy, Phylogeny and Palaeobiology of Early Archosaurs and their Kin. Geological Society Special Publications 379. Geological Society of London, London, pp. 319–351.
Niedźwiedzki, G., Ptaszyński, T., 2007. Large Chirotheriidae tracks in the Early Triassic of Wióry, Holy Cross Mountains, Poland. Acta Geol. Pol. 57 (3), 325–342.
Olsen, P.E., Kent, D.V., Sues, H.-D., Koeberl, C., Huber, H., Montanari, A., Rainforth, E.C., Fowell, S., Szajna, M.J., Hartline, B.W., 2002. Ascent of dinosaurs linked to an iridium anomaly at the Triassic-Jurassic boundary. Science 296, 1305–1307.
Olson, E.C., 1968. The family Caseidae. Fieldiana Geol. 17, 225–349.
Orłowska-Zwolińska, T., 1977. Palynological correlation of the Bunter and Muschelkalk in selected profiles from Western Poland. Acta Geol. Pol. 27 (4), 417–430.
Orłowska-Zwolińska, T., 1984. Palynostratigraphy of the Buntsandstein in sections of western Poland. Acta Palaeontol. Pol. 29 (3-4), 161–194.
Osborn, H.F., 1903. On the primary division of the Reptilia into two sub-classes, Synapsida and Diapsida. Science 17, 275–276.
Peabody, F.E., 1948. Reptile and amphibian trackways from the Moenkopi Formation of Arizona and Utah. Univ. Calif. Publ. Bull. Dep. Geol. Sci. 27, 295–468.
Pereira, M.F., Castro, A., Chichorro, M., Fernández, C., Díaz-Alvarado, J., Martí, J., Rodríguez, C., 2014. Chronological link between deep-seated processes in magma chambers and eruptions: Permo-Carboniferous magmatism in the core of Pangaea (Southern Pyrenees). Gondwana Res. 25, 290–308.
Pérez-López, A., 1993. Estudio de las huellas de reptil, del icnogénero *Brachychiroterium*, encontradas en el Trías Subbético de Cambil. Estud. Geol. 49, 77–86.
Pochat, S., Van Den Driessche, J., 2011. Filling sequence in Late Paleozoic continental basins: a chimera of climate change? A new light shed given by the Graissessac-Lodève basin (SE France). Palaeogeogr. Palaeoclimatol. Palaeoecol. 302, 170–186.
Ptaszyński, T., 2000. Lower Triassic vertebrate footprints from Wióry, Holy Cross Mountains, Poland. Acta Palaeontol. Pol. 45 (2), 151–194.
Reisz, R.R., 1986. Pelycosauria. In: Wellnhofer, P. (Ed.), Handbuch der Paläoherpetologie, 16A. Fischer Verlag, Stuttgart & New York, pp. 1–102.
Reisz, R.R., Maddin, H.C., Fröbisch, J., Falconnet, J., 2011. A new large caseid (Synapsida, Caseasauria) from the Permian of Rodez (France), including a reappraisal of "*Casea*" *rutena* Sigogneau-Russell & Russell, 1974. Geodiversitas 33 (2), 227–246.
Robert, K.J., 1970. Geolegical map of Flamisell and Mañanet valleys, central Pyrenees, in: Zwart, H.J. (1979) (Ed.), The geology of the central Pyrenees. Leidse. Geol. Meded. 50, 1–74.
Robles, S., Llompart, C., 1987. Análisis paleogeográfico y consideraciones paleoicnológicas del Pérmico Superior y del Triásico Inferior en la transversal del rio Segre (Alt Urgell, Pirineo de Lérida). Cuad. Geol. Iber. 11, 115–130.
Romano, M., Nicosia, U., 2014. *Alierasaurus ronchii*, gen. et sp. nov., a caseid from the Permian of Sardinia, Italy. J. Vertebr. Paleontol. 34 (4), 900–913.
Romer, A.S., Price, L.I., 1940. Review of the Pelycosauria. Geol. Soc. Am. Spec. Pap. 28, 1–538.
Ronchi, A., Sacchi, E., Romano, M., Nicosia, U., 2011. A huge caseid pelycosaur from northwestern Sardinia and its bearing on European Permian stratigraphy and palaeobiogeography. Acta Palaeontol. Pol. 56 (4), 723–738.
Rühle von Lilienstern, H., 1939. Fährten und Spuren im Chirotherium-Sandstein von Südthüringen. Fortschritte der Geologie und Palaeontologie 12, pp. 293–387.
Sahney, S., Benton, M.J., 2008. Recovery from the most profound mass extinction of all time. Proc. R. Soc. B 275, 759–765.
Saura, E., 2004. Anàlisi estructural de la zona de les Nogueres Pirineus Centrals PhD Thesis Universitat Autònoma de Barcelona (355 pp.).
Saura, E., Teixell, A., 2006. Inversion of small basins: effects on structural variations at the leading edge of the Axial Zone antiformal stack (Southern Pyrenees, Spain). J. Struct. Geol. 28, 1909–1920.
Schmidt, G., 1931. Das Paläozoikum der spanischen Pyrenäen. Abh. Ges. Wiss. Goettingen, Math.-Phys. Kl. II, 101–195.
Schneider, J.W., Körner, F., Roscher, M., Kroner, U., 2006. Permian climate development in the northern peri-Tethys area—The Lodève Basin, French Massif Central, compared in a European and global context. Palaeogeogr. Palaeoclimatol. Palaeoecol. 240, 161–183.
Sidor, C.A., O'Keefe, F.R., Damiani, R., Steyer, J.S., Smith, R.M.H., Larsson, H.C.E., Sereno, P.C., Ide, O., Maga, A., 2005. Permian tetrapods from the Sahara show climate-controlled endemism in Pangaea. Nature 434, 886–889.
Sidor, C.A., Vilhena, D.A., Angielczyk, K.D., Huttlenlocker, A.K., Nesbitt, S.J., Peecook, B.R., Steyer, J.S., Smith, R.M.H., Tsuji, L.A., 2013. Provincialization of terrestrial faunas following the end-Permian mass extinction. PNAS 110 (20), 8129–8133.
Silva, R.C., Sedor, F.A., Fernandes, A.C.S., 2012. Fossil footprints from the Late Permian of Brazil: an example of hidden biodiversity. J. S. Am. Earth Sci. 38, 31–43.
Sigogneau-Russell, D., Russell, D.E., 1974. Étude du premier caséidé (Reptilia, Pelycosauria) d'Europe occidentale. Bulletin du Muséum national d'Histoire naturelle, Série 3, pp. 145–215 (Section 230).
Smith, R.M.H., Botha-brink, J., 2014. Anatomy of a mass extinction: sedimentological and taphonomic evidence for drought-induced die-offs at the Permo-Triassic boundary in the main Karoo Basin, South Africa. Palaeogeogr. Palaeoclimatol. Palaeoecol. 396, 99–118.
Speksnijder, A., 1985. Anatomy of a strike-slip fault controlled sedimentary basin, Permian of the southern Pyrenees, Spain. Sediment. Geol. 44, 179–223.
Stovall, J.W., Price, L.I., Romer, A.S., 1966. The postcranial skeleton of the giant Permian pelycosaur *Cotylorhynchus romeri*. Bull. Mus. Comp. Zool. 135, 1–30.
Surkov, M.V., Benton, M.K., Twitchett, R.J., Tverdokhlebov, V.P., Newell, A.J., 2007. First occurrence of footprints of large therapsids from the Upper Permian of European Russia. Palaeontology 50 (3), 641–652.
Talens, J., Wagner, R.H., 1995. Stratigraphic implications of Late Carboniferous and Early Permian megafloras in Lérida, south-central Pyrenees; comparison with the Cantabrian Mountains. Coloquios de Paleontología 47. Universidad Complutense, pp. 177–192.
Torsvik, T.H., Cocks, L.R.M., 2013. Gondwana from top to base in space and time. Gondwana Res. 24, 999–1030.
Tourani, A., Benaouiss, N., Gand, G., Bourquin, S., Jalil, N.-E., Broutin, J., Battail, B., Germain, D., Khaldoune, F., Sebban, S., Steyer, J.-S., Vacant, R., 2010. Evidence of an Early Triassic age (Olenekian) in Argana Basin (High Atlas, Morocco) based on new chirotherioid traces. C.R. Palevol 9, 201–208.
Valdiserri, D., Avanzini, M., 2007. A tetrapod ichnoassociation from the Middle Triassic (Anisian, Pelsonian) of Northern Italy. Ichnos 14 (1-2), 105–116.
Valentini, M., Conti, M.A., Mariotti, N., 2007. Lacertoid footprints of the Upper Permian Arenaria di Val Gardena Formation (Northern Italy). Ichnos 14 (3-4), 193–218.
Valentini, M., Nicosia, U., Conti, M.A., 2009. A re-evaluation of *Pachypes*, a pareiasaurian track from the Late Permian. Neues Jb. Geol. Paläontol. Abh. 251 (1), 71–94.
Viennot, P., 1929. Les éruptions basaltiques permiennes dans les Pyrénées. C.R. Soc. Geol. Fr. XXIV, 29–32.
Voigt, S., Hminna, A., Saber, H., Schneider, J.W., Klein, H., 2010. Tetrapod footprints from the uppermost level of the Permian Ikakern Formation (Argana Basin, Western High Atlas, Morocco). J. Afr. Earth Sci. 57, 470–478.
Wagner, R.H., Álvarez-Vázquez, C., 2010. The Carboniferous floras of the Iberian Peninsula: A synthesis with geological connotations. Rev. Palaeobot. Palynol. 16, 239–364.
Ward, P.D., Botha, J., Buick, R., Dekock, M.O., Erwin, D.H., Garrison, G., Kirschvink, J., Smith, R.H.M., 2005. Abrupt and gradual extinction among Late Permian land vertebrates in the Karoo Basin, South Africa. Science 307, 709–714.
Werneburg, R., Steyer, J.-S., Sommer, G., Gand, G., Schneider, J.W., Vianey-Liaud, M., 2007. The earliest tupilakosaurid amphibian with diplospondylous vertebrae from the Late Permian of southern France. J. Vertebr. Paleontol. 27, 26–30.
Williston, S.W., 1911. American Permian Vertebrates. University of Chicago Press, Chicago (145 pp.).
Xu, L., Li, X.-W., Jia, S.-H., Liu, J., 2015. The Jiyuan Tetrapod Fauna of the Upper Permian of China: new pareiasaur material and the reestablishment of *Honania complicidentata*. Acta Palaeontol. Pol. 60 (3), 689–700.

Capítol 6. *Integrated multi-stratigraphic study of the Coll de Terrers late Permian–Early Triassic continental succession from the Catalan Pyrenees (NE Iberian Peninsula): a geologic reference record for equatorial Pangaea*

El capítol 6 correspon al treball enviat a la revista *Global and Planetary Change* el 26 de desembre de 2016 i en revisió des del 30 de desembre de 2016:

Mujal, E., Fortuny, J., Pérez-Cano, J., Dinarès-Turell, J., Ibáñez, J., Oms, O., Vila, I., Bolet, A., Anadón, P., In review. Integrated multi-stratigraphic study of the Coll de Terrers late Permian–Early Triassic continental succession from the Catalan Pyrenees (NE Iberian Peninsula): a geològic reference record for equatorial Pangaea. Global and Planetary Change.

En aquest treball l'autor E. M. ha contribuït en: plantejament del treball; tasques de camp, incloent elaboració del mapa geològic i de la columna estratigràfica, mostreig de roques per làmines primes i anàlisis paleomagnètiques i geoquímiques, i prospecció i documentació de les traces fòssils; preparació de les mostres de roques per paleomagnetisme i geoquímica; elaboració dels models fotogramètrics 3D de les icnites; anàlisis de sedimentologia i icnologia; interpretació i discussió de tots els resultats; redacció del manuscrit; preparació i maquetació de totes les figures; preparació del material suplementari (excepte la part de paleomagnetisme); autor per correspondència amb la revista.

Integrated multi-stratigraphic study of the Coll de Terrers late Permian–Early Triassic continental succession from the Catalan Pyrenees (NE Iberian Peninsula): a geologic reference record for equatorial Pangaea

Eudald Mujal[a]*, Josep Fortuny[b,c], Jordi Pérez-Cano[a], Jaume Dinarès-Turell[d], Jordi Ibáñez[e], Oriol Oms[a], Isabel Vila[f], Arnau Bolet[c], Pere Anadón[e]

[a] Departament de Geologia, Universitat Autònoma de Barcelona, E-08193 Bellaterra, Spain.

[b] Centre de Recherches en Paléobiodiversité et Paléoenvironnements, UMR 7202 CNRS-MNHN-UPMC, Muséum national d'Histoire naturelle, Bâtiment de Paléontologie, 8 rue Buffon, CP38, F-75005 Paris, France.

[c] Institut Català de Paleontologia Miquel Crusafont, ICTA-ICP building, c/ de les columnes, s/n, E-08193 Cerdanyola del Vallès, Spain.

[d] Istituto Nazionale di Geofisica e Vulcanologia, Via di Vigna Murata 605, I-00143 Roma, Italy.

[e] Institut de Ciències de la Terra Jaume Almera, ICTJA-CSIC, c/Lluís Solé i Sabarís s/n, E-08028 Barcelona, Spain.

[f] Departament de la Terra i de l'Oceà (Facultat de Geologia), Universitat de Barcelona, c/Martí i Franqués s/n, E-08028 Barcelona, Spain.

*Corresponding author: E. Mujal, eudald.mujal@gmail.com

Abstract

The most severe biotic crises on Earth history occurred during the Permian–Triassic (PT) transition around 252 Ma. Whereas in the marine realm such extinction event is well-constrained, in terrestrial settings is still poorly known, mainly due to the lack of suitable complete sections. This is utterly the case along the Western Tethys region, located at Pangaea's equator, where terrestrial successions are typically build-up of red beds often characterised by a significant erosive gap at the base of the Triassic strata. Henceforth, documenting potentially complete terrestrial successions along the PT transition becomes fundamental. Here, we document the exceptional Coll de Terrers area from the Catalan Pyrenees (NE Iberian Peninsula), for which a multidisciplinary research is conducted along the PT transition. The red-bed succession, located in a long E-W extended narrow rift system known as Pyrenean Basin, resulted from a continuous sedimentary deposition evolving from meandering (lower Upper Red Unit) to playa-lake/ephemeral lacustrine (upper Upper Red Unit) and again to meandering settings (Buntsandstein facies). Sedimentary continuity is suggested by preliminary cyclostratigraphic analysis that warrants further analysis. Our combined sedimentological, mineralogical and geochemical data infer a humid-semiarid-humid climatic trend across the studied succession. The uppermost Permian strata, deposited under an orbitally controlled monsoonal regime, yields a relatively diverse ichnoassemblage mainly composed of tetrapod footprints and arthropod trace fossils. Such fossils indicate appropriate life conditions and water presence in levels that also display desiccation structures. These levels alternate with barren intervals formed under dry conditions, being thus indicative of strong seasonality. All these features are correlated with those reported elsewhere in Gondwana and Laurasia, and suggest that the Permian–Triassic boundary is recorded somewhere around the

Buntsandstein base. Consequently, Coll de Terrers and the whole Catalan Pyrenees become key regions to investigate in detail the Permian extinction event and the Triassic ecosystems recovery.

Keywords

Permian-Triassic transition; stratigraphy; orbital forcing; X-ray diffraction; tetrapod footprints; Western Tethys.

1. Introduction

The Permian and Triassic periods are characterised by large continental landmasses resulting from the formation of Pangaea, which enhanced global aridity and red-beds deposits (Gibbs et al., 2002; Chumakov and Zharkov, 2003; Roscher and Schneider, 2006; Schneider et al., 2006; Looy et al. 2016; Kustatscher et al., 2017). The Permian–Triassic record has been largely studied, mostly with the aim of unravelling the events that triggered the major biological crisis of Earth's history, i.e., the end-Permian mass extinction (Erwin, 1994). Such event is now well-documented in the marine realm (Payne and Clapham, 2012), but questions still remain open in the case of the continental record (Gastaldo et al., 2015). Benton and Newell (2014) have recently considered several key zones to study both the Permian–Triassic continental record and the Permian–Triassic boundary (PTB), including Western and Central Europe, Russia and Siberia, central India, South China, central-eastern South America, South Africa, Australia and Antarctica. In general, Western Europe successions (Western peri-Tethyan domain) are characterised by an important erosive contact around the PTB (Bourquin et al., 2007, 2011). Recent works have attempted to constrain the Permian–Triassic transition and quantify the lack of record in the case of the Catalan Pyrenees (NE Iberian Peninsula), where long continental successions ranging from the late Carboniferous to the Middle Triassic are known to exist (Gretter et al., 2015; Mujal et al., 2016a). So that, despite the continental Western peri-Tethyan regions are deeply studied, continuous terrestrial Permian–Triassic sections are hardly identified (Bourquin et al., 2011; Kustatscher et al., 2017).

In the present work we introduce and characterise a new section from the Catalan Pyrenees spanning from the uppermost Permian to the lowermost Triassic record. The multidisciplinary study performed on this section includes lithostratigraphy, sedimentology, cyclostratigraphy, mineralogy (X-ray diffraction, XRD), geochemistry (X-ray fluorescence, XRF) and palaeontology (tetrapod and invertebrate ichnology), as well as palaeomagnetism (magnetostratigraphy). This section is free from the Triassic erosive gap, so it is a prospective area to identify the PTB in a continental succession of the Western peri-Tethyan domain, in equatorial Pangaea (Fig. 1A).

2. Geological setting

During the late Palaeozoic and early Mesozoic, the Iberian microplate was located in the equatorial latitudes of Pangaea, in the Western peri-Tethyan region, at the confluence of Gondwana and Laurasia landmasses (Dercourt et al., 2000; Fig. 1A). The microplate rotation at that time generated the exten-

sional (rifting) Iberian, Catalan and Pyrenean basins (De la Horra et al., 2012). The present-day Pyrenean range (located at the NE Iberian Peninsula and originated during the Alpine orogeny; Fig. 1B) was formerly composed of continental sedimentary basins controlled by a transtensional tectonic activity (Speksnijder, 1985; Saura and Teixell, 2006; Gretter et al., 2015). Pyrenean basins accumulated sediments from the late Carboniferous to the Middle Triassic because of the erosion of the Variscan orogen and the associated volcanic episodes (Gisbert, 1981; Martí, 1983; Gisbert et al., 1985; Pereira et al., 2014), related to the breakup of Pangaea (Torsvik and Cocks, 2013). The lithostratigraphic record was defined by Mey et al. (1968) and Nagtegaal (1969), while Gisbert (1981) established the depositional units here used (Fig. 1C). These units are, from base to top: Grey Unit (GU), Transition Unit (TU), Lower Red Unit (LRU), Upper Red Unit (URU) and Buntsandstein facies unit.

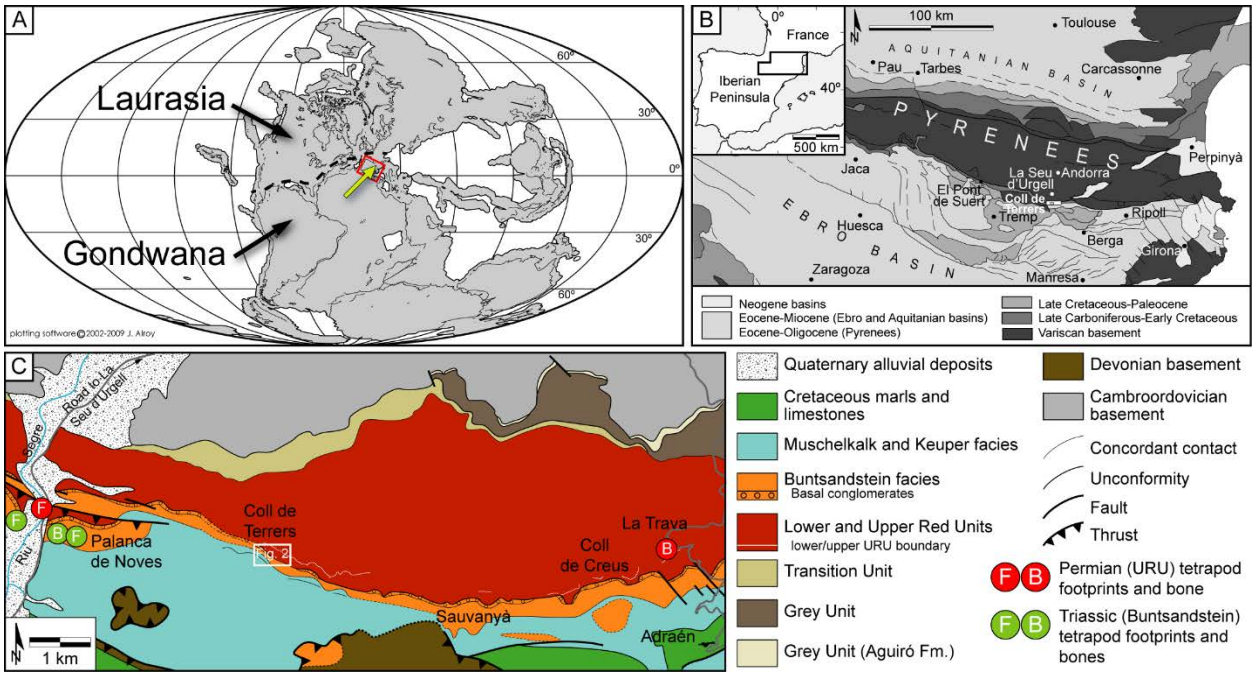

Figure 1. Palaeogeographical and geological setting. A. Pangaea map at 252 Ma (modified from Alroy, 2013); arrow and square show the studied locality; Gondwana/Laurasia boundary (dashed line) from Torsvik and Cocks (2013). B. Regional context. C. Geological map of the studied area (updated from Hartevelt, 1970 and Gisbert, 1981) with the main depositional units and equivalent lithostratigraphic formations; dashed lines correspond to uncertain contacts.

The present work is focused in the red-beds of the URU and its transition to the Buntsandstein facies unit, corresponding to the uppermost Permian and the lowermost Triassic Pyrenean record, respectively (Mujal et al., 2016a). Whereas the Buntsandstein facies is found along the entire Catalan Pyrenees, the URU is only recorded in the eastern part, in the Cadí Basin (Gisbert, 1981; Speksnijder, 1985). The lower portion of the URU is mainly composed of breccias, conglomerates, sandstones and red mudstones with limestone nodules, whereas the upper portion is build-up of red mudstones alternated with thin-bedded and fine-grained sandstone layers constituting metre-scale cyclic sequences (see sections 4.1 and 4.2 below). Due to the basin configuration, the URU is found above an angular unconformity developed on the top of the Variscan basement (Mujal et al., 2017) or the early Permian LRU (Gisbert et al., 1985; Speksnijder, 1985; Gretter et al., 2015). The Triassic Buntsandstein facies are generally of alluvial origin and are composed of basal breccias and conglomerates, followed by a

succession of sandstones and red mudstones, and finally by a red mudstone interval (Gisbert et al., 1985). The Buntsandstein unit is overlaid by the marlstone-limestone succession of the Muschelkalk and Keuper facies deposited during the Middle Triassic transgression. Basin palaeorelief controlled changes in thickness and lateral facies changes of both URU and Buntsandstein.

The URU/Buntsandstein boundary is commonly an angular unconformity (Gisbert et al., 1985; Gretter et al., 2015; Mujal et al., 2016a), as also occur in the other Permian–Triassic Iberian basins (Borruel-Abadía et al., 2015) and generally in the whole Western Europe (Bourquin et al., 2011). This is not the case of the Coll de Terrers area (Alt Urgell, Catalonia, NE Iberian Peninsula; Fig. 1B, C), where a conformable succession between the Permian and Triassic strata is observed (Fig. 2; see section 4 below).

3. Methods

The studied section is 250 m thick and is located in coordinates WGS84 UTM 31N 369341E, 4682768N (base) and 368925E, 4682570N (top). It contains three lithologic units: lower URU, upper URU and Buntsandstein facies that were measured by means of a Jacobs staff and a metre (Fig. 2B); a detailed geological map was also carried out (Fig. 2A). To assist sedimentological determinations, analyses were performed through field observations and thin sections (30 μm thick) obtained from 16 rock samples. The magnetostratigraphic study consisted in the analyses of samples distributed in 39 sites along the URU (Fig. 2B). However, it was found that the succession does not preserve a primary magnetism but, rather, a pervasive remagnetization. Methods, results and discussion of the palaeomagnetic data are provided as Supplementary Data (Text S1).

The lithologic succession of the upper URU and lowermost Buntsandstein has been codified to make it amenable to spectral analysis in order to explore its cyclic nature (Fig. 2C). Two approaches have been applied. The first one (code 1) assigns either 1 or -1 to the respective red mudstones or thin-bedded sandstone layers constituting the basic sequences. The second approach (code 2) assigns the stratigraphic thickness of the sequence throughout the encompassed interval of such sequence. The codified series at 2 cm resolution were used for spectral analysis. The Blackman-Tuckey method implemented in the AnalySeries v.2 software package (Paillard et al., 1996) and the REDFIT program (Schulz and Mudelsee, 2002) were employed. AnalySeries was further used for filtering the time series.

After preliminary prospective mineralogical and elemental analysis by XRD and XRF, sampling was mainly focused on the transition between the three units in order to identify any mineralogical variation. Sampling of lower and upper URU and Buntsandstein accounted for 15, 44 and 15 samples, respectively (Fig. 2B).

For the XRD measurements the samples were pulverised and homogenised to produce randomly-oriented powders. XRD scans were acquired between 4º and 65º in 2θ (0.02º per step) by using a Bruker D8-A25 diffractometer equipped with a Cu X-ray source (Cu Kα radiation) and a LynxEye position sensitive detector. Phase identification was performed by using the DIFFRAC.EVA software together with the Powder Diffraction File PDF-2 and the Crystallography Open Database (COD). Semi-quantitative phase analyses (SQPA) were carried out by using Reference Intensity Ratio (RIR) values for each of the identified phases.

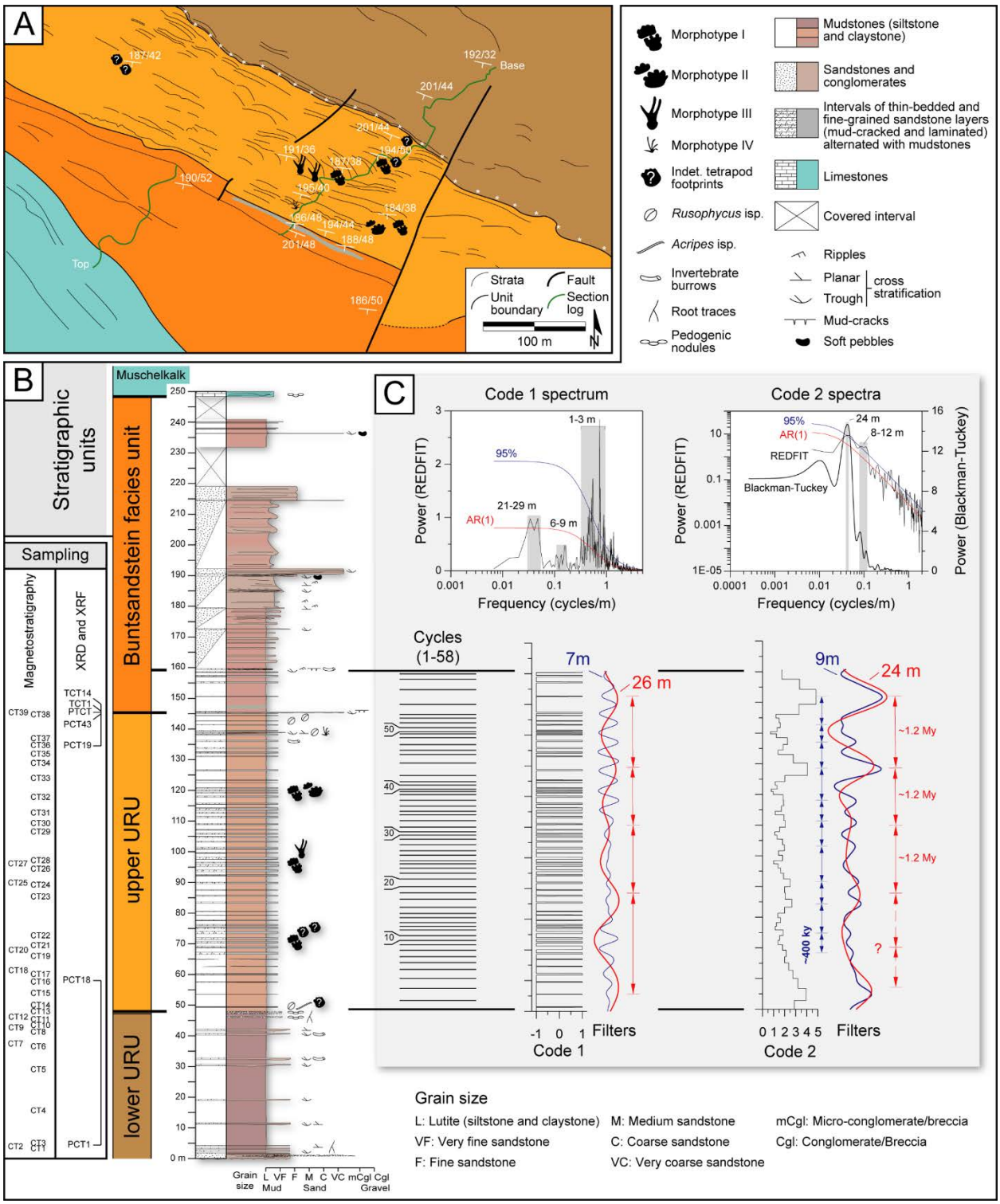

Figure 2. Coll de Terrers setting. A. Detailed geological map. B. Stratigraphic section with location of the magnetostratigraphic, XRD and XRF sample sites. C. Time series analysis of lithologic code 1 and code 2 in the depth domain. Spectral analyses on both series are carried out using the REDFIT program. Blackman–Tukey power spectrum (Band Width = 0.027095 0.563664 < DP(80.000000 %) / P < 2.722162) is also shown for code 2 series. The 95% confidence limits for a red noise test (a fitted AR1 process) for the REDFIT spectra are indicated. The periods in meters for relevant spectral peaks are indicated on the spectra. These spectral peaks are the basis for the frequency used for Gaussian filters and centred at 26 m (0.038383 ± 0.025 bandpass) and 7 m (0.160307 ± 0.12 bandpass) for code 1 and centred at 24 m (0.042828 ± 0.03 bandpass) and 9 m (0.11 ± 0.08 bandpass) respectively (see text for discussion).

The elemental composition of the samples was investigated by XRF measurements. For this purpose, a Bruker Tracer IV. Geo energy-dispersive XRF analyser equipped with a large area (30 mm^2) silicon drift detector and a 40 kV Rh X.-ray tube was employed. For each sample, two different XRF scans were obtained: one measurement excited with low voltage (15 keV) to optimize the detection of light elements ($13 < Z < 28$), and a second measurement excited with large voltages (40 keV) to detect heavier elements ($Z > 28$).

A palaeontological prospection was also carried out. Tetrapod footprints and invertebrate trace fossils were found and studied *in situ*, documented through photographs and schemes (processed in a vector based software), and situated in the measured section and in the geological map (Fig. 2A, 2B). Tetrapod footprints were analysed following the methods of Leonardi (1987). Additionally, seven 3D photogrammetric models were performed from selected specimens (including manus-pes sets and isolated ichnites). Photographs were obtained with a digital compact camera Sony DSC-T200 8.1 Megapixel and processed using open access software following the methods of Mujal et al. (2016b): Visual SFM v.0.5.24 (http://www.ccwu.me/vsfm/; to obtain the point cloud), MeshLab v.1.3.2 (http://meshlab.sourceforge.net; to create, scale and orientate the 3D mesh), and ParaView v.4.1.0 (http://www.paraview.org; to create the colour depth maps and contour lines). An *ex situ* slab bearing small tetrapod footprints was collected and is stored at Institut Català de Paleontologia Miquel Crusafont (Sabadell, Spain) and labelled IPS-99097.

4. Coll de Terrers section: results and interpretation

The analysed Coll de Terrers section (Cadí Basin of the Pyrenean rift system) is a red bed succession dipping south-westwards. The three units of the succession (lower URU, upper URU and Buntsandstein facies; Figs. 2, 3) correspond to three different sedimentary settings. In the following sections we present and interpret the detailed lithologic frame of the three units and the analytic and palaeontological data.

4.1. Stratigraphy and sedimentology

The Coll de Terrers deposits represent tectonically controlled sequences (Gisbert et al., 1985; Spieksnijder, 1985; Gretter et al., 2015). At Coll de Terrers, the URU overlays in angular unconformity the Lower Red Unit (LRU), which corresponds to a red-beds succession of volcanosedimentary origin of early Permian age (Pereira et al. 2014; Mujal et al. 2016b). Out from Coll de Terrers, the basal portion of the lower URU (here not studied) is composed of polymictic conglomerates and breccias with coarse sandstone matrix corresponding to alluvial braided facies (Gisbert, 1981; Gretter et al., 2015).

These coarse deposits are covered by fine- to medium-grained sandstones with occasional microconglomeratic levels, plant fragments and root traces (base of the measured section; Fig. S1). Sandstones rapidly grade to wine-red mudstones with occasional fine- to medium-grained sandstone body channels with lateral accretions and cross stratifications, of low lateral continuity and with sporadic vertical and tubular invertebrate burrows (Fig. S1). Some mudstone intervals exhibit pedogenic carbonate nodules with diameters ranging from millimetre up to 1 cm. The whole interval, of 45.5 m in

the measured section (Fig. 2), is interpreted as corresponding to distal meandering fluvial (sandstone bodies) and floodplain systems (mudstone intervals), where palaeosol levels were developed (Gisbert, 1981; Gretter et al., 2015).

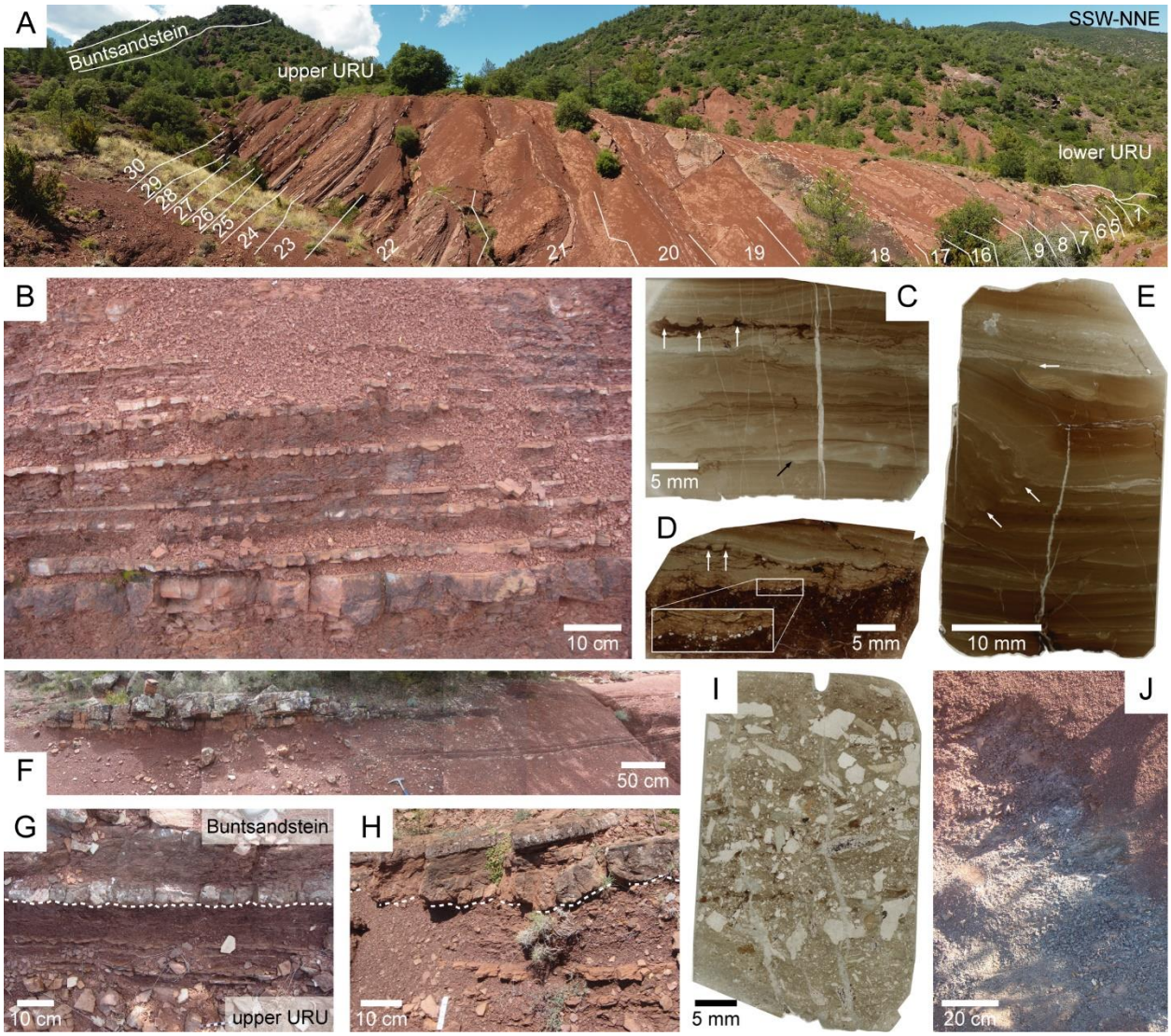

Figure 3. Coll de Terrers section. A. Overview of the studied units with partial labelling of the orbital cycles (numbers). B. Thin-bedded and fine-grained sandstone interval of cycle 22; note the thickest basal layer and the common load structures in most of sandstone layers. C-E. Thin sections of sandstone layers including: parallel and cross laminae; fining upwards of the laminae; mud drapes with load structures (white vertical arrows in C, D); long exposure levels (black arrow in C); small pedogenic nodules at the sandstone/mudstone interface (D); and section of a tetrapod footprint in lower laminae (white arrows in E). F. Fine-grained sandstone channel at the topmost part of the upper URU (cycle 49). G, H. Upper URU/Buntsandstein boundary (white dashed line), represented by a quartz microbreccia. I. Thin section of the basal Buntsandstein mircrobreccia, with most of the pebbles of quarts, but also including feldspars. J. Grey mudstone interval at the base of the Buntsandstein facies and overlying red mudstones.

The lower/upper URU boundary is represented by three levels of large carbonate nodules (up to 15 cm of diameter) generally septariform (i.e., radial and concentric networks of cracks filled with calcite; Fig. S2). The mudstones just below the boundary display vertical and sinuous greenish reduction marks corresponding to root traces as well as slickensides (Fig. S2C). Mudstone intervals as those of the lower URU separate the nodular levels, with a total thickness of 2 m in average. These nodules

indicate long periods of pedogenesis, where palaeosols were well-developed. Such boundary can be observed and traced along almost 7 km (Fig. 1C), dividing the URU in two sequences of different depositional settings.

The overlying upper URU deposits (Fig. 3) are 97.3 m thick in the measured section. They build up a cyclic or rhythmic sequence of red-orange mudstones alternated with 54 thin-bedded and fine-grained sandstone intervals (Figs. 2, 3A). Thickness of the mudstone intervals oscillates from 0.2 to 6.2 m along the succession, with an average of 1.5 m. Occasionally, the red-orange mudstones preserve small nodules mostly accumulated in the interface with the fine-grained sandstone layers (Fig. 3D). The thin-bedded and fine-grained sandstone intervals range from 0.03 m to 0.8 m thick (average of 0.38 m). These intervals consist of laminated layers around 2-5 cm thick (and up to 15 cm thick) alternated with 2-3 cm thick mudstone layers (Fig. 3B). Sandstone layers are orange-brownish and occasionally greenish-greyish. The number of thin-bedded sandstone layers in each interval oscillates from 1 to 15, but they commonly contain 6-7 layers.

These alternating intervals are of long lateral continuity (~450 m observed, which is the lateral extension of the outcrop; Figs. 2, 3A). Within each interval, the basal sandstone layer is thicker (5-10 cm, up to 15 cm) than the rest (2-5 cm in average). The lower boundary of some basal sandstone layers is transitional. Layers decrease in thickness and lateral continuity to the top, building up thinning and fining upwards sequences (Fig. 3B). The lower half of the layers is generally irregular due to load structures (flames, balls and pillows; Fig. 3B, 3C). The uppermost surface of all layers is mud-cracked, sometimes preserving ripple marks. In some cases, two periods of desiccation are observed in each layer: the lower half presents a genesis of mud-cracks not expressed in the upper half, which shows a second genesis. Laminations are either parallel (building up fining upwards sequences), or cross laminated (with flow and wave ripples) (Fig. 3C-E). Thin sections reveal thin mud drapes covering laminae (Fig. 3C, 3D). Laminae overlying mud drapes often present load structures (Fig. 3C). Towards the top of the upper URU (138-139 m of the measured section) we observed fine- to medium-grained and cross-stratified sandstone channels, 0.5 to 3 m long and up to 30 cm thick, and laterally changing to the thin-bedded and fine-grained sandstone layers (Fig. 3F).

Tetrapod footprints (see section 4.4.1 below) are mostly found in the basal sandstone layers, which provide extensive outcropping surfaces. Some small footprints are found in layers above the basal one (in some cases observed in cross section). In a particular case, the lower half of a layer preserved a tetrapod footprint covered by the uppermost laminae (Fig. 3E). Invertebrate trace fossils with tiny, well-defined features (see section 4.4.2 below) are also found in the fine-grained sandstone layers, usually preserved as casts.

The whole set of sedimentary structures suggests a relatively dry setting if compared with the lower URU. The upper URU is here interpreted as a distal alluvial plain system (fan fringe/playa-lake, or ephemeral lacustrine). The muddy portions of the succession would indicate conditions of less energy in the depositional environment. In contrast, the coarser intervals (i.e., the 54 intervals of thin-bedded sandstone layers) would indicate more energetic conditions.

Such duality of environments has been recorded as a monsoonal system related to the formation of Pangaea (Parrish and Peterson, 1988; Kutzbach and Ziegler, 1993; Roscher and Schneider, 2006;

Roscher et al., 2011; Tabor et al., 2011) established in the equatorial region since the early Permian (Tabor and Montañez, 2002). Therefore, the thin-bedded sandstone layers would correlate with maximum monsoonal periods and the thick mudstone intervals would correlate with periods of reduced monsoonal activity. Similar monsoonal systems are those of the Salagou formation from the French Lodève Basin (Roscher and Schneider, 2006; Schneider et al., 2006), although these deposits have recently been dated as early–middle Permian (Michel et al., 2015).

The overlying Buntsandstein succession is 103 m thick, being one of the thinnest observed in the Catalan Pyrenees. The base of the Buntsandstein is represented by a 20 to 50 cm thick microbreccia of quartz pebbles with subordinated feldspar and lithics, and a matrix of red coarse-grained sandstones and mudstones (Fig. 3G-I). It is slightly erosive, and the topmost portion is composed of fine- to very fine-grained laminated sandstone, which is mud-cracked. The composition of this microbreccia is equivalent to that of the Buntsandstein basal conglomerates from other Pyrenean regions (e.g., Gretter et al., 2015; Fig. 3I), and can be traced laterally to the well-developed conglomeratic sequences (Figs. 1, 2). This microbreccia overlies a fine-grained sandstone interval of six layers from the upper URU (Fig. 3G, 3H).

The basal microbreccia is overlaid by a 13.5 m thick sequence composed of red mudstones, with a 1 m thick grey interval at the lower part (at 146.7-147.7 m in the measured section; Fig. 3J). Four intervals of thin-bedded and fine-grained sandstone layers as those of the upper URU are found in the red mudstones above the grey interval. Despite slight differences in colour and composition (see section 4.3 below) this interval also displays the cyclicity observed in the upper URU attributed to the monsoonal recurrence.

The successive interval consists of fine- to medium-grained channelized sandstones with trough and planar cross stratifications, ripples and other flow structures, as well as vertical burrows; thin conglomeratic layers (10-30 cm thick) occasionally constitute the base of the sandstone bodies (lag deposits). These bodies build up fining-upwards sequences, and often grade to metric red mudstone intervals with occasional carbonate nodules of pedogenic origin (Fig. 2). These facies are interpreted as alluvial fans with braided systems evolving to meandering and floodplain settings. The carbonate-dominated Muschelkalk facies, resulting from the Middle Triassic marine transgression, cover the Buntsandstein deposits.

4.2. Cyclostratigraphy

The upper URU and the first 13.5 m of the Buntsandstein facies are built up of alternating mudstones and thin-bedded sandstone intervals with a cyclic stacking pattern. We have defined the basic sequences or cycles to include two half muddy parts and the interbedded interval with sandstone layers (i.e., sandstones interpreted to represent the maximum enhanced monsoonal periods). Thus, a basic sequence starts and finishes in the middle of the relatively thick muddy interval layers representing periods of reduced monsoonal action. The total number of sequences is 58: 53-54 at the upper URU and 4-5 at the Buntsandstein facies, where sequence 54 starts in the upper URU and finishes in the Buntsandstein. Spectral analysis of the code 1 time series in the depth domain (Fig. 2C) displays significant peaks in a band including periods in the range 1-3 m, which correspond to the main thickness

of the basic sequences. Other peaks which are not found to be significant are located in bands corresponding to periods of 6-9 m and 21-29 m, respectively. The use of this simple lithologic code 1 is intrinsically limited. The stacking pattern of the basic sequences readily suggest some kind of cyclic modulation as there appears to be recurring variations of their thickness (Figs. 2B, 2C, 3A). Code 2 time series better accounts for such observations and should be more suited to infer modulations acting on the basic sequences. Indeed, spectral analysis of code 2 series (Fig. 2C) display significant peaks both at the 8-12 m band and around 24 m. These are compatible with the inferred bands on the code 1 time series. Consequently, a short-eccentricity origin (~100 kyr duration) may be attributed to the basic sequences while the band with periods of 8-12 m would represent the 400 kyr long eccentricity cycle. Moreover, in this context, the cyclicity with periods around 24 m might fit with the very long 1.2 Myr obliquity modulation cycle, which have already been detected in the Permian (Fang et al., 2015; Li et al., 2016). The alternative interpretation of the basic cycle as precession cycles (~21 kyr) appears less likely as the 24 m period would be difficult to fit to any orbital period despite the 8-12 m could still fit to short eccentricity. Collectively, we favour the interpretation of the basic sequences as short eccentricity cycles driven by depositions in a monsoonal climate system. We conclude that the upper URU and lowermost Buntsandstein represent about 5.8 Myr of monsoonal deposition.

4.3. Mineralogy and elemental succession

Coll de Terrers section bulk rock mineralogy as studied by XRD allowed us to identify the following main minerals (in parentheses, SQPA values obtained with the RIR method are given): quartz (3-39.9 %), calcite (18.3-49.1 %), albite (0.8-18.5 %), clinochlore (4.5-33.9 %), hematite (0-5.3 %), kaolinite (1.3-18.9 %) and muscovite/illite (5.4-45.3 %). Analcime (0-1.4 %) was only detected in two clusters found at the uppermost URU (between 135.5 m and 141.6 m of the measured section) (Fig. 4). Other minor phases (each one of less than 1 % in abundance) were found on specific levels, including microcline (between 14.5 m and 49.44 m) and rutile (between 135.5 m and 148.1 m). Fig. 4 shows the main mineral variations from the lower to the upper URU (18 samples from 4.4 m to 58.0 m of the measured section) and from the upper URU to the Buntsandstein facies (56 samples from 134.5 m to 148.1 m of the measured section).

The lower and upper URU display distinctive proportions of some minerals like quartz and kaolinite, which are abundant in the lower URU and depleted in the upper URU (Fig. 4). On the contrary, significantly larger amounts of albite and muscovite/illite are found in the upper URU relative to the lower URU. The simultaneous reduction of kaolinite and increase of albite may indicate a shift from humid to semiarid conditions (Schneider et al., 2006), which is in accordance with the sedimentary structures from the lower and upper URU, respectively (Figs. 2, 3, S1, S2). A similar palaeoclimatic trend of the Pyrenean units was proposed by Gascón and Gisbert (1987), who documented an aridification increase in the Permian. De la Horra et al. (2012) also reported a humid to semiarid climate transition in the middle-late Permian of the Iberian Basin, and Gómez-Gras and Alonso-Zarza (2003), Linol et al. (2009) and Liebrecht et al. (2016) documented semiarid conditions for the uppermost Permian deposits of the Balearic Islands. The sizable decrease of quartz contents in the upper URU is possibly related to reduced chemical weathering (see also Williams et al., 2012), as this mineral is

more resistant than feldspars and rock fragments (Coney et al., 2007). In turn, analcime occurs both as a primary mineral in alkaline igneous rocks but can also be authigenically formed (Remy and Ferrel, 1989; Schenider et al., 2006). The latter is the most possible origin of this mineral in Coll de Terrers, as no signals of igneous rocks have been found in the succession.

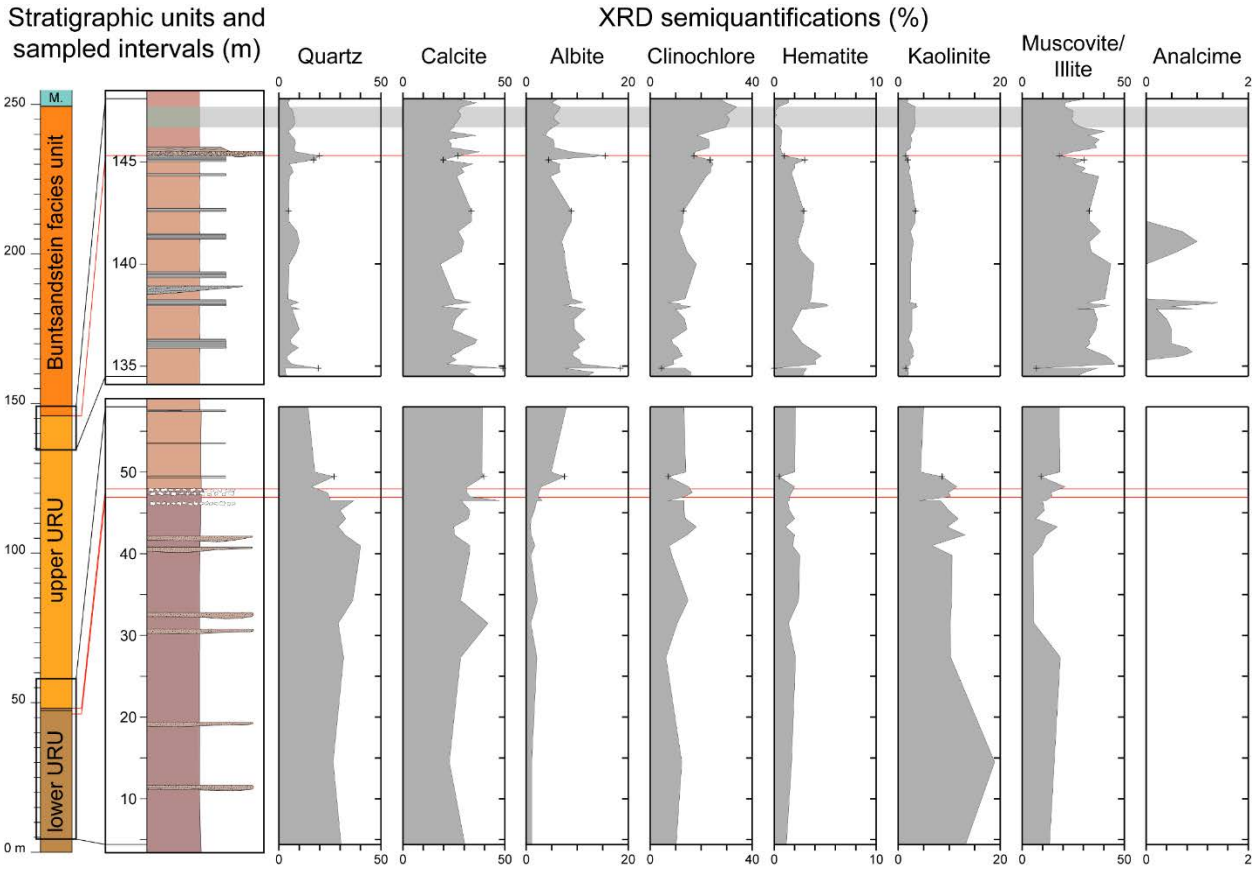

Figure 4. Semiquantification of main minerals (in percentage) obtained by XRD. "+" correspond to sandstone samples. Red lines correspond to the septarian nodules (double line; lower/upper URU boundary) and to the upper URU/Buntsandstein boundary. Grey interval corresponds to the grey mudstones at the lowermost Buntsandstein facies.

From the uppermost URU (142.6 m of the measured section) to the lowermost Buntsandstein red mudstones, significant increase of clinochlore contents accompanied with reduced hematite contents (as well as a slight decrease of albite) have been observed. Abundance of quartz and muscovite/illite remain nearly constant between the upper URU and the Buntsandstein facies. Peaks of albite and quartz are found in the basal Buntsandstein microbreccia, most probably corresponding to pebbles (Fig. 3G-I). In the grey interval of the basal Buntsandstein red mudstones (146.7-147.7 m of the measured section; Fig. 3H) albite and kaolinite slightly increase, clinochlore highly increases, muscovite/illite decreases and hematite is depleted. To sum up, the slight differences in mineral proportions found by XRD are not sufficiently significant to suggest a climatic change between these units. Thus, we conclude that most probably semiarid conditions persisted across the upper URU and lowermost Buntsandstein, also supporting continuity in sedimentation throughout these units.

Trends of calcite are not considered here, as this mineral infills postdepositional fractures cross-cutting the succession (Fig. 3C-E). Thus, part of the measured calcite is not from the rock composition but of diagenetic origin instead.

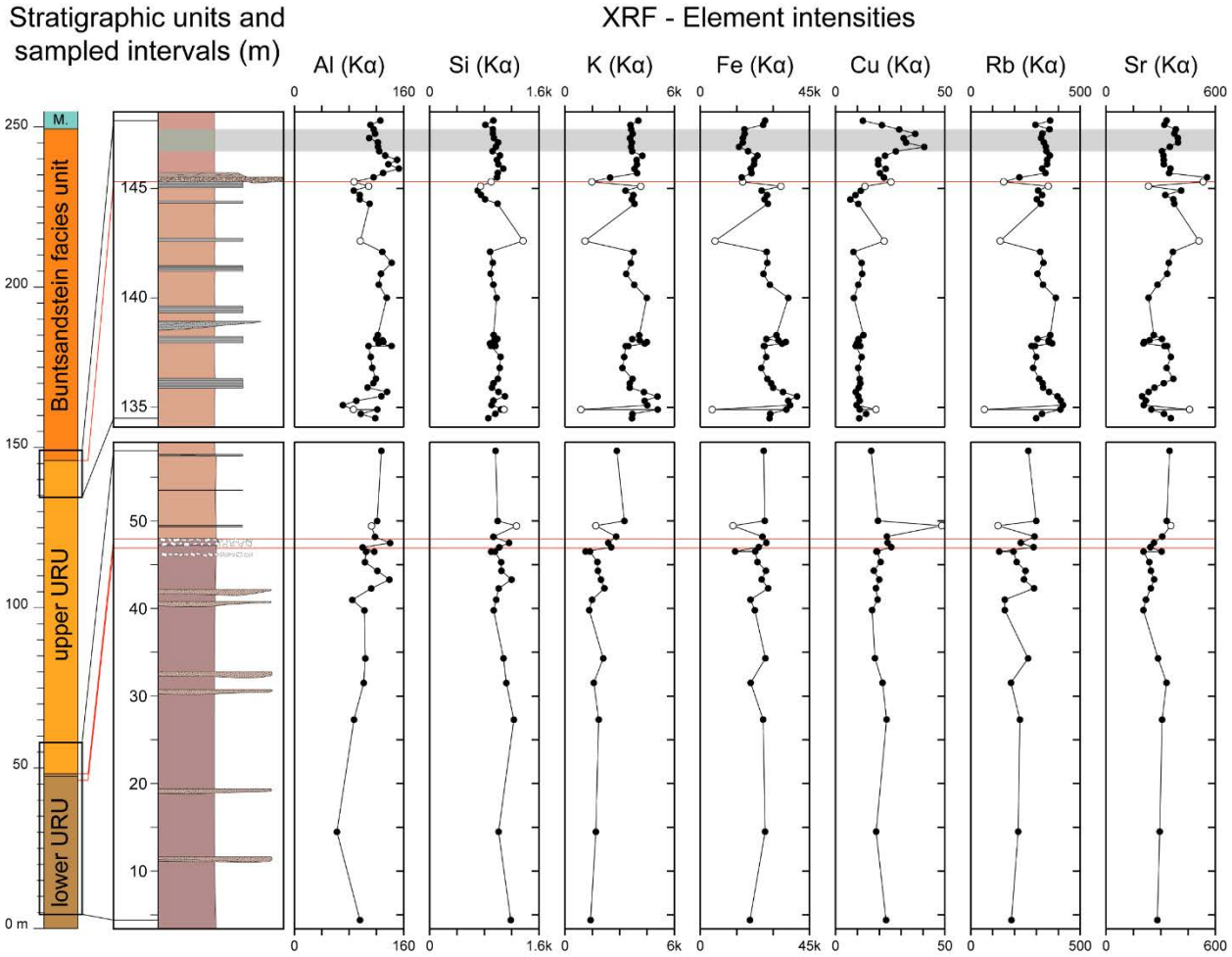

Figure 5. Element intensities obtained by XRF. Black and white circles correspond to mudstone and sandstone samples, respectively. Red lines and grey interval as in Fig. 4.

The mineralogical data was complemented with XRF measurements, which allowed us to monitor XRF signals for a range of major and trace elements (Al, Si, K, Fe, Cu, Rb and Sr in Fig. 5; Ca, Ti, Cr, Ni and Pb in Fig. S3). The most notable intensity trends (Fig. 5) reveal several changes across the three units:

1) Increase of K (and also of Rb, which displays an equivalent trend) from the lower to the upper URU, consistent with the muscovite/illite increasing.

2) Significant decrease of Fe accompanied by increased intensity of the Cu peak, across the upper URU/Buntsandstein boundary, coincident with the hematite reduction. Copper is generally related to environments with low oxygen levels (Hofmann et al., 2000; Hiete et al., 2006), which could be linked to the decrease of hematite observed by XRD. This mineral is formed in oxic conditions, and therefore the observed hematite reduction may be a consequence of lower atmospheric oxygen levels (Hiete et al., 2006; Benton and Newell, 2014).

3) Slight decrease of Al, K and Fe signals in the Buntsandstein grey mudstone interval, relative to neighbouring materials, and increase of Cu and Sr (and possibly a minor increase of Ni) signals. These observations are coincident with the clinochlore increase, muscovite/illite reduction and hematite depletion, which could be related to anoxia in the lacustrine/playa-lake water (Hiete et al., 2006; see section 5 below).

4.4. Palaeontological content

The Coll de Terrers fossil assemblage is mainly composed of tetrapod footprints and invertebrate trace fossils located at the upper URU. In the lower URU and Buntsandstein facies only invertebrate burrows and root trace fossils were identified. Thus the main focus of the section is on the Permian upper URU fossil record.

4.4.1. Vertebrate footprints

Prior to this study, the known URU vertebrate fossil record was limited to the unrecovered large tetrapod footprints from Palanca de Noves (stratigraphically located 116 m below the Triassic angular unconformity; Robles and Llompart, 1987), and to a synapsid caseid vertebra from La Trava (stratigraphically located 35 m below the Triassic angular unconformity; Mujal et al. 2016a). Coll de Terrers yields four tetrapod footprint morphotypes (I-IV), as well as several unclassifiable rounded and oval-shaped deep tracks characterized by large expulsion rims. Footprints are preserved in concave epirelief in the fine-grained sandstone layers of the upper URU. Such layers were cohesive substrates that enhanced footprinting. Herein we also re-analyse the footprints reported by Robles and Llompart (1987) to study the complete succession of tetrapod footprints along the Pyrenean URU. These ichnites are currently lost due to construction of the road to the town of La Seu d'Urgell during the nineties, so our reanalysis is based on the descriptions and photographs published by these authors.

- Morphotype I (Figs. 6A, B, S4, S5)

Description: This morphotype is found in the basal fine-grained sandstone layer of the sequences 9 (at 70.20 m; Fig. S4A), 23 (at 95.20 m; Figs. 6A, S4B-I) and 38 (at 119.80 m; Figs. 6B, S5) of the measured section. Tracks of this morphology are settled in alternating manus-pes sets. Manus impressions are pentadactyl, semiplantigrade to plantigrade and wider than long. Manus digits, displayed in arch form, are short, mostly preserved as rounded tip impressions, with thin and shallow phalangeal pad marks (Fig. S5C). A low expulsion rim appears in the posterior (proximal) part of the tips of some tracks (Fig. S4B, C). Digit III is the longest, followed by digits IV, II and I. Digit V, the shortest, is just a faint impression. Digits I and II are the deepest, followed by digit III, digit IV is much less impressed. The palm is much wider than long, with a concave and shallow posterior margin. A rounded and deep impression is observed below digit I. The deepest part of the palm is an oval-shaped impression below digit III. Pes tracks are generally poorly preserved, they are longer than wide, pentadactyl and plantigrade, and in some cases partially overprint manus (Fig. 6A, S4C-I). When preserved, pedal digits are also displayed in arch form (Figs. 6B, S4A, S5). Digits are short and stubby, preserving oval- to round-shaped tips, slightly wider than long. In one track digits are elongated (Fig. S4G). Digit III is the longest, and digit V is the smallest. The posterior and outer half of the sole is the deepest impressed part of the footprint, in some cases surrounded by an expulsion rim (Fig. S4A). Trackway pace angulation is estimated to be around 90º in both manus and pes tracks. Manus tracks are slightly rotated inwards, whereas pes tracks are slightly rotated outwards.

Remarks: The quadrupedal tracks, displayed in alternating manus-pes sets, with low pace angulations and the shape of both manus and pes impressions are characters found in the *Dicynodontipus* tracks of

the late Permian *Cistecephalus* Assemblage Zone from the South African Karoo basin (de Klerk, 2002). This ichnogenus is also recorded in the Early and Middle Triassic from Australia (Retallack, 1996) and Germany and Britain (Haubold, 1971). The different track preservations are related to substrate rheology (i.e., moisture and water content). Such variety of preservations, as well as the partial overprinting of pes to manus impressions, and the footprint depth patterns, were also observed by de Klerk (2002) in the late Permian of South Africa. All these features suggest that the Coll de Terrers tracks are most probably close related to the South African *Dicynodontipus* footprints if not the same. The lack of more detailed tracks and complete trackways preclude ichnogeneric assignation. Overall, the Coll de Terrers tracks could represent the first record of *Dicynodontipus* in the Permian of Western Europe. If true, this record suggests a late Permian age for the upper URU of Coll de Terrers.

- Morphotype II (Figs. 6C, S6)

Description: Footprints of this morphology are found in different fine-grained sandstone layers of the sequence 39, at 120 m of the measured section (Figs. 6C, S6). Tracks are arranged in manus pes sets. Tracks are nearly rounded and slightly wider than long. Manus (about 10 cm wide, 7 cm long) are smaller and more oval-shaped than pes tracks (about 15 cm wide and long). Manus are semiplantigrade, with only three short and rounded digits preserved (I, II and III, in increasing length). Digit II is the most deeply impressed, followed by digit I. Digit III is slightly shallower than palm impression, which is deeper below digit I (Fig. 6C). Manus is slightly rotated inwards respect to pes impression. Pes tracks are nearly rounded, plantigrade to semiplantigrade, mostly preserving digits I to IV, in increasing length and depth. Digit I is much shorter than digit II; digits III and IV are nearly equal in length. A rounded and relatively deep impression is observed in the sole below digit I. The outer half of the sole is the deepest impressed part. A shallow ridge divides the sole between digit I and its basal pad from the rest of the footprint.

Remarks: The slightly wider than long footprints and their size, with pes larger than manus impressions and the stubby digits in increasing length from I to IV, are traits of *Pachypes*, a late Permian ichnogenus recorded from Italy (Valentini et al., 2009), Morocco (Voigt et al., 2010), Niger (Smith et al., 2015) and possibly from Russia (Valentini et al., 2009; but see Gubin et al., 2003; Surkov et al., 2007; Voigt et al., 2010). Track preservations preclude a confident assignation, but all the previous characters suggest *Pachypes* (or a close related one) as the most favoured ichnotaxon for Morphotype II.

- Morphotype III (Figs. 6D, S7)

Description: This morphotype is preserved in the basal layer of the sequence 27, at 100.98 m of the measured section (Figs. 6D, S7). Footprints are deeply impressed, bordered by relatively high and wide expulsion rims. They preserve three thin and long digits, representing about 2/3 of the total footprint length. Two of the three digits are nearly parallel, while the other digit is separated, with a higher angle of divarication. Digit tips are rounded. The heel, narrower than the total digits width, shows different shapes, appearing as a smoothed triangle, slightly curved (convex), or separated by a ridge from the

rest of the impression (Fig. S7A-F, H, I). Some tracks are rather aligned and alternated, possibly corresponding to the same trackway, although patterns are not regular (Fig. S7G, J). If these tracks correspond to a trackway, the most separated digit would correspond to digit I, as it would be in the footprint inner (medial) part.

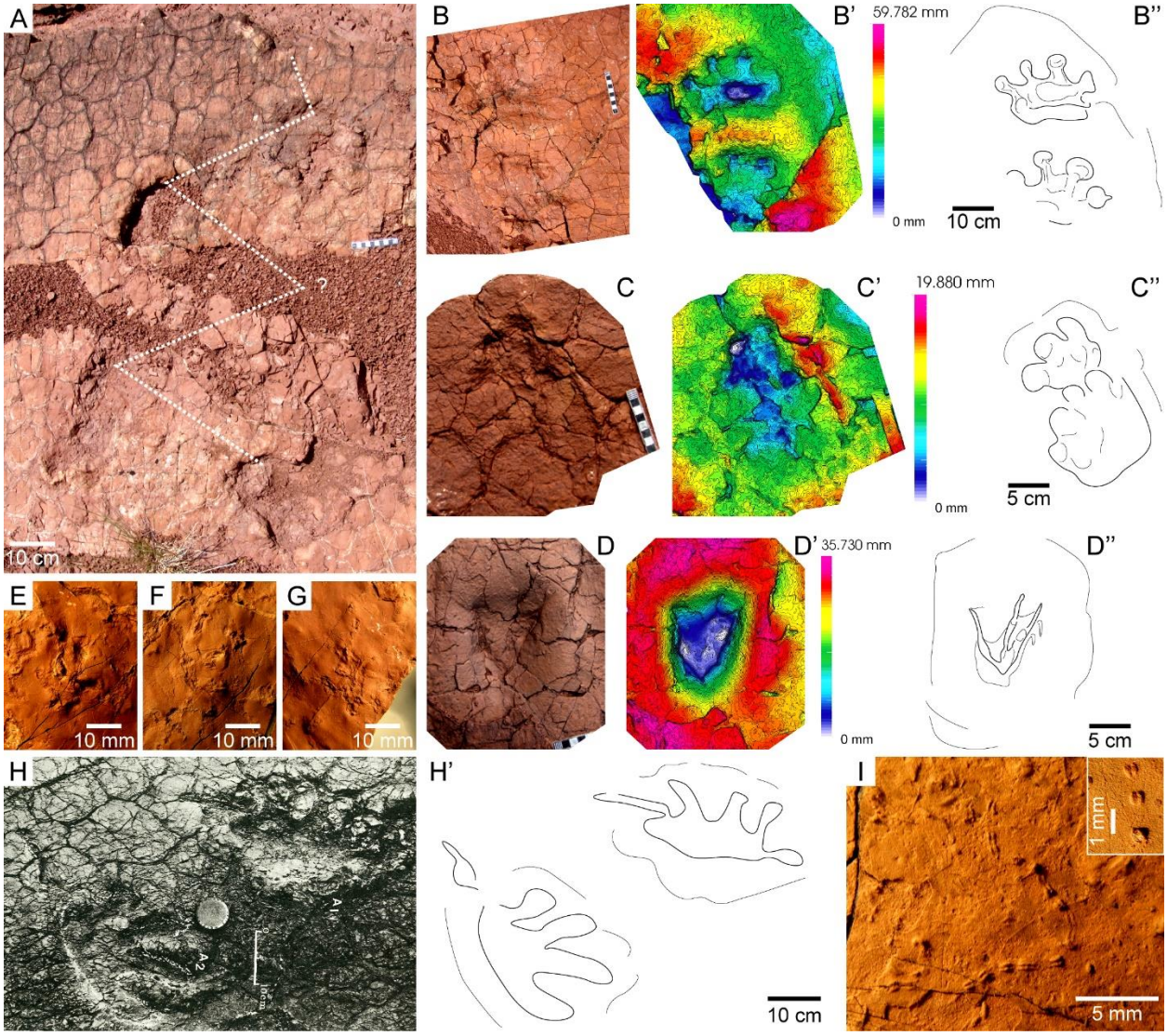

Figure 6. Ichnology of the upper URU, including tetrapod footprints (A-H) and arthropod ichnites (I). A, B. Morphotype I, including a partial trackway with manus paces in dashed white line (A) and a well-preserved manus and partial pes with the 3D model and ichnites outline (B). C. Morphotype II manus-pes set, with the 3D model and ichnites outline. D. Morphotype III, with the 3D model and ichnite outline. E-G. Morphotype IV, including three left tracks. H. Footprints from Palanca de Noves (photo of "forms A" modified from Robles and Llompart, 1987) and ichnites outline. I. Ichnites preliminary attributed to *Acripes* and *Rusophycus*.

Remarks: The asymmetrical fork-like shape of these footprints, only preserving three digits, is unknown from any Permian tetrapod footprint morphotype. Therefore, this shape most probably results from a specialized gait in a soft (but cohesive) substrate. Anatomical features are hardly preserved, precluding a confident assignation. In addition, the original track surface may be covered or eroded, thus some tracks may correspond to overtracks or undertracks, respectively. This occurs in microbial

mats from tidal flats, where water content variation and surface mud-cracking are frequent (Marty et al., 2009), hence being similar to the upper URU sandstone layer substrates.

- Morphotype IV (Figs. 6E-G, S8)

Description: These footprints were found in two *ex situ* blocks 7 cm thick (including IPS-99097, Fig. S8) at the uppermost URU, close to the sandstone channel (sequence 49) at 138.5 m of the measured section. Footprints are pentadactyl, digitigrade and longer than wide. Measuring about 2.5x2 cm, they are the smallest vertebrate ichnites of Coll de Terrers. Digits are thin and long, in increasing length from I to IV, which are curved inwards. Occasionally digit I is not preserved. Digit V, rotated and curved outwards, is between digits I and II in length. Digit tips are clawed. Despite the fact that surfaces are plenty of tracks, no manus-pes sets nor trackways are recognized.

Remarks: Small-sized footprints with this asymmetrical shape, due the relative length of the slender and curved digits, may be attributed to either *Dromopus* or *Rhynchosauroides* (e.g., Haubold, 1971). *Dromopus* is mostly recognized in Lower Permian deposits (Marchetti, 2016), whereas *Rhynchosauroides* is identified in the Upper Permian record (Valentini et al., 2007, 2009). Similar footprints from the late Permian of the Nigerian Moradi formation were attributed to *Dromopus* by Smith et al. (2015) although further detailed studies are necessary for a confident ichnotaxonomy. Therefore, and due to track preservation, we refer Morphotype IV to a *Dromopus-Rhynchosauroides* plexus awaiting further analysis.

- Footprints published by Robles and Llompart (1987) (Fig. 6H)

Description: These authors described four ichnites preserved in concave epirelief and located in the URU, 116 m below the Triassic unconformity at the Palanca de Noves site. Footprints are pentadactyl and plantigrade to semiplantigrade, probably corresponding to the same trackway. Robles and Llompart (1987) differentiated four forms: A_1, A_2, B_1 and B_2. Ichnites A_1 and A_2 correspond to a manus and a pes, respectively, building up a right couple. B_1 and B_2 correspond to a pes and a manus, respectively, from two different (but consecutive) left sets. Manus is much wider (ca. 35 cm) than long (ca. 19 cm), and with relatively long digits (about 1/3 of the total footprint length) with rounded tips. Digit I is elongated and rotated backwards. Digit III is the longest, followed by digit IV and digit II. Digit V is slightly shorter than digit I. The palm, wider than long, is oval shaped. Pes track is wider (ca. 33 cm) than long (ca. 20 cm). Digits III and IV are the longest, followed by digit II. Digits I and V, similar in length, and much shorter than the others. In the right manus-pes set, manus is rotated inwards and closer to the trackway midline than pes track, which is nearly parallel to the midline. If these footprints build up a single trackway, pace angulation is relatively low, about 90º.

Remarks: These tracks were correlated to different trackmakers by Robles and Llompart (1987): the forms A were identified as temnospondyl or seymouriamorph tracks, and the forms B as a reptile-like track or a chirotheriid. Nevertheless, these tracks most probably correspond to a single trackway, thus such morphological variations are related to locomotion and substrate rheology. Two ichnogenera present the characters described above: 1) the *Dicynodontipus* tracks from the *Cistecephalus* Assemblage Zone (late Permian) at the South African Karoo Basin (de Klerk, 2002), and 2) the *Merifontichnus* tracks from the La Lieude formation (middle Permian) at the French Lodève Basin (Gand et al., 2000; Gand

and Durand, 2006) and possibly from the late early Permian of the Italian Orobic Basin (Marchetti, 2016). Due to the available data, ichnotaxonomy should remain open, although considering the age of the succession (see discussion in section 5.2 below), *Merifontichuns* is the favoured ichnogenus for these ichnites.

4.4.2. Invertebrate trace fossils and plant remains

Invertebrate ichnites occur in the three Coll de Terrers units. In the distal meandering and floodplain systems of the lower URU, sandstone channels preserve either vertical or oblique, cylindrical and slightly sinuous bioturbations infilled by wine-reddish mudstone (Fig. S1E). Plant fragments and root traces are also preserved along the lower URU (Fig. S1F, S2B).

Several fine-grained sandstone layers of the upper URU yield both vertical and horizontal (and ramified) cylindrical bioturbations of up to 1 cm of diameter (Fig. S9A-E). When present, vertical burrows are relatively abundant (Fig. S9A). Gisbert (1981) attributed the vertical burrows to bivalves. Otherwise, ramified and horizontal burrows may correspond to arthropods. The lowermost surfaces of some fine-grained sandstone layers preserve abundant trace fossils with two differentiated morphologies: 1) Ichnites of <1 mm to 3 mm long, oval-shaped and bilobated (i.e., "coffee grain-like" shape; Figs. 6I, S9G-J), attributed to *Rusophycus*, which is a common Permian-Triassic resting trace fossil (Gand et al., 2008); 2) relatively long and sinuous ichnites composed of two parallel ribbons with a medial ridge, often associated with *Rusophycus* (Figs. 6I, S9I, S9J); these impressions resulted from locomotion, probably corresponding to *Acripes* (or close related) ichnogenus (Gand et al., 2008). These ichnites were impressed in a submerged substrate, as their trackmakers, notostracan arthropods (triopsids), are unable to move out of water (Gand et al., 2008). Associated with some of these arthropod ichnites, several globular structures possibly corresponding to pellets are also recognized (Fig. S9J).

4.4. Correlation with the Pyrenean record

The Coll de Terrers succession is integrated with those from Palanca de Noves at the Segre river valley (3.87 km Westwards; Gisbert et al., 1985; Robles and Llompart, 1987) and La Trava-Coll de Creus (6.85 km Eastwards; Gretter et al., 2015; Mujal et al., 2016a), which present significant differences (Figs. 1, 7). The major and traceable feature is the Westwards and Eastwards thickening of the Buntsandstein facies, which overlie the URU in angular unconformity and local conformity in the studied area (Fig. 7). Such thickening was the result of erosive depocentres located to the W and E of Coll de Terrers (e.g., the number of upper URU cycles at Coll de Creus is less than 30, whereas Coll de Terrers preserves 54 cycles; Fig. 1C). Coll de Terrers remained as a topographic high where accommodation was reduced (e.g., the Buntsandstein unit thickness at Coll de Terrers is of 103 m and in Palanca de Noves is of 213 m). The cycles at the lowermost part of the Buntsandstein from Coll de Terrers have not been identified at any other area of the Catalan Pyrenees. Instead, in the other successions the basal conglomerates of alluvial braided systems are overlaid by fine- to medium-grained sandstones and mudstones of fluvial (mostly meandering) and floodplain systems (Mujal et al., 2016a). This feature denotes that in Coll de Terrers the basal Buntsandstein deposits record a singular environment of low energy (i.e., playa-lake or ephemeral lacustrine) instead of the coarse braided systems

found in other Pyrenean regions (Gisbert et al., 1985; Gretter et al., 2015). As a result, the Coll de Terrers Permian deposits were not exposed to any major erosion, and the Permian-Triassic succession is in continuity (i.e., strike and dip angles, and sedimentary setting do not change across the URU/Buntsandstein boundary, thus the usual Triassic angular unconformity is not present at all). This feature is exceptional in the Pyrenees and probably within the continental deposits of Western Europe (Bourquin et al., 2007, 2011; Gretter et al., 2015).

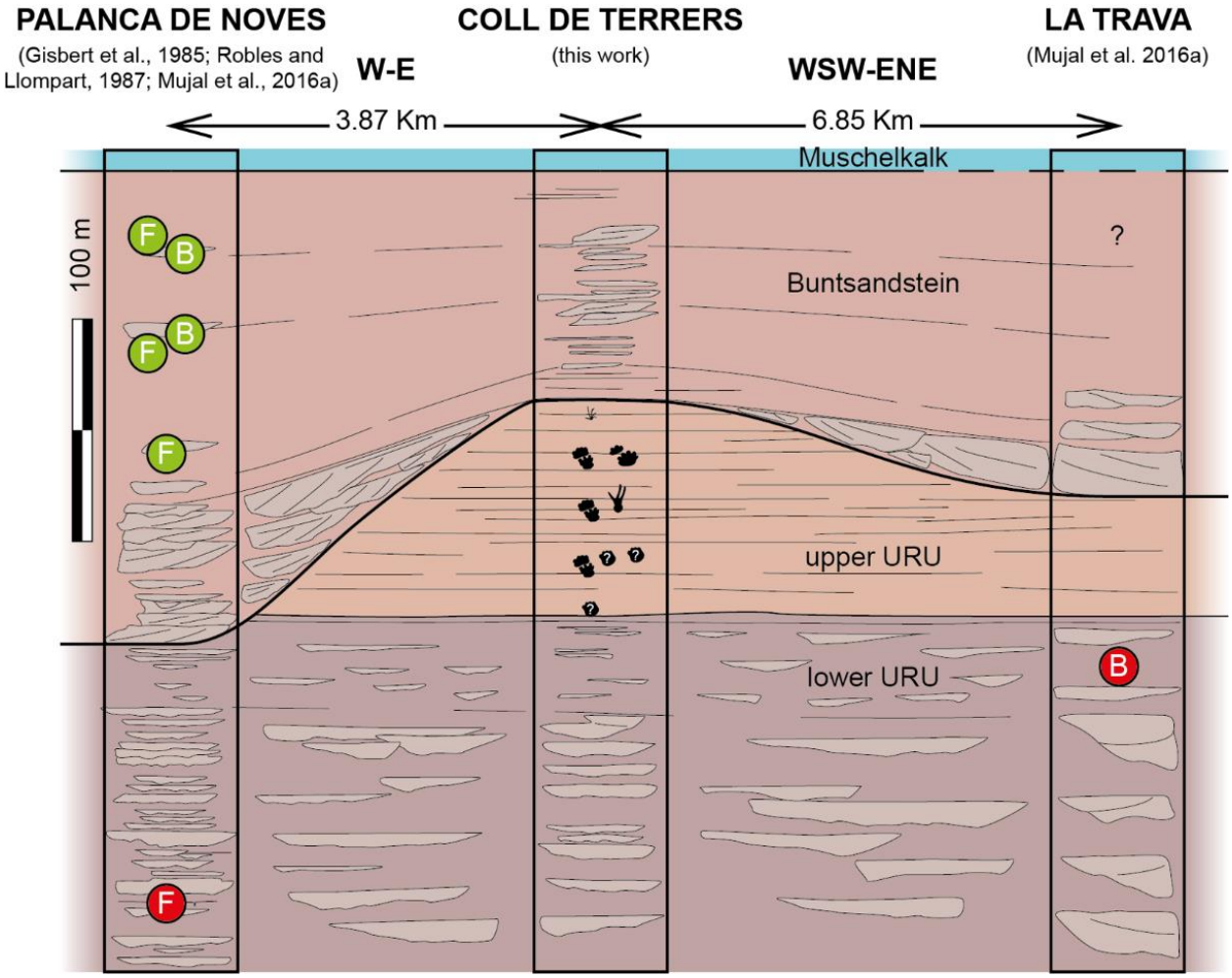

Figure 7. Correlation of the URU-Buntsandstein sequences with the stratigraphic position of the URU vertebrate remains. Previously published tetrapod bones (B) and footprints (F) are indicated in red for the URU and in green for the Buntsandstein facies. Symbols of Coll de Terrers tetrapod footprints as in Fig. 2.

5. Discussion

The Permian–Triassic transition from the Catalan Pyrenees has been recently investigated by Mujal et al. (2016a). These authors documented a lack of record of about 15-19 Myr between the Permian and Triassic successions in sections preserving well-developed conglomerates at the base of the Buntsandstein from Palanca de Noves and La Trava sections. In this last section, a synapsid caseid vertebra of the lower URU uppermost part was tentatively correlated to the Wordian (middle Permian), thus suggesting that the upper URU is younger. The correlation of the Pyrenean lower and upper URU fossil localities shows that the Palanca de Noves tracks reported by Robles and Llompart

(1987) were stratigraphically below the caseid vertebra (Fig. 7). These ichnites were preserved in thin mudstone and thin-bedded sandstone intervals settled in a succession with abundant levels of conglomeratic alluvial channels (Robles and Llompart, 1987), thus corresponding to the lower URU. In our analyses we found that these ichnites could be attributed to either *Merifontichnus* or *Dicynodontipus*. Considering the inferred age for the caseid vertebra (early middle Permian), the Palanca de Noves tracks, which are older than the vertebra, more likely correspond to *Merifontichnus*. This ichnogenus is known from the middle Permian La Lieude formation of France (Gand et al., 2000; Gand and Durand, 2006), whereas *Dicynodontipus* is known from the late Permian *Cistecephalus* Assemblage Zone of South Africa (de Klerk, 2002) and the late Permian of the Northern Italian Bletterbach Gorge, Dolomites (Kustatscher et al., 2017 and references therein).

These biostratigraphic inferences can be compared and coupled with the sedimentological and mineralogical trends of the succession. The lower to upper URU deposits record a transition from humid to semiarid conditions (Fig. 8). This climatic shift is possibly related to that of the upper portion of the Alcotas formation in the Iberian Basin (De la Horra et al., 2012) and also to the climatic shift documented in the early late Permian of northern Pangaea (Retallack et al., 2006; Roscher and Schneider, 2006; Słowakiewicz et al., 2009). This may imply that the lower/upper URU boundary could be correlated with the middle-late Capitanian (around the middle Permian extinction event) (Retallack et al., 2006; Sheldon et al., 2014; Day et al., 2015). Nevertheless, the lower/upper URU boundary possibly represents a paraconformity or sedimentary hiatus (i.e., long periods of exposition and development of levels with large nodules; Figs 8, S2); no evidences of the middle Permian extinction have been identified in the Pyrenees so far.

The upper URU records a cyclic alternation of facies, from mudstones to fine-grained sandstones, related to a monsoon system of orbital recurrence (Figs. 2, 3A, 3B). Such duality of facies would represent the seasonality proposed in the late Permian palaeoclimatic model of Roscher et al. (2011). Similarly, late Permian seasonality has also been documented in the Central Pangaean Moradi formation of Niger (Looy et al., 2016) and the Southern Pangaean Karoo Basin of South Africa (Gastaldo et al., 2015). The tetrapod footprint morphotypes I and II recovered in Coll de Terrers were potentially produced by similar (or the same) trackmakers as those corresponding to *Dicynodontipus* and *Pachypes* (i.e., dicynodonts and pareiasaurs, respectively), being present at the Karoo Basin (de Klerk, 2002) and Northern Italy (Kustatscher et al., 2017) and at the Moradi formation (Smith et al., 2015), respectively. In fact, the upper URU mudstones are barren of fossils, but the thin-bedded sandstone layers preserve tetrapod footprints, possibly indicative of periods of more favourable conditions for life development. The presence of burrows and notostracan ichnites may indicate that the fine-grained sandstone layers acted as a source of food. These ichnites were impressed in a submerged substrate, as their trackmakers are unable to move out of water (Gand et al., 2008), further denoting different conditions than those of the muddy intervals. Noteworthy, the thin-bedded sandstone layers record periods of subaerial exposure (Figs. 3B-E, 6A, 8) that, together with the notostractan ichnites, indicate recurrent dry and wet periods. This is indicative of a similar seasonality to that of Central Pangaea (Looy et al., 2016).

The correlation of the monsoonal sequences with 400 kyr eccentricity cycles implies that the upper URU and the lowermost Buntsandstein were deposited along ~5.8 Myr. In this way, the aridification observed at the upper URU would be at least of 5.3-5.4 Myr older than the upper URU/Buntsandstein boundary. The lack of any major erosion and the URU/Buntsandstein concordant contact both suggest that the Permian–Triassic boundary (PTB) could be preserved somewhere in the uppermost URU or lowermost Buntsandstein, possibly in the URU/Buntsandstein boundary itself (Fig. 8). Note also that the URU/Buntsandstein boundary does not show a disruption in the cyclicity (Fig. 2). This agrees with the suggested correlation of the upper URU with the early late Permian aridification and with the South African *Cistecephalus* Assemblage Zone. The presence of tractive structures in the uppermost URU at Coll de Terrers (e.g., channel at 138.5 m of the measured section; Fig. 3F) denote a higher water flow (i.e., increase in water flow) than that of the thin-bedded sandstone layers. This switch to more energetic conditions at the uppermost URU culminated with the basal Buntsandstein microbreccia (Figs. 3G-I, 8). A similar energetic increase of the sedimentary style has been documented in the Permian-Triassic transition of the Iberian Basin (Arche and López-Gómez, 2005), Russia (Newell et al., 2010; Benton and Newell, 2014), South Africa (Ward et al., 2000) and central India (Chakraborty and Sarkar, 2005). This energetic increase is related to the loss of plants that fix the substrate on account of the end-Permian extinction (Retallack et al., 1998, 2006; Michaelsen, 2002; Benton and Newell, 2014).

Another peculiar sedimentological feature of Coll de Terrers is the sudden switch from red to grey mudstones in the lowermost Buntsandstein (Fig. 3J). Accordingly, this 1-m-thick grey mudstone interval shows a sudden shift of several minerals and elements (Figs. 4, 5). Particularly, the hematite depletion and the increase of Cu and Sr (and also the minor increase that seems to occur in the case of Ni) possibly denote anoxic conditions. Grey intervals with Cu enrichments, related to anoxia, are recorded in the lowermost Buntsandstein of the Germanic Basin (Hiete et al., 2006). Noteworthy, the end-Permian extinction is correlated with oceanic anoxia and acidification (Grice et al., 2005; Meyer and Kump, 2008) that influenced atmosphere (Kump et al., 2005). In this way, in marine sections of South China, spikes of Cu and Ni related to the Siberian volcanism coincide with the end-Permian extinction event (Rothman et al., 2014). Strontium increase across the PTB has been related to increased acidic conditions in the Iberian Basin (Borruel-Abadía et al., 2016). With the present elemental data, such interpretations for Coll de Terrers still remain open, although peaks of Sr and Al are also observed at the lowermost Buntsandstein mudstones (Fig. 5). Coney et al. (2007) suggested that no distinct geochemical signatures are found across the PTB in the South African Karoo Basin, although that could be due to the lithological differences of the analysed sections. On the contrary, Williams et al. (2012) found geochemical trends correlated with the global record in the Australian Sidney Basin. Further geochemical analysis at Coll de Terrers will shed light on this terrestrial record and its potential correlation with marine sections.

Regarding the age of the Buntsandstein facies, Mujal et al. (2016a) established a late Olenekian (late Early Triassic) age for the portion of the unit overlying the basal conglomerates at Palanca de Noves, where no monsoonal sequences as those of Coll de Terrers are observed. The well-developed conglomeratic deposits from Palanca de Noves would correspond to by-pass deposits, and thus may not

preserve the lowermost Triassic record, as also occurs in La Trava (Fig. 7). Therefore, the basal conglomerates at Palanca de Noves are directly overlaid by meandering deposits (Mujal et al., 2016a). The 4-5 monsoonal sequences from the Coll de Terrers Buntsandstein correspond to the earliest Triassic record. Both sedimentological and mineralogical data indicate that these deposits formed under semiarid conditions, and thus they are probably related to the Early Triassic greenhouse crises (Retallack et al., 2011; Retallack, 2013). The overlying meandering deposits correlate with those of Palanca de Noves and La Trava (Fig. 7) and indicate a shift towards more humid conditions. At Palanca de Noves, such deposits yield a relatively diverse tetrapod ichnofauna and scarce bone remains (Fig. 7) related to the Early-Middle Triassic vertebrate recovery (Mujal et al., 2016a). All these features are possibly indicative of the transition to cooler temperatures at the end of the Early Triassic (Rey et al., 2016).

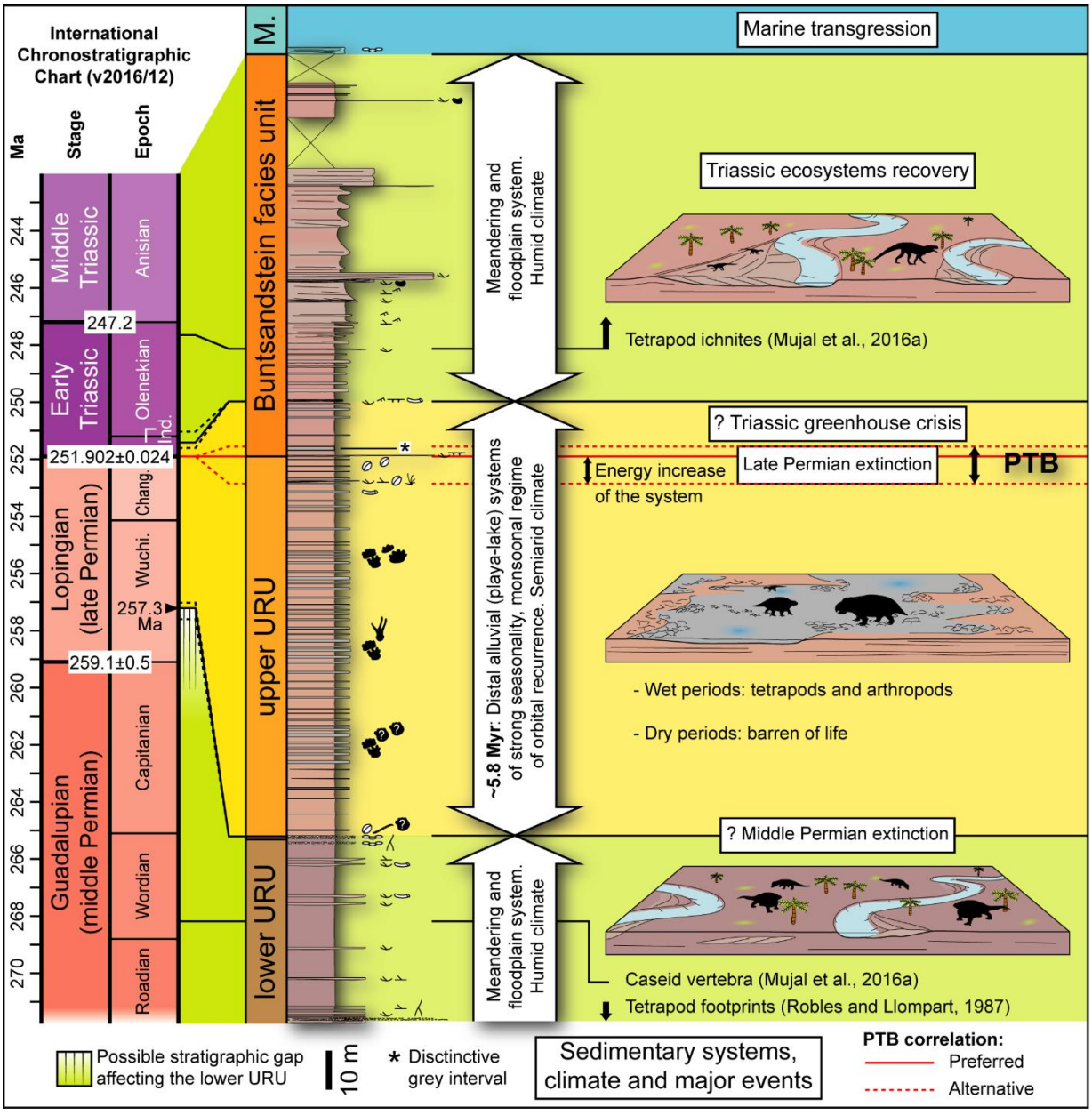

Figure 8. Suggested correlation of Coll de Terrers section with the International Chronostratigraphic Chart (v2016/12) by Cohen et al. (2013 updated) and major events recorded at the studied area. Ind.: Induan. Chang.: Changhsingian. Wuchi.: Whuciapingian. M.: Muschelkalk facies.

Further prospections, analyses and major efforts, including more detailed XRD and XRF studies and isotopic analyses as well, are required to elucidate the age of the Permian-Triassic deposits of Coll de Terrers, and other Pyrenean areas as well, and the potential biological crises recorded therein.

6. Conclusions

The Catalan Pyrenees, together with other regions from the Western peri-Tethyan domain, are a key target to decipher the late Palaeozoic–early Mesozoic events. Here we have provided new data on the continental Permian–Triassic transition of a recently identified area, Coll de Terrers. The sedimentary succession of the uppermost Permian units records different environments that, supported by the XRD analyses, point towards a transition from humid to semiarid climate that correlates with the late Permian aridification. The tetrapod ichnoassemblage also suggests a late Permian age for the uppermost Permian.

The late Permian succession was deposited under a monsoonal regime (already documented in equatorial Pangaea) in a low-energy setting (i.e., a distal alluvial plain), and orbital forcing imprint recurrence conditions (i.e., potential eccentricity and long-term obliquity cycles, hitherto unknown in the Permian–Triassic record of the Iberian Peninsula). The continuous sedimentary succession and the lack of any major erosion across the uppermost Permian and lowermost Triassic deposits imply the potential record of the Permian-Triassic boundary. This is supported by a sudden increase of the system energy close to the Permian–Triassic transition (documented in both northern and southern Pangaea), and also by the lack of any major erosion and sedimentary hiatus as well as by the preliminary cyclostratigraphic results.

In summary, Coll de Terrers records events and features globally recognized in Permian–Triassic terrestrial successions. This area, located in a narrow rift system at the Gondwana and Laurasia confluence, emerges as a reference zone to investigate the Permian–Triassic transition in terrestrial settings often characterised by scarcity of stratigraphic record. This is the first contribution to improve correlations between northern and southern Pangaean regions, shedding new light on the terrestrial Permian extinction events.

Acknowledgments

We acknowledge fieldwork support by Josep Marmi and Mireia Plà, preparation of thin rock samples by Luis Gordón and Marc Puigcerver at UAB, and XRD and XRF data acquisition and analysis by Josep Elvira and Soledad Álvarez at ICTJA-CSIC. E. Mujal acknowledges N.-E. Jalil (MNHN), S. Jiquel, B. Marandat, L. Marivaux, M. Vianey-Liaud, P.-O. Antoine and all ISE-M staff their kind help in the collection visits. E. Mujal obtained financial support from the PIF grant of the Geology Department at UAB, and from the Erasmus+ program of the UAB performed at the Palaeontology Department from the Institut des Sciencies de l'Evolution (Université de Montpellier, France). E. Mujal received funding from the SYNTHESYS Project http://www.synthesys.info/ (FR-TAF-3621, FR-TAF-4808) which is financed by European Community Research Infrastructure Action under the FP7 "Capacities" Program. J. Fortuny acknowledges the support of the postdoc grant "Beatriu de Pinós" 2014 – BP-A 00048 from the Generalitat de Catalunya. This work received support from CERCA programme at Institut Català de Paleontologia (ICP) and from the projects "Vertebrats del Permià i el Triàsic de Catalunya i el seu context geològic" and "Evolució dels ecosistemes amb faunes de vertebrats del Permià i

el Triàsic de Catalunya" (ref. 2014/100606), based at ICP and financially supported by the Departament de Cultura (Generalitat de Catalunya).

References

Alroy, J., 2013. Online paleogeographic map generator. http://paleodb.org/?a=mapForm

Arche, A., López-Gómez, J., 2005. Sudden changes in fluvial style across the Permian-Triassic boundary in the eastern Iberian Ranges, Spain: Analysis of possible causes. Palaeogeography, Palaeoclimatology, Palaeoecology 229, 104-126. https://dx.doi.org/10.1016/j.palaeo.2005.06.033

Benton, M.J., Newell, A.J., 2014. Impacts of global warming on Permo-Triassic terrestrial ecosystems. Gondwana Research 25(4), 1308-1337. https://dx.doi.org/10.1016/j.gr.2012.12.010

Borruel-Abadía, V., Barrenechea, J.F., Galán-Abellán, A.B., Alonzo-Azcárate, J., De la Horra, R., Luque, F.J., López-Gómez, J., 2016. Quantifying aluminium phosphate-sulphate minerals as markers of acidic conditions during the Permian-Triassic transition in the Iberian Ranges, E Spain. Chemical Geology 429, 10-20. http://dx.doi.org/10.1016/j.chemgeo.2016.03.007

Borruel-Abadía, V., López-Gómez, J., De la Horra, R., Galán-Abellán, B., Barrenechea, J.F., Arche, A., Ronchi, A., Gretter, N., Marzo, M., 2015. Climate changes during the Early-Middle Triassic transition in the E. Iberian plate and their palaeogeographic significance in the western Tethys continental domain. Palaeogeography, Palaeoclimatology, Palaeoecology 440, 671-689. https://dx.doi.org/10.1016/j.palaeo.2015.09.043

Bourquin, S., Bercovici, A., López-Gómez, J., Diez, J.B., Broutin, J., Ronchi, A., Durand, M., Arche, A., Linol, B., Amour, F., 2011. The Permian-Triassic transition and the onset of Mesozoic sedimentation at the northwestern peri-Tethyan domain scale: Palaeogeographic maps and geodynamic implications. Palaeogeography, Palaeoclimatology, Palaeoecology 299(1-2), 265-280. https://dx.doi.org/10.1016/j.palaeo.2010.11.007

Bourquin, S., Durand, M., Diez, J.B., Broutin, J., Fluteau, F., 2007. The Permian-Triassic boundary and lower Triassic sedimentation in western European basins: An overview. Journal of Iberian Geology 33(2), 221-236.

Chakraborty, T., Sarkar, S., 2005. Evidence of lacustrine sedimentation in the Upper Permian Bijori Formation, Satpura Gondwana basin: Palaeogeographic and tectonic implications. Journal of Earth System Science 114(3), 303-323. https://dx.doi.org/10.1007/BF02702952

Chumakov, N.M., Zharkov, M.A., 2003. Climate during the Permian-Triassic biosphere reorganizations. Article 2. Climate of the Late Permian and Early Triassic: General inferences. Stratigraphy and Geological Correlation 11(4), 55-70.

Cohen, K.M., Finney, S.C., Gibbard, P.L., Fan, J.-X., 2013 (updated). The ICS International Chronostratigraphic Chart. Episodes 36, 199-204.

Coney, L., Reimold, W.U., Hancox, P.J., Mader, D., Koeberl, C., McDonald, I., Struck, U., Vajda, V., Kamo, S.L., 2007. Geochemical and mineralogical investigation of the Permian-Triassic boundary in the continental realm of the southern Karoo Basin, South Africa. Palaeoworld 16, 67-104. https://dx.doi.org/10.1016/j.palwor.2007.05.003

Day, M.O., Ramezani, J., Bowring, S.A., Sadler, P.M., Erwin, D.H., Abdala, F., Rubidge, B.S., 2015. When and how did the terrestrial mid-Permian mass extinction occur? Evidence from the tetrapod record of the Karoo Basin, South Africa. Proceedings of the Royal Society B 282, 20150834. http://dx.doi.org/10.1098/rspb.2015.0834

de Klerk, W.J., 2002. A dicynodont trackway from the Cistecephalus assemblage zone in the Karoo, East of Graaff-Reinet, South Africa. Palaeontologia Africana 91(38), 73-91.

De la Horra, R., Galán-Abellán, A.B., López-Gómez, J., Sheldon, N.D., Barrenechea, J.F., Luque, F.J., Arche, A., Benito, M.I., 2012. Paleoecological and paleoenvironmental changes during the continental Middle-Late Permian transition at the SE Iberian Ranges, Spain. Global and Planetary Change 94-95, 46-61. https://dx.doi.org/10.1016/j.gloplacha.2012.06.008

Dercourt, J. Gaetani, M., Vrielynck, B., Barrier, E., Biju-Duval, B., Brunet, M.F., Cadet, J.P., Crasquin, S., Sandulescu, M., 2000. Peri-Tethys Atlas, Palaeogeographical maps, CCGM/CGMW, Paris: 24 maps and explanatory notes: I-XX, 1-269.

Erwin, D.H., 1994. The Permo-Triassic extinction. Nature 367, 231-236. https://dx.doi.org/10.1038/367231a0

Fang, Q., Wu, H., Hinnov, L.A., Jing, X., Wang, X., Jiang, Q., 2015. Geologic evidence for chaotic behaviour of the planets and its constraints on the third-order eustatic sequences at the end of the Late Paleozoic Ice Age. Palaeogeography, Palaeoclimatology, Palaeoecology 440, 848-859. http://dx.doi.org/10.1016/j.palaeo.2015.10.014

Gand, G., Durand, M., 2006. Tetrapod footprint ichno-associations from French Permian basins. Comparisons with other Euramerican ichnofaunas. In: Lucas, S.G., Cassinis, G., Schneider, J.W. (Eds.), Non-Marine Permian Biostratigraphy and Biochronology. Geological Society of London Special Publication 265. London, pp. 157-177. https://dx.doi.org/10.1144/GSL.SP.2006.265.01.07

Gand, G., Garric, J., Demathieu, G. R. S., Ellenberger, P., 2000. La palichnofaune de vertébrés tétrapodes du Permien supérieur du Bassin de Lodève (Languedoc-France). Palaeovertebrata 29(1), 1-82.

Gand, G., Garric, J., Schneider, J., Walter, H., Lapeyrie, J., Martin, C., Thiery, A. 2008. Notostraca trackways in Permian playa environments of the Lodève basin (France). Journal of Iberian Geology 34(1), 73-108. https://dx.doi.org/10.1002/adma.200802733

Gascón, F., Gisbert, J., 1987. La evolución climática del Stephaniense, Pérmico y Buntsandstein del Pirineo catalán en base al estudio de paleosuelos. Cuadernos de Geología Ibérica 11, 97-114.

Gastaldo, R.A., Kamo, S.L., Neveling, J., Geissman, J.W., Bamford, M., Looy, C.V., 2015. Is the vertebrate-defined Permian-Triassic boundary in the Karoo Basin, South Africa, the terrestrial expression of the end-Permian marine event? Geology 43(10), 939-942. https://dx.doi.org/10.1130/G37040.1

Gibbs, M.T., Rees, P.M., Kutzbach, J.E., Ziegler, A.M., Behling, P.J., Rowley, D.B. 2002. Simulations of Permian Climate and Comparisons with Climate-Sensitive Sediments. The Journal of Geology 110(1), 33-55. https://dx.doi.org/10.1086/324204

Gisbert, J., 1981. Estudio geológico-petrológico del Estefaniense-Pérmico de la Sierra del Cadí (Pirineo de Lérida): Diagénesis y sedimentología. Ph.D. Thesis. University of Zaragoza, Spain.

Gisbert, J., Martí, J., Gascón, F., 1985. Guía de la excursión al Stephaniense, Pérmico y Triásico inferior del Pirineo catalán. II Coloquio de estratigrafía y paleogeografía del Pérmico y Triásico de España. 79 pp.

Gómez-Gras, D., Alonso-Zarza, A.M., 2003. Reworked calcretes: their significance in the reconstruction of alluvial sequences (Permian and Triassic, Minorca, Balearic Islands, Spain). Sedimentary Geology 158, 299-319. https://dx.doi.org/10.1016/S0037-0738(02)00315-9

Gretter, N., Ronchi, A., López-Gómez, J., Arche, A., De la Horra, R., Barrenechea, J.F., Lago, M., 2015. The Late Palaeozoic-Early Mesozoic from the Catalan Pyrenees (Spain): 60 Myr of environmental evolution in the frame of the western peri-Tethyan palaeogeography. Earth-Science Reviews 150, 679-708. https://dx.doi.org/10.1016/j.earscirev.2015.09.001

Grice, K., Cao, C., Love, G.D., Böttcher, M.E., Twitchett, R.J., Grosjean, E., Summons, R.E., Turgeon, S.C., Dunning, W., Jin, Y., 2005. Photic zone euxinia during the Permian-Triassic superanoxic event. Science 307(5710), 706-709. https://dx.doi.org/10.1126/science.1104323

Gubin, Y.M., Golubev, V.K., Bulanov, V.V, Petuchov, S.V., 2003. Pareiasaurian tracks from the Upper Permian of Eastern Europe. Paleontological Journal 37(5), 514-523.

Hartevelt, J.J.A., 1970. Geology of the upper Segre and Valira valleys, central Pyrenees, Andorra/Spain. Leidse. Geol. Meded. 45, 349-354.

Haubold, H., 1971. Ichnia Amphibiorum et Reptiliorum fossilium. In: Wellnhofer, P. (Ed.). Encyclopedia of Paleoherpetology 18. Fischer Verlag, Stuttgart and Portland, 124 pp.

Hiete, M., Berner, U., Heunisch, C., Röhling, H.-G., 2006. A high-resolution inorganic geochemical profile across the Zechstein-Buntsandstein boundary in the North German Basin. Zeitschrift Der Deutschen Gesellschaft Für Geowissenschaften, 157(1), 77-105. https://dx.doi.org/10.1127/1860-1804/2006/0157-0077

Hofmann, A., Tourani, A., Gaupp, R., 2000. Cyclicity of Triassic to Lower Jurassic continental red beds of the Argana Valley, Morocco: implications for palaeoclimate and basin evolution. Palaeogeography, Palaeoclimatology, Palaeoecology 161, 229-266.

Kump, L.R., Pavlov, A., Arthur, M.A., 2005. Massive release of hydrogen sulphide to the surface ocean and atmosphere during intervals of oceanic anoxia. Geology 33(5), 397-400. https://dx.doi.org/10.1130/G21295.1

Kustatscher, E., Bernardi, M., Petti, F.M., Franz, M., van Konijnenburg-van Cittert, J.H.A., Kerp, H., 2017. Sea-level changes in the Lopingian (late Permian) of the northwestern Tethys and their effects on the terrestrial palaeoenvironments, biota and fossil preservation. Global and Planetary Change 148, 166-180. http://dx.doi.org/10.1016/j.gloplacha.2016.12.006

Kutzbach, J.E., Ziegler, A.M., 1993. Simulation of Late Permian climate and biomes with an atmosphere-ocean model: Comparisons with observations. Philosophical Transactions of the Royal Society B 341, 327-340. https://dx.doi.org/10.1098/rstb.1993.0118

Leonardi, G., 1987. Glossary and Manual of Tetrapod Footprint Palaeoichnology. Departamento Nacional de Produção Mineral, Brasilia (117 pp.).

Li, M., Huang, C., Hinnov, L., Ogg, J., Chen, Z.-Q., Zhang, Y., 2016. Obliquity-forced climate during the Early Triassic hothouse in China. Geology (2016). https://dx.doi.org/10.1130/G37970.1

Liebrecht, T., Fortuny, J., Galobart, À., Müller, J., Sander, P.M., 2017. A large, multiple-tooth-rowed captorhinid reptile (Amniota: Eureptilia) from the upper Permian of Mallorca (Balearic Islands, western Mediterranean). Journal of Vertebrate Paleontology 37(1): e1251936. http://dx.doi.org/10.1080/02724634.2017.1251936

Linol, B., Bercovici, A., Bourquin, S., Diez, J.B., López-Gómez, J., Broutin, J., Durand, M., Villanueva-Amadoz, U., 2009. Late Permian to Middle Triassic correlations and palaeogeographical reconstructions in south-western European basins: New sedimentological data from Minorca (Balearic Islands, Spain). Sedimentary Geology 220, 77-94. https://dx.doi.org/10.1016/j.sedgeo.2009.06.003

Looy, C.V., Ranks, S.L., Chaney, D.S., Sanchez, S., Steyer, J.-S., Smith, R.M.H., Sidor, C.A., Myers, T.S., Ide, O., Tabor, N.J., 2016. Biological and physical evidence for extreme seasonality in central Permian Pangea. Palaeogeography, Palaeoclimatology, Palaeoecology 451, 210-226. https://dx.doi.org/10.1016/j.palaeo.2016.02.016

Marchetti, L., 2016. New occurrences of tetrapod ichnotaxa from the Permian Orobic Basin (Northern Italy) and critical discussion of the age of the ichnoassociation. Papers in Palaeontology 2(3), 363-386. https://dx.doi.org/10.1002/spp2.1045

Martí, J., 1983. La formación volcánica estefaniense Erill Castell (Pirineo de Lérida). Acta Geológica Hispánica 18 (1), 27-33.

Marty, D., Strasser, A., Meyer, C.A., 2009. Formation and Taphonomy of Human Footprints in Microbial Mats of Present-Day Tidal-flat Environments: Implications for the Study of Fossil Footprints. Ichnos 16, 127–142. https://dx.doi.org/10.1080/10420940802471027

Mey, P.H.W., Nagtegaal, P.J.C., Roberti, K.J., Hartevelt, J.J.A., 1968. Lithostratigraphic subdivision of post-Variscan deposits in the South-Central Pyrenees, Spain. Leidse Geologische Mededelingen 41, 221–228.

Meyer, K.M., Kump, L.R., 2008. Oceanic euxinia in Earth history: Causes and consequences. Annual Reviews of Earth and Planetary Sciences 36, 251-288. https://dx.doi.org/10.1146/annurev.earth.36.031207.124256

Michaelsen, P., 2002. Mass extinction of peat-forming plants and the effect on fluvial styles across the Permian-Triassic boundary, northern Bowen Basin, Australia. Palaeogeography, Palaeoclimatology, Palaeoecology 179, 173-188.

Michel, L.A., Tabor, N.J., Montañez, I.P., Schmitz, M.D., Davydov, V.I., 2015. Chronostratigraphy and paleoclimatology of the lodève Basin, France: Evidence for a pan-tropical aridification event across the carboniferous-permian boundary. Palaeogeography, Palaeoclimatology, Palaeoecology 430, 118-131. https://dx.doi.org/10.1016/j.palaeo.2015.03.020

Mujal, E., Fortuny, J., Oms, O., Bolet, A., Galobart, À., Anadón, P., 2016b. Palaeoenvironmental reconstruction and early Permian ichnoassemblage from the NE Iberian Peninsula (Pyrenean Basin). Geological Magazine 153(4), 578-600. https://dx.doi.org/10.1017/S0016756815000576

Mujal, E., Gretter, N., Ronchi, A., López-Gómez, J., Falconnet, J., Diez, J.B., De la Horra, R., Bolet, A., Oms, O., Arche, A., Barrenechea, J.F., Steyer, J.-S., Fortuny, J., 2016a. Constraining the Permian/Triassic transition in continental environments: Stratigraphic and paleontological record from the Catalan Pyrenees (NE Iberian Peninsula). Palaeogeography, Palaeoclimatology, Palaeoecology 445, 18-37. https://dx.doi.org/10.1016/j.palaeo.2015.12.008

Nagtegaal, P.J.C., 1969. Sedimentology, paleoclimatology, and diagenesis of post-Hercynian continental deposits in the south-central Pyrenees, Spain. Leidse Geologische Mededelingen 42, 143–238.

Newell, A.J., Sennikov, A.G., Benton, M.J., Molostovskaya, I.I., Golubev, V.K., Minikh, A.V., Minikh, M.G., 2010. Disruption of playa-lacustrine depositional systems at the Permo-Triassic boundary: evidence from Vyazniki and Gorokhovets on the Russian Platform. 1. Journal of the Geological Society of London, 167, 695–716. https://dx.doi.org/10.1144/0016-76492009-103

Paillard, D., Labeyrie, L., Yiou, P., 1996. Macintosh program performs time-series analysis. Eos Trans. AGU, v. 77, no. 379. p. (http://www.agu.org/eos_elec/96097e.html).

Parrish, J.T., Peterson, F., 1988. Wind directions predicted from global circulation models and wind directions determined from eolian sandstones of the western United States-A comparison. Sedimentary Geology 56(1-4), 261-282. https://dx.doi.org/10.1016/0037-0738(88)90056-5

Payne, J.L., Clapham, M.E., 2012. End-Permian Mass Extinction in the Oceans: An Ancient Analog for the Twenty-First Century? Annual Reviews of Earth and Planetary Sciences 40, 89-111. https://dx.doi.org/10.1146/annurev-earth-042711-105329

Pereira, M.F., Castro, A., Chichorro, M., Fernández, C., Díaz-Alvarado, J., Martí, J., Rodríguez, C., 2014. Chronological link between deep-seated processes in magma chambers and eruptions: Permo-Carboniferous magmatism in the core of Pangaea (Southern Pyrenees). Gondwana Research 25(1), 290-308. https://dx.doi.org/10.1016/j.gr.2013.03.009

Remy, R.R., Ferrell, R.E., 1989. Distribution and Origin of Analcime in Marginal Lacustrine Mudstones of the Green River Formation, South-Central Uinta Basin, Utah. Clays and Clay Minerals 37(5), 419-432. https://dx.doi.org/10.1346/CCMN.1989.0370505

Retallack, G.J., 1996. Early Triassic therapsid footprints from the Sydney Basin, Australia. Alcheringa 20, 301-314.

Retallack, G.J., 2013. Permian and Triassic greenhouse crises. Gondwana Research 24, 90-103. https://dx.doi.org/10.1016/j.gr.2012.03.003

Retallack, G.J., Metzger, C.A., Greaver, T., Jahren, A.H., Smith, R.M.H., Sheldon, N.D., 2006. Middle-Late Permian mass extinction on land. Bulletin of the Geological Society of America 118(11-12), 1398-1411. https://dx.doi.org/10.1130/B26011.1

Retallack, G.J., Seyedolali, A., Krull, E.S., Holser, W.T., Ambers, C.P., Kyte, F.T., 1998. Search for evidence of impact at the Permian-Triassic boundary in Antarctica and Australia. Geology 26(11), 979-982.

Retallack, G.J., Sheldon, N.D., Carr, P.F., Fanning, M., Thompson, C.A., Williams, M.L., Jones, B.G., Hutton, A. 2011. Multiple Early Triassic greenhouse crises impeded recovery from Late Permian mass extinction. Palaeogeography, Palaeoclimatology, Palaeoecology 308(1-2), 233-251. https://dx.doi.org/10.1016/j.palaeo.2010.09.022

Rey, K., Amiot, R., Fourel, F., Rigaudier, T., Abdala, F., Day, M.O., Fernandez, V., Fluteau, F., France-Lanord, C., Rubidge, B.S., Smith, R.M., Viglietti, P.A., Zipfel, B., Lécuyer, C., 2016. Global climate perturbations during the Permo-Triassic mass extinctions recorded by continental tetrapods from South Africa. Gondwana Research 37, 384-396. https://dx.doi.org/10.1016/j.gr.2015.09.008

Robles, S., Llompart, C., 1987. Análisis paleogeográfico y consideraciones paleoicnológicas del Pérmico superior y Triásico inferior en la transversal del río Segre (Alt Urgell, Pirineo de Lérido). Cuadernos de Geología Ibérica 11, 115-130.

Roscher, M., Schneider, J.W., 2006. Permo-Carboniferous climate: Early Pennsylvanian to Late Permian climate development of central Europe in a regional and global context. In: Lucas, S.G., Cassinis, G., Schneider, J.W. (Eds.), Non-Marine Permian Biostratigraphy and Biochronology. Geological Society of London Special Publication 265. London, 265, pp. 95-136. https://dx.doi.org/10.1144/GSL.SP.2006.265.01.05

Roscher, M., Stordal, F., Svensen, H., 2011. The effect of global warming and global cooling on the distribution of the latest Permian climate zones. Palaeogeography, Palaeoclimatology, Palaeoecology 309(3-4), 186-200. https://dx.doi.org/10.1016/j.palaeo.2011.05.042

Rothman, D.H., Fournier, G.P., French, K.L., Alm, E.J., Boyle, E.A., Cao, C., Summons, R.E., 2014. Methanogenic burst in the end-Permian carbon cycle. PNAS 111(15), 5462-5467. https://dx.doi.org/10.1073/pnas.1318106111

Saura, E., Teixell, A., 2006. Inversion of small basins: effects on structural variations at the leading edge of the Axial Zone antiformal stack (Southern Pyrenees, Spain). Journal of Structural Geology 28(11), 1909-1920. https://dx.doi.org/10.1016/j.jsg.2006.06.005

Schneider, J.W., Körner, F., Roscher, M., Kroner, U., 2006. Permian climate development in the northern peri-Tethys area - The Lodève basin, French Massif Central, compared in a European and global context. Palaeogeography, Palaeoclimatology, Palaeoecology, 240(1-2), 161-183. https://dx.doi.org/10.1016/j.palaeo.2006.03.057

Schulz, M., Mudelsee, M., 2002. REDFIT; estimating red-noise spectra directly from unevenly spaced paleoclimatic time series. Computer & Geosciences 28, 421-426.

Sheldon, N.D., Chakrabarti, R., Retallack, G.J., Smith, R.M.H., 2014. Constraining geochemical signatures on land from the Middle and Late Permian extinction events. Sedimentology 61, 1812-1829. https://dx.doi.org/10.1111/sed.12117

Słowakiewicz, M., Kiersnowski, H., Wagner, R., 2009. Correlation of the Middle and Upper Permian marine and terrestrial sedimentary sequences in Polish, German, and USA Western Interior Basins with reference to global time markers. Palaeoworld 18(2-3), 193-211. https://dx.doi.org/10.1016/j.palwor.2009.04.009

Smith, R.M.H., Sidor, C.A., Tabor, N.J., Steyer, J.-S., 2015. Sedimentology and vertebrate taphonomy of the Moradi Formation of northern Niger: A Permian wet desert in the tropics of Pangaea. Palaeogeography, Palaeoclimatology, Palaeoecology 440, 128-141. https://dx.doi.org/10.1016/j.palaeo.2015.08.032

Speksnijder, A., 1985. Anatomy of a strike-slip fault controlled sedimentary basin, Permian of the Southern Pyrenees, Spain. Sedimentary Geology 44, 179-223.

Surkov, M.V, Benton, M.J., Twitchett, R.J., Tverdokhlebov, V.P., Newell, A.J., 2007. First occurrence of footprints of large therapsids from the Upper Permian of European Russia. Palaeontology 50(3), 641-652.

Tabor, N.J., Montanez, I.P., 2002. Shifts in late Paleozoic atmospheric circulation over western equatorial Pangean: Insights from pedogenic $d^{18}O$ compositions. Geology 30(12), 1127-1130. https://dx.doi.org/10.1130/0091-7613(2002)030<1127:SILPAC>2.0.CO;2

Tabor, N.J., Smith, R.M.H., Steyer, J.-S., Sidor, C.A., Poulsen, C.J., 2011. The Permian Moradi Formation of northern Niger: Paleosol morphology, petrography and mineralogy. Palaeogeography, Palaeoclimatology, Palaeoecology 299, 200-213. https://dx.doi.org/10.1016/j.palaeo.2010.11.002

Torsvik, T.H., Cocks, L.R.M., 2013. Gondwana from top to base in space and time. Gondwana Research 24, 999-1030. http://dx.doi.org/10.1016/j.gr.2013.06.012

Valentini, M., Conti, M.A., Mariotti, N., 2007. Lacertoid Footprints of the Upper Permian Arenaria di Val Gardena Formation (Northern Italy). Ichnos 14(3-4), 193-218. https://dx.doi.org/10.1080/10420940601049974

Valentini, M., Nicosia, U., Conti, M.A., 2009. A re-evaluation of pachypes, a pareiasaurian track from the late permian. Neues Jahrbuch Fur Geologie Und Palaontologie - Abhandlungen 251(1), 71-94. https://dx.doi.org/10.1127/0077-7749/2009/0251-0071

Voigt, S., Hminna, A., Saber, H., Schneider, J.W., Klein, H., 2010. Tetrapod footprints from the uppermost level of the Permian Ikakern Formation (Argana Basin, Western High Atlas, Morocco). Journal of African Earth Sciences 57(5), 470-478.https://dx.doi.org/10.1016/j.jafrearsci.2009.12.003

Ward, P.D., Montgomery, D.R., Smith, R., 2000. Altered river morphology in South Africa related to the Permian-Triassic extinction. Science 289, 1740-1743. https://dx.doi.org/10.1126/science.289.5485.1740

Williams, M.L., Jones, B.G., Carr, P.F., 2012. Geochemical consequences of the Permian-Triassic mass extinction in a non-marine succession, Sydney Basin, Australia. Chemical Geology 326-327, 174-188. http://dx.doi.org/10.1016/j.chemgeo.2012.07.021